DEVELOPMENT OF MAGNESIUM BASED HYBRID NANOCOMPOSITE

BY

OGUNLAKIN NASIRUDEEN OLALEKAN

A Thesis Presented to the

DEANSHIP OF GRADUATE STUDIES

KING FAHD UNIVERSITY OF PETROLEUM & MINERALS

DHAHRAN, SAUDI ARABIA

In Partial Fulfillment of the
Requirements for the Degree of

MASTER OF SCIENCE

In

MATERIAL SCIENCE AND ENGINEERING

APRIL, 2016

KING FAHD UNIVERSITY OF PETROLEUM & MINERALS

DHAHRAN- 31261, SAUDI ARABIA

DEANSHIP OF GRADUATE STUDIES

This thesis, written by **OGUNLAKIN NASIRUDEEN OLALEKAN** under the direction of his thesis advisor and approved by his thesis committee, has been presented and accepted by the Dean of Graduate Studies, in partial fulfillment of the requirements for the degree of **MASTER OF SCIENCE IN MATERIALS SCIENCE & ENGINEERING.**

Dr. Syed Fida Hassan
(Advisor)

Dr. Zuhair Mattoug Gasem
Department Chairman

Dr. Saheb Nouari
(Member)

Dr. Salam A. Zummo
Dean of Graduate Studies

Dr. Tahar Laoui
(Member)

25/4/16

Date

Dedication

I dedicate this work to Almighty Allah for his guidance and protection over me, and also to my loving parent for their care and support.

ACKNOWLEDGMENTS

Alhamdulillah, I thank Allah, for giving me the strength, the means and skills to carry out this work. I thank my parents for guiding and sponsoring me to acquire basic and higher education. Also, I say thanks to my wife and the rest of my family members for their patience and support.

I am grateful to King Fahd University of Petroleum and Minerals (KFUPM) and the Ministry of Higher Education (MoHE), Saudi Arabia for awarding me the scholarship to undertake my MS degree program.

My sincere appreciation goes to my Advisor; Dr. Syed Fida Hassan, Associate Professor, Department of Mechanical Engineering, KFUPM who assisted me a lot to develop my research skills and for his valuable advice in this work. I also acknowledge the contributions of my committee members; Dr. Nouari Saheb and Dr. Tahar Laoui to the success of my thesis work, their valuable advices, influence and suggestions were instrumental to the success of this work.

My profound gratitude goes to Mr. Faheemdeen Patel and Mr Murthada Baig for their adequate technical assistance to me, especially during the compaction and the extrusion process of this work. I acknowledge the assistance of Mr. Akolade Idris of CENT, Mr. Mohammad Latif Hashmi of Materials Science Laboratory, Mr. Ali Sabeer of Mechanical Workshop for their enormous support.

I thank the entire MS student of Material Science and Engineering for their advices and hands of help we extend to each other in the laboratory. Mr Araoye Razaq, Mr Lawal Taoreed Taiwo, Mr AbdulHakim Yussuf, Mr Ismaeel Aliyu and the entire member of the Nigeria Community in KFUPM (NCUPM) also deserve my gratitude for their help and support.

Finally, I express my gratitude to anyone I didn't mention that has assisted or contributed to the success of this research in one way or the other.

TABLE OF CONTENTS

ACKNOWLEDGMENTS ..... **VI**

TABLE OF CONTENTS ..... **VIII**

LIST OF TABLES ..... **XI**

LIST OF FIGURES ..... **XII**

LIST OF ABBREVIATIONS ..... **XVI**

ABSTRACT ..... **XVIII**

ملخص الرسالة ..... **XXI**

CHAPTER 1 INTRODUCTION **1**

CHAPTER 2 LITERATURE REVIEW **5**

2.1 Magnesium Based Composite and Nanocomposite **5**

2.2 Types of Reinforcement. **6**

2.3 Processing Of Magnesium Based Composite **8**

2.3.1 Liquid/Melt Based Processing 8

2.3.2 Solid / Powder Based Processing 10

2.4 Microstructure of magnesium based composites **17**

2.4.1 Grain refinement of magnesium matrix 17

2.5 Mechanical Properties of Magnesium Based Composites **23**

2.5.1. Hardness 23

2.5.2. Tensile Properties 24

2.5.3. Compressive Properties 31

2.6 Summary **34**

CHAPTER 3 MATERIALS AND EXPERIMENTAL PROCEDURE **36**

3.1 Raw Materials **36**

3.2 Material Processing **36**
3.2.1 Blending 36
3.2.2 Powder Compaction/Consolidation 37
3.2.3 Sintering 38
3.2.4 Extrusion 38
3.2.5 Density Measurement 39
3.2.6 X-ray Diffraction Studies 40
3.2.7 Microstructural Characterization 40
3.2.8 Mechanical Characterization 41
3.2.9 Fracture characterization 43

CHAPTER 4 EXPERIMENTAL RESULTS **44**

4.1 Magnesium-Nickel Composite **44**
4.1.1 Macrostructural Characteristics 44
4.1.2 Density Measurement 45
4.1.3 X-RAY Diffraction Studies 45
4.1.4 Microstructural Characteristics 47
4.1.5 MECHANICAL PROPERTIES 50
4.1.6 Fractography 53

4.2 Magnesium-TiO_2 Nanocomposite **55**
4.2.1 Macrostructural Characteristics 55
4.2.2 Density Measurement 56
4.2.3 X-RAY Diffraction Studies 56
4.2.4 Microstructural Characteristics 59
4.2.5 Mechanical Properties 62
4.2.6 Fractography 66

4.3 Magnesium-Hybrid Nanocomposite **69**
4.3.1 Macrostructural Characteristics 69
4.3.2 Density Measurement 69
4.3.3 X-Ray Diffraction Studies 70
4.3.4 Microstructural Characteristics 72
4.3.5 Mechanical Properties 75
4.3.6 Fractography 78

CHAPTER 5 DISCUSSIONS **80**

5.1. Mg-Ni Composite **80**
5.1.1. Synthesis of reinforced and monolithic magnesium 80
5.1.2. Microstructural characteristics 80
5.1.3. Mechanical characteristics 82

5.2. Mg-TiO_2 nanocomposite **85**
5.2.1. Synthesis of reinforced and monolithic magnesium 85

5.2.2. Density Measurements....85
5.2.3. Microstructural characteristics....85
5.2.4. Mechanical characteristics....86
5.2.5. Tension-Compression Asymmetry (TCA) of Mg-TiO_2 nanocomposite....88

5.3. Magnesium hybrid nanocomposite....90
5.3.1. Synthesis of hybrid nanocomposite....90
5.3.2. Microstructural characteristics....90
5.3.3. Mechanical characteristics....91

CHAPTER 6 CONCLUSIONS....94

CHAPTER 7 RECCOMENDATIONS....96

REFERENCES....97

VITAE....115

LIST OF TABLES

Table 1: Results of Density, porosity and grain size 45

Table 2: Results of Microhardness and Macrohardness for Mg-Pure and Mg-1.50Ni..... 50

Table 3: Result of room temperature tensile testing for Mg-Pure and Mg-1.50Ni..... 51

Table 4: Result of room temperature compressive testing for Mg-Pure and Mg-1.50Ni composite 52

Table 5: Results of Density, Porosity and Grain size measurement for Mg-TiO_2 nanocomposites..... 56

Table 6: Results of Microhardness and Macrohardness for Mg-TiO_2 nanocomposites ... 62

Table 7: Result of room temperature tensile testing for Mg-Pure and Mg-TiO_2 nanocomposites..... 63

Table 8: Result of room temperature compressive testing for Mg-Pure and Mg-TiO_2 nanocomposites..... 64

Table 9: Results of Density. Porosity and Grain size Measurement for hybrid sample . 69

Table 10: Results of Microhardness and Macrohardness of Mg-Pure and Mg-1.50Ni-0.33TiO_2 sample..... 75

Table 11: Result of room temperature tensile testing for Mg—Pure and Mg-1.50Ni-0.33TiO_2 sample..... 76

Table 12: Result of room temperature compressive testing for Mg-Pure and Mg-1.50Ni-0.33TiO_2 sample..... 77

LIST OF FIGURES

Figure 1: Mixing of Matrix and reinforcement [79] 12

Figure 2: Relationship between green density and compacting pressure [81]..... 14

Figure 3: Bonding Mechanism in powder sintering [81]..... 15

Figure 4: Optical microscopy micrographs of Mg/SiC nanocomposites extruded at (a) 250 °C; and (b) 350 °C adapted from ref. [89]..... 20

Figure 5: Optical micrographs showing the grain morphology of (a) Mg/(1 vol Al2O3&0.1 vol Cu), (b) Mg/(1 vol Al2O3&0.3 vol Cu), (c) Mg/(1 vol Al2O3&0.6 vol Cu), and (d) Mg/(1 vol Al2O3&0.9 vol Cu) nanocomposites. Adapted from ref. [48]..... 23

Figure 6: Bubble chart illustrating the improvement in 0.2% yield strength and ductility for magnesium nanocomposites adapted from reference [47] 29

Figure 7: Schematic diagrams showing the powder consolidation steps. a) loose particles are filled into the die cavity b) & c) Pressure is applied uniaxially d) removing the green billet from the die 37

Figure 8: Photograph of tube furnace used for sintering 38

Figure 9: Schematic of tensile specimen 42

Figure 10: Photograph of some a) sintered billets and b) extruded rods showing no visible macrostructural defect 44

Figure 11: X-ray diffraction spectrum of samples in direction parallel to extrusion direction 46

Figure 12: X-ray diffraction spectrum of samples in direction perpendicular to extrusion direction 46

Figure 13: Scanning electron micrographs showing elemental nickel particle: (a) distribution pattern and (b) interfacial characteristics in Mg-1.50Ni composite and c) EDX linescan analysis showing elements across the line indicating good interfacial integrity 48

Figure 14: Optical micrographs showing grain morphology in: (a) monolithic magnesium, and (b) and (c) elemental nickel reinforced magnesium, respectively. 49

Figure 15: Tensile Stress-Strain curves of Mg-Pure and Mg-150Ni composites 51

Figure 16: Compressive Stress-Strain curves of Mg-Pure and Mg-1.50Ni composites ... 52

Figure 17: Scanning electron fractographs showing: ductile pseudo-dimple in (a) and (b), and inter-crystalline feature in (c) for monolithic magnesium, and brittle- ductile matrix in (d) with particle cracking in (e) for elemental nickel particle reinforced magnesium respectively..... 53

Figure 18: Compressive fracture surface image of a & b) pure magnesium and (c &d) Ni reinforced magnesium composite..... 54

Figure 19: Photograph of some a) compacted billets b) sintered billets and c) extruded rods of TiO_2 reinforced samples 55

Figure 20: X-ray diffraction spectrum of Mg-TiO2 samples in direction parallel to extrusion direction 57

Figure 21: X-ray diffraction spectrum of Mg-TiO2 samples in direction perpendicular to extrusion direction 58

Figure 22: EDX analysis of Mg-TiO2 nanocomposite sample..... 59

Figure 23: Representative FESEM images reinforcement distribution in (a) Mg-033TiO2 b) Mg-066TiO2 c) Mg-100TiO2 samples (few pointed arrows indicate TiO2 nanoparticles) 60
Figure 24: Representative optical micrograph of (a) Mg-033TiO2, (b) Mg-066TiO2 and (c) Mg-100TiO2 61
Figure 25: Tensile Stress-Strain curves of for Mg-Pure and Mg-TiO2 nanocomposites . 63
Figure 26: Compressive Stress-Strain curves of developed composites for Mg-Pure and Mg-TiO2 nanocomposites 65
Figure 27: Tensile compressive yield stress of Pure Mg and Mg/TiO2 composites indicating the Tensile Compression Asymmetry 65
Figure 28: Scanning electron fractographs showing the tensile fracture surface of a) & b) monolithic Mg, c) & d) Mg-033TiO_2 e) & f) Mg-066TiO_2 g) & h) Mg-100TiO_2 67
Figure 29: Scanning electron fractographs showing the compressive fracture surface of a) & b) monolithic Mg, c) & d) Mg-033TiO2 e) & f) Mg-066TiO2 g) & h) Mg-100TiO2 68
Figure 30: Photograph of some hybrid (Mg-1.50Ni-0.33TiO_2) samples 69
Figure 31: X-ray diffraction spectrum of pure Mg and Mg-1.50Ni-0.33TiO_2 samples in direction parallel to extrusion direction 71
Figure 32: X-ray diffraction spectrum of pure Mg and Mg-1.50Ni-0.33TiO_2 samples in direction perpendicular to extrusion direction 71
Figure 33: EDX analysis of Mg-150-0.33TiO2 nanocomposite sample 72
Figure 34: SEM image of hybrid sample showing distribution of reinforcement 73

Figure 35: EDX mapping of Mg-150Ni-033TiO2 sample 74

Figure 36: Micrograph of etched hybrid nanocomposite..... 74

Figure 37: Tensile Stress-Strain curves of developed Mg-Pure and Mg-1.50Ni-0.33TiO2 sample..... 76

Figure 38: Compressive Stress-Strain curves of developed composites for Mg-Pure and Mg-1.50Ni-0.33TiO2 sample..... 77

Figure 39: Scanning electron fractographs showing the tensile fracture surface of Mg-150Ni-033TiO2 samples at different magnification. 78

Figure 40: Scanning electron fractographs showing the compressive fracture surface of Mg-150Ni-033TiO_2 samples at different magnification. 79

LIST OF ABBREVIATIONS

HCP	:	Hexagonal Crystal Structure
MNC	:	Magnesium Nanocomposite
DMD	:	Disintegrated Melt Deposition
MDD	:	Mechanical Disintegration and Deposition
BPS	:	Blend-Press-Sinter
SPS	:	Spark Plasma Sintering
CTE	:	Coefficient of Thermal Expansion
YS	:	Yield Strength
CYS	:	Compressive Yield Strength
UTS	:	Ultimate Tensile Strength
UCS	:	Ultimate Compressive Strength
WoF	:	Work of Fracture
CNT	:	Carbon Nanotube
PSN	:	Particle Simulated Nucleation
XRD	:	X-Ray Diffraction
SEM	:	Scanning Electron Microscope
EDS	:	Energy Dispersive Spectroscopy

FESEM	:	Field Emission Scanning Electron Microscope
ASTM	:	American Society for Testing and Materials
Mg-Pure	:	Monolithic Magnesium Sample
Mg-0.33TiO_2	:	Magnesium nanocomposite reinforced with 0.33vol% TiO_2
Mg-0.66TiO_2	:	Magnesium nanocomposite reinforced with 0.66vol% TiO_2
Mg-1.00TiO_2	:	Magnesium nanocomposite reinforced with 1.00vol% TiO_2
Mg-1.5Ni-0.33TiO_2	:	Magnesium composite reinforced with 1.5vol% Ni and 0.33vol% TiO_2

ABSTRACT

Full Name : [Ogunlakin Nasirudeen Olalekan]

Thesis Title : [Development of Magnesium Based Hybrid Nanocomposite]

Major Field : [Material Science and Engineering]

Date of Degree : [April, 2016]

This thesis focused on development of magnesium based composite with enhanced mechanical properties. Near dense monolithic magnesium, micron sized nickel particle reinforced magnesium composite and TiO_2 nanoparticle reinforced magnesium nanocomposite were successfully developed using the cost effective powder metallurgy process of blend-press-sinter followed by hot extrusion. Hybrid nanocomposite consisting of 1.5 volume% nickel and 0.33volume% TiO_2 was also developed using similar technique.

The developed monolithic and reinforced magnesium composites were characterized to determine the microstructural evolution, particle distribution and grain morphology using appropriate characterization techniques such as XRD, SEM and FE-SEM. The samples were also subjected to microhardness, macrohardness, tensile and compressive tests to determine the effect of the reinforcements on the mechanical properties of magnesium.

The nickel reinforcement particles dispersion was reasonably uniform with good matrix-reinforcement interfacial integrity. The small volume fraction of elemental nickel particle reinforcement refined grain morphology and significantly improved the hardness and tensile strength of the magnesium matrix without affecting the yield strength. However, ductility was adversely affected. The tensile strength was increased by ~21% with a ~26% decrease in the fracture strain, the reinforcement changed the tensile fracture mode of

magnesium matrix from pseudo-ductile to brittle mode dominated by nickel particle fracture. The room temperature compression properties of the synthesized nanocomposites reveal an increase in the 0.2% compressive yield strength and ultimate compressive strength of pure magnesium up to ~81% and ~23% respectively with a ~18% decrease in the fracture strain.

In the TiO_2 reinforced magnesium nanocomposites, microstructural characterization of the nanocomposites reveal significant reduction in grain size of pure magnesium with addition of titanium oxide nanoparticles. The room temperature tensile properties of the synthesized nanocomposites revealed no significant improvement in the strength characteristics of magnesium with the addition of TiO_2 nanoparticles, the tensile fracture strain of the synthesized nanocomposites was found to marginally surpass that of pure magnesium and a maximum fracture strain of ~17% with the addition of 0.33 vol.% TiO_2 was obtained. The room temperature compression properties of the synthesized nanocomposites reveal an increase in the 0.2% compressive yield strength and ultimate compressive strength of pure magnesium with no significant change in the fracture strain. With addition of 1.00 vol.% TiO_2, the 0.2% compressive yield strength and the fracture strain of pure magnesium increased by ~65%% and ~37% respectively. With the addition of TiO_2 nanoparticles, the level of anisotropy/asymmetry of pure magnesium measured using tensile compression asymmetry values was found to be lower than that of the synthesized pure magnesium and a minimum of ~1 for Mg-1.00vol.% TiO_2 nanocomposite was observed.

The microstructural characterization of the magnesium hybrid nanocomposite reveals significant grain refinement beyond that of individual nickel and TiO_2 particle

reinforcements. The simultaneous addition of 1.5vol.% nickel and 0.33vol% TiO_2 significantly improved the hardness, tensile strength and fracture strain of the magnesium matrix but with adverse effect on its the yield strength. The room temperature compression properties of the hybrid nanocomposites reveal an increase in the 0.2% compressive yield strength and ultimate compressive strength of pure magnesium up to ~112% and ~29% respectively with a ~12 % decrease in the fracture strain.

ملخص الرسالة

الاسم الكامل : أوغنلكن ناصرالدين أولاليكن

عنوان الرسالة : التنمية من المغنيسيوم تستند المركبة النانوية الهجين

التخصص : علم المواد والهندسة

تاريخ الدرجة : April, 2016

هذه الاطروحة تركز على تطوير المغنيسيوم تستند المهجنة التي يدخل فيها المغنسيوم بشكل اساسي مع خواص ميكانيكية محسنة. المغنسيوم شبه موحد الكثافة ومركبات المغنسيوم المدعمة بجزيئات النيكل الميكرونية الحجم ومركبات المغنسيوم المدعمة بجزيئات (اكسيد التيتانيوم) النانوية الحجم طورت بنجاح باستخدام طريقة ميتالوجيا المساحيق (او تعدين المساحيق) الاقتصادية التي تعتمد على الخلط والكبس وعملية التصليد الحراري ثم عملية السحب(البثق) الحار. الجزيئات النانوية المهجنة التي تحتوي على النيكل ب1.5% حجما واكسيد التيتانيوم بنسبة 0.33% حجما كانت قد طورت كذلك باستخدام تقنية(طريقة) مشابهة.

مركبات المغنسيوم الموحدة المطورة والمدعمة تميزت لتحدد ثورة البناء الميكروني وتوزيع الجزيئات و مورفولوجيا الحبيبات باستخدام تقنيات ملائمة مثل حيود الاشعة السينية و المجهر الالكتروني الماسح و مجهر مجال انبعاث المسح الالكتروني. العينات كانت قد عرضت كذلك لاختبارات الصلابة المكرونية والصلابة الماكرونية والشد والكبس(الضغط) لتحديد تأثير التدعيمات على الخصائص الميكانيكية للمغنسيوم.

توزيع دعائم جزيئات النيكل كانت موحدة بشكل جيد مع ارتباط جيد بين المكونات. النسبة الحجمية الضئيلة من جزيئات النيكل الداعمة حسنت مورفولوجيا الحبيبات وطورت بشكل واضح الصلابة ومقاومة الشد في مصفوفة المغنسيوم بدون التأثير على مقاومة الخضوع (التشوه). مع ذلك فان الطواعية قد تأثرت. مقاومة الشد كانت قد ازدادت بنسبة 21% تقريبا مع 26% نقص في اجهاد الكسر. التدعيمة غيرت طريقة الكسر بالشد لمصفوفة

المغنسيوم من شبه الطواعية الى الهشاشة التي تطغى على سلوك الانكسار للنيكل. خصائص الكبس في درجة حرارة الغرفة للجزيئات النانوية الاصطناعية كشفت زيادة في مقاومة الخضوع ومقاومة الكبس 0.2% في المغنسيوم النقي الى 81% تقريبا و 23% تقريبا على التوالي مع نقص في اجهاد الانكسار بنسبة 18% تقريبا.

في المغنيسيوم النانوية للمغنسيوم المدعمة باكسيد التيتانيوم, خصائص البناء النانوي للمركبات النانوية كشفت نقص واضح في حجم الحبيبات في المغنسيوم النقي مع اضافة الجزيئات النانوية لاكسيد التنتانيوم. خصائص الشد عند درجة حرارة الغرفة للمركبات النانوية الاصطناعية لم تكشف عن تطور واضح في خصائص القوة في المغنسيوم مع اضافة الجزيئات النانوية لاكسيد التيتانيوم, لوحظ اجهاد الانكسار للشد في المغنيسيوم النانوية المصنعة بأنه يفوق قليلا ذلك الذي وجد في المغنسيوم النقي و اجهاد الكسر الاقصى وصل الى 17% مع اضافة 0.33% حجما من اكسيد التيتانيوم. خصائص الكبس عند درحة حرارة الغرفة للمركبات النانوية كشفت زيادة في مقاومة الخضوع 0.2% ومقاومة الكبس(الضغط) للمغنسيوم النقي و لم يوجد تغير واضح في اجهاد الكسر. مع اضافة 1% حجمت من اكسيد التيتانيوم؛ مقاومة الخضوع لضغط الكبس 0.2% واجهاد الكسر للمغنسيوم النقي زادت بنسبة 65% و37% تقريبا على التوالي. مع اضافة الجزيئات النانوية لاكسيد التيتانيوم؛ فان تباين الخواص للمعنسيوم النقي الذي قد تم قياسه باستخدام تباين قيم الشد والكبس؛ وجد بأنه اقل من ذلك الذي لجزيئات المغنسيوم النقي المصنع ب 1 تقريبا كحد ادنى للمغنسيوم المخلوط مع 1% حجما من جزيئات النانو لاكسيد التيتانيوم.

خصائص البناء الميكروني لمركبات المغنسيوم النانوية المهجنة كشفت عن نقاوة واضحة للحبيبات اكثر من تلك التي وجدت لجزيئات التدعيم الفردية من النيكل واكسيد التيتانيوم. الاضافة المتزامنة من النيكل بنسبة 1.5% حجما وجزيئات اكسيد التيتانيوم بنسبة 0.33% حجما طورت الصلابة ومقاومة الشد واجهاد الكسر لمصفوفة المغنسيوم بشكل واضح لكنها على العكس من ذلك اثرت على مقاومة الخضوع. خصائص الضغط عند درجة حرارة الغرفة للجزيئات النانوية المهجنة كشفت عن زيادة في مقاومة الخضوع للكبس 0.2% ومقاومة الكبس للمغنسيوم النقي حتى 112% و29% على التوالي مع نقص يساوي 12% في اجهاد الكسر.

CHAPTER 1

INTRODUCTION

The increasing demand for fuel conservation in automobiles and aircrafts, and the increasing need to reduce emissions to lower environmental impact had prompted many industries to search for new advanced materials to replace conventional materials, in lieu of this, many research works had focused on the development of new lightweight materials as the key and unavoidable solution for the future in structural and other applications. Consequently, magnesium based materials have gained much interest in this regard in recent years as a promising light weight material due to their unique properties; magnesium is the lightest known structural metal having a density of 1.74g/cm^3 which is approximately two-third the density of aluminum, two-fifth that of titanium and one-fourth that of steel[1]. Aside its low density, magnesium is abundant in both seawater and earth crust, it is the third most dissolved mineral in seawater having an availability of 1.1 kg/m3 and also the sixth most abundant element in the earth's crust comprising of 2% by mass[2]. Magnesium offers high specific stiffness, specific strength, high damping capacity, excellent castability and superior machinability[3]. The production of magnesium worldwide has increased from 588000 metric tons in 2009 to around 877000 metric tons in 2013 to meet the increase in demand for magnesium[4].

Since the commercial exploitation of magnesium in 1886, it had found relevance in several industries. In the automobile industry, advanced materials have been used to replace

conventional steel parts to reduce fuel consumption and improve performance, magnesium based materials have been used in parts like gear box housing, fuel tank cover, seat frames and steering wheel by leading automobile makers and had led to significant weight reduction[5,6]. In aerospace industry, weight reduction is more crucial and several weight saving alternatives have been introduced, however, magnesium still possesses more advantage over other materials (high impact and good high temperature properties when compared to structural plastic and less expensive than metal fiber laminates) and has found extensive use in both military and civil aircrafts in parts which includes the thrust reversal, gearbox, engines and helicopter transmission casings[7,8]. In the electronic industries magnesium has potential in replacing plastics due to its greater strength improvement, heat transfer and ability to shield electromagnetic interference and radio frequency when compared to plastics[8], they are recently used in the housing of electronic gadgets. In recent years, there is an increasing interest in magnesium for biomedical applications due to its biodegradability, biocompatibility and similar mechanical properties to human cortical bone, magnesium-based material is a promising biocompatible implant material for load bearing application due to its light weight and high fracture toughness compared to hydroxyapatite[9–12]. The ability of magnesium-based alloys to store hydrogen up to 7.6wt% with good reversibility also makes it a potential material for hydrogen storage applications[13–16].

However, the wider application of magnesium has been limited due to some of its inherent properties which include low ductility, low toughness, high thermal expansion coefficient and high oxidation rate. The low formability of magnesium arises from its hexagonal crystal structure (HCP) which has limited available slip systems[17]. Plastic deformation

in magnesium materials is accommodated by twinning in addition to slip, the directional nature of twinning gives rise to a large difference in the yield behavior of magnesium in tension and compression resulting in large asymmetry between tensile and compressive yield stress of the material, this large asymmetry further limits the application of magnesium. Most of the identified problems with magnesium have been addressed by the development of new magnesium alloys; aluminum has been the primary alloying elements as it is found to increase the tensile strength through the formation of $Mg_{17}Al_{12}$ intermetallic phase, other elements such as rare earth metals like neodymium and yttrium also significantly improve the property of magnesium through precipitation hardening. In some application however, the property improvements obtained through alloying and precipitation hardening is not sufficient, this had led to the development of magnesium matrix composite where reinforcements such as whiskers, particulates and fibers are used to achieve improved property beyond alloying[18]. The most common type of reinforcements has been metals and ceramics, metallic oxides and carbon nanotubes have also provided improved strength and ductility [19–21]. The addition of micro-sized metallic and carbide ceramic reinforcements generally increases the strength of magnesium but deteriorates the intrinsically limited ductility of magnesium[22–24] while recent studies have shown that the addition of nano-sized reinforcement improves the strength without any adverse effect on its ductility [7,25,26].

The high potential of magnesium to meet the requirements of the continually increasing demand for lighter weight material will increase the need for magnesium based nanocomposite, hence this present work is focused on the development of a magnesium based composite with simultaneous improvement in strength and ductility. In this research

work, micron sized metallic nickel (Ni) particulates and nano sized titanium dioxide (TiO_2) have been uniformly distributed into magnesium matrix individually and combined (hybrid). The developed composites were characterized to determine the microstructural evolution and were subjected to hardness, tensile and compressive tests to determine the effect of the reinforcements on the mechanical properties of magnesium.

CHAPTER 2

LITERATURE REVIEW

2.1 Magnesium Based Composite and Nanocomposite

Magnesium based materials have promising properties which makes them excellent candidates in applications where light saving is crucial, they have high specific strength, high specific stiffness, good high temperature creep resistance and high damping capacity.

Magnesium based composites are a class of material with magnesium as the matrix and another material added as the reinforcing phase. The main aim of adding the reinforcement is to improve a certain or overall properties of magnesium, some of the properties improved with the addition of reinforcement include strength, hardness, stiffness, creep resistance and ductility, the final property of the composite can be controlled by judicial selection of the reinforcement and processing method. The choice of reinforcement is influenced by the desired application, processing route and cost, previous studies on magnesium based composites suggests that several micron size (size ranging from 1 to 100μm) particulate reinforcement which includes metals, oxides, carbides, borides, nitrides and metals have been added to magnesium to improve its mechanical properties due to their availability, competitive cost and well established processing route[27]. The addition of appropriate micron sized metallic reinforcement to magnesium had led to significant strength increment but with deteriorating effect on its limited ductility due to particle cracking and void formation at matrix-reinforcement interface[28], the quest for simultaneous

improvement in the strength and ductility of magnesium had led to the development of magnesium nanocomposites(MNC). Magnesium based nanocomposite is a composite in which the particle size of one or more of its constituent is less than 100nm[29], Recent studies on MNC have revealed that the incorporation of small volume fraction of nanosized particles led to simultaneous improvement in the strength and ductility of magnesium. Addition of more than one reinforcement (hybrid) at nano scale to magnesium had also been researched on by few researchers with the overall aim of achieving significant simultaneous improvement in strength and ductility[23,30–32]. The final properties of a composite material however depends largely on the processing route, type, size, shape, morphology and volume fraction of reinforcement, secondary processing and the heat treatment.

2.2 Types of Reinforcement.

Reinforcements are introduced intentionally into magnesium matrix to achieve the desired final property. The judicial selection of the right reinforcement is very crucial to improve the properties of the magnesium matrix in order to meet the desired application. Reinforcements can be generally classified based on their type, size, and shape. The type of reinforcement can be metallic or non-metals, the size of reinforcement can range from micron size to nanoscale, the shape of the reinforcement is also important as shapes with sharp edges such as angular particles can act as local stress raiser, thereby reducing the ductility of the composite. In reality, powder particles are not perfect and might show characteristics of more than one shape type. The shape index and aspect ratio is used to quantify the shape of powder particles, while the shape index relates the surface area of the particle to its volume, the aspect ratio is the ratio of the particles largest dimension to its

smallest dimension, a perfect sphere have an aspect ratio of 1 while a rough acicular shape can have aspect ratio ranging from 3 to 25.

The choice of reinforcement in a matrix composite depends majorly on the desired application, the manufacturing technique and cost. A composite for structural application requires high modulus and low density reinforcement, in bio-application, the biocompatibility and biodegradability of the reinforcement is crucial while the thermal conductivity and the thermal expansion coefficient are important in thermal management application.

A numbers of micron size particulate reinforcements which includes metals (Ti, Ni, Cu, Mo), nitrides (ZrN, BN, TiN, AlN), borides (ZrB_2, TiB_2), oxides (Al_2O_3, Y_2O_3, TiO_2) and carbides (SiC, ZrC, TiC, B_4C) [3,18,33–37] have been reportedly added to the magnesium and led to strength improvement but with deteriorating effect on its limited ductility. Recent studies however reveals that nano sized reinforcement improves the strength without adverse effect on the ductility, nanosized ceramic reinforcement is the most commonly used reinforcement in magnesium based nano composites, they range from carbide, borides, or oxides [19,21,38–47]. The use of hybrid reinforcement majorly consisting of a metal and ceramic reinforcement have recently been studied to further improve mechanical properties [31,32,45,48–53].

2.3 Processing Of Magnesium Based Composite

Magnesium based materials have been synthesized with several techniques over the years, the selection of synthesis technique is very essential as it affects the final microstructural features of the composite, materials with similar composition will yield different properties if synthesized with different technique. The processing techniques can be grouped into two major categories[54,55]:

1. Liquid/Melt Based Processing
2. Solid/Powder Based Processing

The solid phase processing has the advantage of the ability to incorporate any amount of reinforcement into the matrix and also eliminates undesirable reaction between reinforcement and matrix that can degrade the composite property.

2.3.1 Liquid/Melt Based Processing

Melt based processing involves the dispersion of the reinforcement into molten magnesium. The basic type is the stir casting where the reinforcement is stirred into the molten magnesium by mechanical means before the melt is cast into mold or die to produce the desired shape. The homogenous distribution of the reinforcement into the magnesium matrix is very crucial to avoid having a weaker region rich in reinforcement or matrix, as such stir casting have not been routinely used to produce nanoparticle reinforced magnesium due to the low wettability and high specific surface area of the nanoparticle in the molten metal which makes it more challenging to uniformly disperse nanoparticle in the melt.

Several advancements have been made to achieve uniform distribution and avoid agglomeration of the nanoparticle in the molten matrix. Lan et al [56] first fabricated a nano SiC reinforced magnesium composite by an innovative ultrasonic method, it involves the use of ultrasonic agitation to disperse the nanoparticle in the melt prior to casting; the ultrasonic cavitation in combination with local temperature exceeding 5000^{o}C can break apart the nanoparticles. Nanoparticle reinforcement dispersed in magnesium matrix using ultrasonic method resulted in composites with a well dispersed particle in the matrix but some clusters of particle were discovered in the microstructure, the composite generally show a significant increase in the strength and ductility relative to the monolithic magnesium [56–63].

Another method employs the atomization of the molten melt to ensure a relatively uniform distribution of the nanoparticles. One of such technique is the spray forming or spray atomization and deposition [3]. In this process, the melt is thoroughly mixed with the reinforcement prior to pouring. The molten stream is impacted and disintegrated by a highly energetic inert gas usually argon or water jets into fine droplets which are collected into a billet, when the droplets strikes the substrate, most of them are in the semi-solid state and a preform is formed with continuous deposition of the droplet. This process can be used to produce materials of various form reducing the need for secondary processing on the material. The composites from this method results in fine equiaxed grain structures due to the rapid cooling however, the lack of precise process control and the low process yield of this process has hindered the widespread use of spray casting.

Another technique that uses the atomization of molten melt is the disintegrated melt deposition (DMD) which combines the advantages of conventional casting method and

spray process. It is one of the most cost effective methods tested successfully to produce magnesium based composites. It has been widely used to produce magnesium based nanocomposites[17,20,38,40,41,46,49,51,52,61,63–72]. The nanoparticles are added into the molten magnesium matrix and superheated to 750^{o}C and stirred mechanically inside a graphite crucible under an inert atmosphere, the stirrer impeller is usually coated with a water based wash to prevent any possibility of contamination of the melt, the melt is then discharged through a orifice of about 10mm diameter located at the bottom of the chamber after which the melt is subsequently disintegrated by twin jets of Argon gas oriented normal to the stream. The disintegrated composite melt is subsequently deposited onto a metallic substrate to form a billet.

A new advancement of the disintegrated melt deposition called Mechanical Disintegration and Deposition (MDD) method have been developed to minimize the cost of the spray process while retaining the scientific advantage of the method. It involves the disintegration of the melt through mechanical means rather than the use of inert gas as in the disintegrated melt technique. Gupta et al[73] have successfully used this method to synthesize both reinforced and unreinforced magnesium based composite.

2.3.2 Solid / Powder Based Processing

The solid based processing route has been employed extensively in the production of magnesium based composites, it involves the synthesis of material below the melting temperature of the matrix, The powder metallurgy technique generally involves three basic primary processes: 1) the blending of magnesium powder and the reinforcement to achieve uniform dispersion of the reinforcement in the magnesium matrix, 2) the pressing/consolidation of the blended powder into billets (green compacts) and 3) the

sintering of the billet to achieve full densification. These primary processes have improved overtime with different innovation to achieve a better composite property at the end. The synthesized composite could be processed further with a secondary processing technique such as extrusion, rolling and forging to further reduce porosity and form it into the desired shape. The major advantage of this technique is the ability to incorporate any amount of reinforcement in the matrix allowing for the production of a combination of matrix and reinforcement which cannot be achieved through the liquid based processing technique.

i. Powder Mixing/Blending

The process of blending and/or mixing is very important in powder metallurgy as it establishes the initial homogeneity of the composite. Blending is a mechanical alloying process in which the powder particles are subjected to repeated cycles of cold welding, fracture and rewelding of the particles to achieve uniform size and shape distribution, blending can be carried out carried out on individual powder particles prior to mixing[69,74–78]. Mixing is the combination and homogeneous distribution of different material, it can be performed by several mechanical techniques which includes rotating containers such as drums or cones and different stirring mechanisms. Mixing can also be achieved with a ball milling machine without the use of milling media. The mechanism of mixing is such that the free fall and vibration of particles are avoided as they can lead to segregation of particles. The mixing time could range from minutes to days depending on several factors, the time should be sufficient enough to achieve to achieve the desired uniform distribution of particles and should not be longer than needed to avoid change in shape, size and work hardening of the powder particles [79].

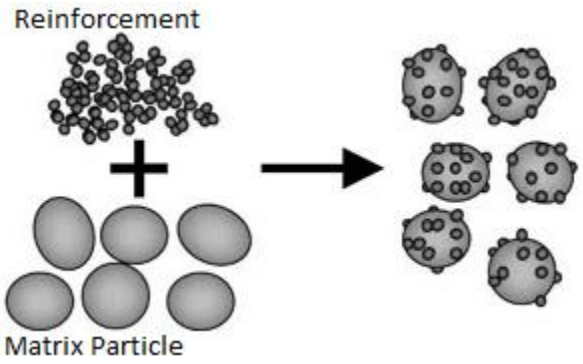

Figure 1: Mixing of Matrix and reinforcement [79]

ii. Compaction/Consolidation

Compaction involves the pressing of loosed powders either at room temperature or at elevated temperature to form a geometrical solid part called a green compact, the strength of the green compact is dependent on the compaction parameters (pressure and time) and powder characteristics, its geometry is similar to that of the final part prior to secondary processing, though some shrinkage might occur during sintering. The pressing force required depends on the powder types and the desired density, the force could be uniaxial or isostatic. In uniaxial pressing, the loosed blended powder is poured in the cavity of a die, and pressure is applied in a single direction with the die in direct contact with the powder while in isostatic pressing, a pressure barrier exist between the powder and the pressurizing medium and the pressure is applied from all direction. Lubrication is important during compaction and must be applied in correct quantities as excess lubrication can be collected in the space between particles and prevent proper compaction. Isostatic pressing have been employed to produce nanoparticle reinforced magnesium composite achieving near full densification [75,80], however a setback for the isostatic process is its higher

production cost and slower processing speed, hence uniaxial pressing is commonly employed.

In the initial stage of powder compaction, the density of the powder is increased due to the rearrangement of each powder particles, a more efficient packing of the particles lead to the elimination of gaps, pores and spaces between particles, at this stage, the resistance of the powders to the applied pressure is relatively lower, density increases rapidly applied pressure and the contact points between the particles are well established. As compaction continues, the force between the contact points is increased and a type of bonding called the cold pressure welding occurs at these points between the particles, this gives the green compacts the required structural integrity for further processing. As the compaction pressure increases, the resistance to material movement is increased by friction and work hardening of the powder, there is an increase in stress between the contact points and leads to material deformation, plastic flow and interlocking of particles occur, the volume decrease and density increases continually but a lower rate compare to the initial stage until the maximum density (the green density) is attained. Figure 2 shows the typical relationship between the compacting pressure and green density indicating how the rate of increase in density drops off between the initial stage of particle repacking and the later stage of plastic deformation.

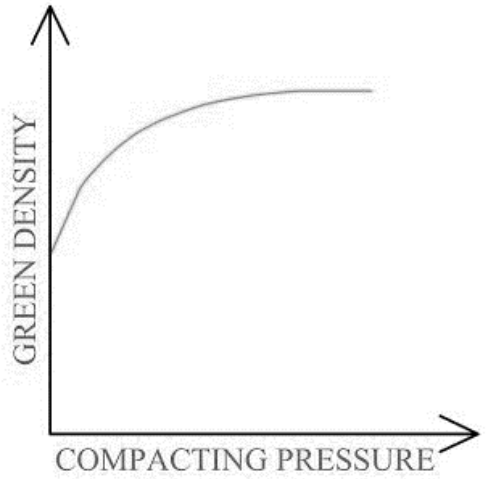

Figure 2: Relationship between green density and compacting pressure [81]

iii. Sintering

Sintering is an essential process in powder metallurgy; it involves the heating of the green compacts to a temperature below the melting point usually until the particles merge and the compact solid becomes denser, the sintering temperature is usually between 70 to 90 percent of the melting temperature of the matrix, this will initial bonding between the pressed particles and greatly enhance the strength. During sintering, the initial structure of each individual particle disappear and the material forms a whole mass, the porosity and volume is further reduced, all added addictive such as lubricants and binders are also burnt off during sintering to maintain the material purity in the final form, shrinkage occurs during sintering and should be accounted for earlier. Sintering is very important in powder metallurgy process as it increases the density, strength, ductility, thermal and electrical conductivity of the final product.

Diffusion is considered to be the main mechanism of bonding during sintering, other bonding mechanism that may occur includes plastic flow, grain growth, recrystallization and phase material transport depending on the process parameters and powder properties.

While diffusion mechanism reduces the distance between two particles, the phase material transport adds material to the space while maintaining the inter-particle distance as illustrated in Figure 3 where D1 is the initial inter-particle distance and D2 and D3 are the distances as a result of diffusion and phase material transport respectively.

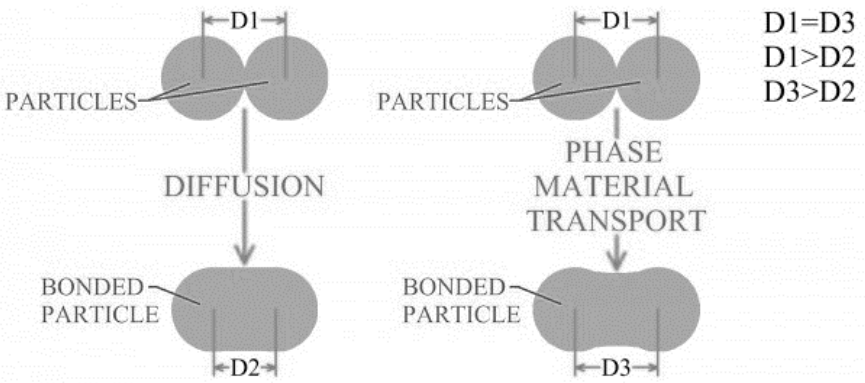

Figure 3: Bonding Mechanism in powder sintering [81]

The main sintering process parameters are time, temperature and furnace atmosphere, the heating and cooling rate is also important. The temperature of sintering is usually between 70 to 90% of the matrix melting temperature, the sintering time is dependent on the material and should be long enough to allow complete bonding of particles and the furnace atmosphere should be controlled to avoid oxidation.

Conventional sintering is most commonly used to sinter magnesium nanocomposites; it involves the heating of the green compacts at moderate temperature (400-500^{o}C) in an inert atmosphere, the sample is heated from the outside and the thermal energy is transferred towards the inner part through convection, conduction and radiation of the heat. Due to this, the temperature at the outer part of the sample is usually higher than the temperature of the inner core of the material which could lead to relatively poor microstructural

characteristics of the core. Accordingly, it is advisable to sinter for an extended period to allow for uniform distribution of heat within the material.

Microwave sintering is an alternative to conventional sintering. In microwave heating, heat is generated from the inner core of the material and radiated outward to the outer surface due to the penetrative power of microwaves. This also leads to higher temperature at the core compared to the outer surface which could lead to a relatively poor microstructure of the outer surface of the material.

With the aim of gaining the advantage of both types of sintering, the hybrid microwave sintering was developed and had been used extensively to produce magnesium nanocomposite [44,51,62,82–87]. It involves the introduction of a heating susceptor such as SiC particles or rod to assist in the reduction of the thermal gradient during sintering of the material. Enhanced property, reduction in sintering time and significant energy savings have been achieved with the use of hybrid microwave sintering.

Another mode of sintering is the spark plasma sintering (SPS) or pulsed electric current sintering (PECS); this method involves the simultaneous compaction and sintering of the powder material. It utilizes uniaxial directional force and a pulsed direct electric current in a low atmospheric pressure environment to perform high speed consolidation of the powder. It has the advantage of high sintering speed and high reproducibility. It is referred to as a rapid sintering method. J.Liu et al [88] recently synthesized SiC nanoparticle reinforce magnesium with significant improvement in yield strength and detainment of the malleability of magnesium using the SPS technique.

2.4 Microstructure of magnesium based composites

The study of the microstructure of particle reinforced magnesium composite is very important as it reveals important information related to the properties of the composite. It is also important to study the distribution of reinforcement in the matrix and the interfacial characteristics between them. Optical microscopy, Scanning electron microscopy and X-ray diffraction techniques are the most common techniques used to investigate the microstructural analysis of magnesium based composites. Grain refinement, interfacial characteristics, reinforcement distribution and crystallographic texturing are important microstructural features of magnesium based composites that need to be investigated.

2.4.1 Grain refinement of magnesium matrix

Generally, examination of the microstructure of the reinforced magnesium composite indicates a typically refined equiaxed grains compare to the monolithic magnesium. The reduction in grain size of the composite have been largely attributed to the ability of the reinforcement particle to act as nucleation site for magnesium grains during recrystallization and the pinning effect of the reinforcement on the grain boundaries to restrict the amount of grain growth occurring during recrystallization.

The degree of grain refinement depends on the processing technique and parameters, type and amount of reinforcement added.

i. Effect of processing technique and parameters on grain refinement

The processing technique plays an important role in the degree of grain refinement as evident from several research works. A study by Hassan and Gupta on 50nm sized Al_2O_3 reinforced Magnesium produced by the powder based technique of BPS and the melt based

technique of Disintegrated Melt Deposition (DMD), it was observed that, for the composite produced by the BPS method, the grain size was reduced from 60 to 31μm while the grain size dropped significantly from 49 to 14μm for the same amount of 1.1vol % of Al_2O_3 in the composite produced by the DMD technique [20]. In another research work by Hassan and Gupta on nano Y_2O_3 reinforced magnesium synthesized by both BPS and DMD method, comparing the same volume percent of 0.7% Y_2O_3, the DMD composite clearly showed a reduced grain size from 49 to 6μm compare to the BPS composite that have grain size of approximately 15μm for the reinforced composite and 60μm for monolithic magnesium [42]. The superior grain refinement observed in the material processed with the DMD technique was ascribed to the joined impact of the presence of high amount of uniformly distributed nano-Al_2O_3 reinforcement which can act as nuclei for recrystallization and also restrict further growth of new grain during solidification and the vigorous stirring of the melt before its disintegration and subsequent deposition at high temperature. Other research works have also show that the DMD technique is more effective in grain refinement compared to the BPS technique.

Several processing parameter also affects the degree of grain refinement. Research work by Hassan and Gupta on the effect of extrusion ratio on the microstructure of nano-Y_2O_3 reinforced magnesium showed that an increase in the extrusion ratio leads to higher degree of grain refinement, in this research, magnesium nanocomposite containing 0.7 vol% of Y_2O_3 powder were synthesized by powder metallurgy technique using hybrid microwave sintering technique. The sintered billets were extruded at 350^oC using three different extrusion ratios of 12:1, 19:1, and 25:1. Microstructural examination reveals a decrease in grain size as the extrusion ration is increased. also the distribution of the grain size also

becomes more homogenous, this was attributed to the increase in the level of deformation while the increase in homogeneity of the microstructure was attributed to the limited thermal exposure of the grains following recrystallization which inhibits the tendency of abnormal grain growth [87].

Another research work by K.B. Nie et al [89] on the effect of extrusion temperature on the microstructure of nano SiC reinforced magnesium AZ91 alloy revealed that the grain size of the matrix decrease with increasing extrusion temperature, in this research work, the scale of grain size distribution is also reduced indicating that full dynamic recrystallization (DRX) occurred during the extrusion. Microstructural analysis also reveals the presence of two separate zones in the extruded sample, one zone contains bands of nano SiC particle that are parallel to the extrusion direction while the other zone consist of refined-grain found in between the bands of nano SiC particle, as shown in Figure 4. A decrease in the amount of SiC band was also observed as the extrusion temperature is increased. The magnesium matrix can easily flow into the SiC nanoparticles at higher temperature because it has a higher flow velocity than the SiC reinforcement; this led to an improved distribution of the reinforcement and an increase in the amount of dispersed nano SiC particles as the extrusion temperature is increased. The dispersed SiC particles can introduce larger strain in the magnesium matrix that can lead to severer dynamic recrystallization and also inhibit further grain growth of recrystallized grains, this led to the gradual refinement of the grains of matrix in the reinforced nanocomposites.

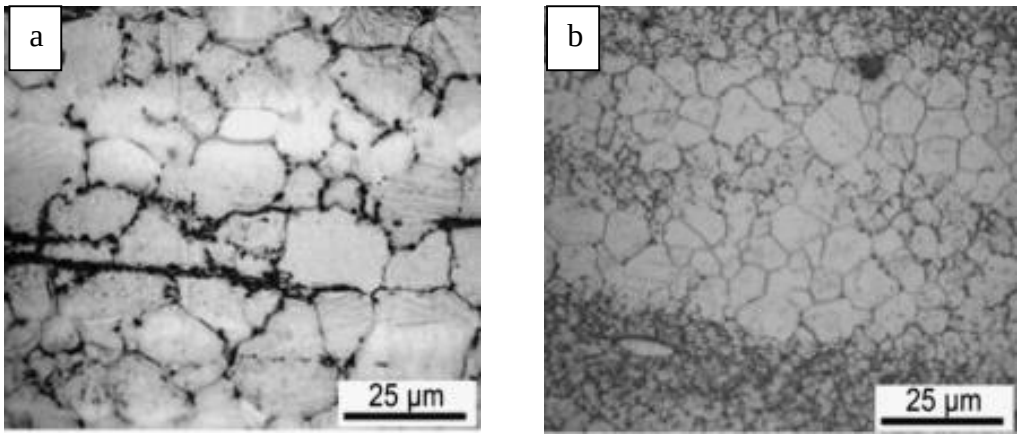

Figure 4: Optical microscopy micrographs of Mg/SiC nanocomposites extruded at (a) 250 °C; and (b) 350 °C adapted from ref. [89]

The effect of sintering technique employed in the BPS technique was also studied by Hassan et al on nano-Y_2O_3 reinforced magnesium, In their study, they utilized two types of sintering technique: the conventional heating technique and the microwave assisted rapid sintering technique to sinter the monolithic and reinforced nanocomposites followed by hot extrusion of the samples, the conventional sintering technique was carried out in a tube furnace under inert atmosphere at 500^oC for 120mins while the microwave sintered sample was heated to a temperature close to the melting point of the matrix for 13mins, extrusion of the sintered billets was carried out at 350 °C with an extrusion ratio of 25:1. Microstructural examination of all the samples revealed minimal porosity and fairly uniform distribution of Y_2O_3 in the Mg matrix. Significant grain refinement was observed in the case of conventionally sintered samples and was attributed to the long sintering duration at high temperature enabling the complete recrystallization of the reinforced nanocomposites [90].

Effect of ball milling prior to the DMD technique was studied by Sankaranarayanan et al [49] on hybrid (5.6Ti and 2.5n-Al_2O_3) reinforced magnesium, the effect of pre synthesizing

the reinforcement prior to their addition to magnesium was studied, microstructural examination reveals that ball milling the particles prior to their addition is very effective in achieving uniform distribution of reinforcement and high degree of grain refinement, this is attributed to the ability of smaller particles due to the ball milling to provide more active site for magnesium nucleation.

Multidirectional forging have also been found to drastically reduce grain size of magnesium grains as evident in the work of Nie et al and Xia et al [91,92]

ii. Effect of amount and type of reinforcement on grain refinement.

Studies have shown that the addition of size reinforcement up to a certain amount will achieve some degree of grain refinement, experimental results reveals that the effectiveness of the reinforcement to achieve grain refinement varies from one reinforcement to another. For a particular reinforcement, the degree of grain refinement seemingly depends on the amount of reinforcement added. Studies have shown that for a particular reinforcement and a particular processing technique, a certain amount of the reinforcement will be needed to achieve significant reduction in grain size.

In the study of nano reinforced Al_2O_3, Hassan et all developed 0.2, 0.66 and 1.11 vol % of Al_2O_3 reinforced magnesium using the BPS technique followed by hot extrusion, it was observed that a significant grain reduction was not observed until the addition of approximately 1.1 volume % Al_2O_3 for the composite, this was attributed to the fact that the restriction of grain growth could have been favored by the presence of high volume fraction of nano-Al_2O_3 particles [93].

Another study on nano Y_2O_3 content of 0.2, 0.66 and 1.11 vol % in magnesium composite synthesized by the DMD technique followed by hot extrusion by S.F Hassan revealed that grain refinement of magnesium matrix is enhanced up to the addition of 0.66-vol% of nano-Y_2O_3 reinforcement, beyond which the possibility of nano size particulate clustering is high and would halt further grain refinement. [94].

Meenashisundaram et al [38]synthesized nano TiO_2 reinforced magnesium with 0.58, 0.97, 1.98 and 2.5 vol% titania using the DMD technique followed by hot extrusion, microstructural analysis reveals an inverse relationship between the amount of reinforcement and the grain size, the grain size reduced from 45μm for pure magnesium to 21μm for 2.5vol% magnesium.

Sankaranarayanan et al [17] studied the effect of addition of nano sized boron carbide on the microstructure of pure magnesium, in his work, pure Mg-metal reinforced with 0.35, 1.04 and 1.74 vol% nano-size B_4C particulates were synthesized using the DMD technique followed by hot extrusion. Microstructural examination indicates a good interfacial integrity attributed to the good wettability between magnesium and boron carbide promoted by the presence of impurities as found by Zhang et all [95] that the presence of impurity promotes the wettability between magnesium and boron carbide. Significant grain refinement was also observed with the addition of boron carbide as the grain size decreased form 28μm for pure Mg to 11μm for 1.74 vol% B_4C addition.

Limited study on the effect of hybrid reinforcement on the grain morphology of magnesium is available in open literature, a study by K.S Tun et al on the effect of hybrid reinforcement of Cu and Al_2O_3 reveals significant grain refinement due to the combined effect of Cu and Al_2O_3 when compared to their individual effect, grain size was reduced from 21μm to 7 μm

for composite containing 1vol% Al_2O_3 and 0.9 vol% Cu as shown in Figure 5, effectiveness of Cu in grain refinement is attributed to the cumulative effect of Mg_2Cu intermetallic formed at the boundary in assisting grain recrystallization[48].

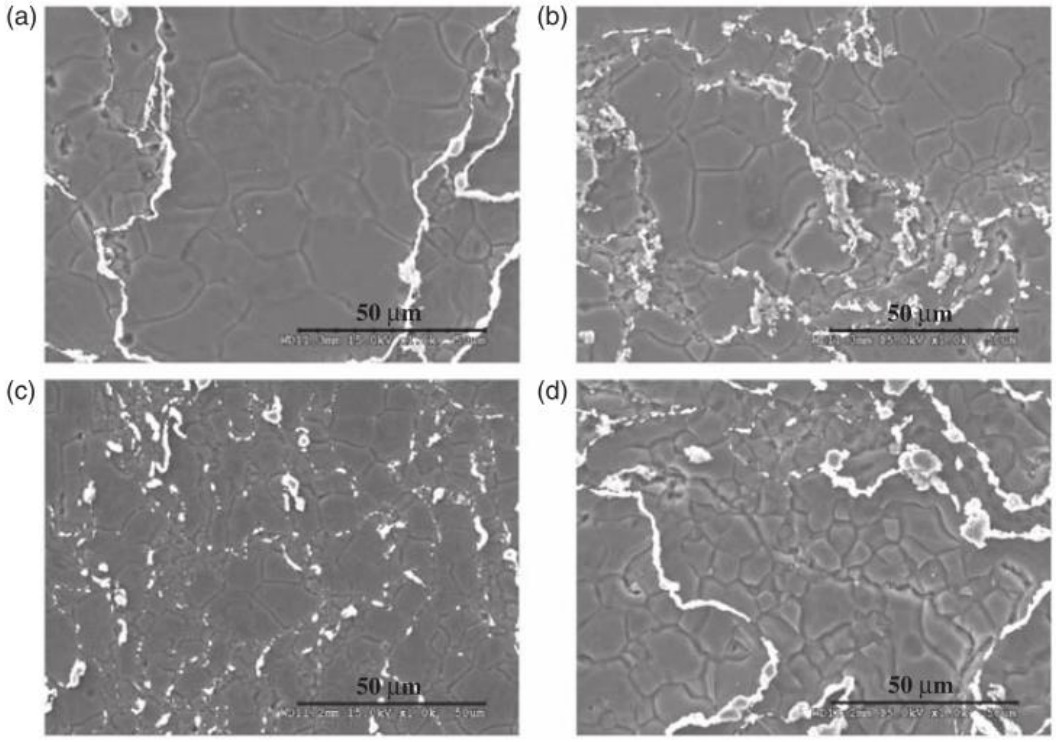

Figure 5: Optical micrographs showing the grain morphology of (a) Mg/(1 vol Al2O3&0.1 vol Cu), (b) Mg/(1 vol Al2O3&0.3 vol Cu), (c) Mg/(1 vol Al2O3&0.6 vol Cu), and (d) Mg/(1 vol Al2O3&0.9 vol Cu) nanocomposites. Adapted from ref. [48]

2.5 Mechanical Properties of Magnesium Based Composites

2.5.1. Hardness

The hardness of a material quantifies its resistance to plastic deformation, it is not a fundamental property of the material and only represents an arbitrary value used to provide a relative idea of material properties[96], it is divided into two classes: the micro hardness and macro hardness, micro hardness test uses forces typically less than 2N. Addition of harder and stronger reinforcement to magnesium had led to an increase in the hardness of

the magnesium matrix. The increase in hardness is attributed to three main reasons: a) the increase in dislocation density due to mismatch of CTE and elastic modulus between reinforcement and matrix b) reduction in grain size as seen earlier under grain refinement section and c) the presence of harder metallic or ceramic particles as reinforcement acting as a local constrain to matrix deformation.

2.5.2. Tensile Properties

One of the major attractions of composite materials is the improvement in tensile properties such as yield Strength, ultimate tensile strength and ductility. Incorporation of harder and stiffer reinforcement particle into the matrix of magnesium had led to an improved mechanical property relative to pure magnesium. In many of the research papers available, a sizeable increase in the strength of magnesium have been shown due to addition of micron sized metallic reinforcement while an improvement in ductility of magnesium have been observed due to the addition of metallic oxide nanoparticles and ceramics in general. The tensile property of magnesium nanocomposite also greatly depends on the processing method and type of reinforcement. The explanations for the observed improvement in these properties due to the addition of particulate reinforcement and processing methods are summarized here.

i. Tensile Strength:

The improvements in strength observed in nanoparticle reinforced magnesium have been attributed to four potential strengthening mechanisms:

- *Hall-Petch effect:* Dislocation pile up at grain boundary is increased due to finer grain size induced in the matrix by the addition of nanoparticles, the effect of grain

size on the strength of the material is commonly predicted using equation 1[97,98] :

$$\sigma_y = \sigma_o + K_y d^{-1/2} \quad \textbf{(1)}$$

where σ_0 is the original strength of the material (MPa), K*y* is a constant (MPa √ m) depending on the material, and *d* is the grain size (m) of the material. The grain size of the matrix in nanoparticle reinforced composite depends on the particle size and volume fraction of the particle, this relationship has been expressed by the Zener equation [66] :

$$d_m = \frac{4\alpha d_p}{3V_p} \quad \textbf{(2)}$$

where α is a proportionality constant, dp is the particle size, and Vp is the particle volume.

- *Orowan Strengthening:* the impeding of dislocation motion by the nanoparticles. The mismatch in the coefficient of thermal expansion between the reinforcement and the matrix will result in the geometrically necessary dislocation around each particles which results in high work hardening rate and strengthening of the nanocomposite. The Orowan effect in strengthening of magnesium based nanocomposite is predicted by equation (3) [99–101]:

$$\sigma_{orowan} = \frac{0.13 G_m b}{d_p\left[\left(\frac{1}{2V_p}\right)^{\frac{1}{3}} - 1\right]} \ln\left(\frac{d_p}{2b}\right) \quad \textbf{(3)}$$

where d_p is the particle diameter (m), G_m is the matrix shear modulus (Pa), *b* is the Burger's vector (m), and V_p is the volume fraction of the particles

- *CTE and EM Mismatch:* Thermally induced residual stress due to difference in coefficient of thermal expansion (CTE) and elastic modulus (EM) between the nanoparticle and the magnesium matrix is accommodated through the formation of geometrically necessary dislocations (GNDs). The combined effect of CTE and EM mismatch on the strengthening of the matrix can be estimated with the Taylor's equation [102]:

$$\Delta\sigma_{CTE+EM} = \sqrt{3}\beta Gb(\sqrt{\rho^{CTE}} + \sqrt{\rho^{EM}}) \quad \textbf{(4)}$$

where β is a constant, ρ^{CTE} and ρ^{EM} are the density of the geometrically necessary dislocations due to CTE and EM mismatch respectively and are estimated by the following expressions [103]:

$$\rho^{CTE} = \frac{A\Delta\propto\Delta T v_p}{b b_d (1-v_p)} \quad \textbf{(5)}$$

$$\rho^{EM} = \frac{6v_p}{\pi {d_p}^3}\varepsilon \quad \textbf{(6)}$$

where A is a geometric constant, $\Delta\propto$ is the difference in CTE and ΔT is the difference between test and processing temperature.

- *Load Transfer Effect:* Transfer of load by shearing from the softer Mg matrix to the stiffer and harder reinforcement contributes to strengthening of the matrix material. In particulate reinforced composite, a modified shear lag model proposed by Nardone and Prewo is commonly used to predict the contribution due to load transfer to the strengthening of the matrix[104,105]

$$\Delta\sigma_l = V_p\sigma_m[\frac{(l+t)A}{4l}] \quad \textbf{(7)}$$

where V_p is the volume fraction of particles in the matrix, σ_m is the yield strength of the matrix, l is the size of the particulate parallel to the load direction, t is the thickness of the particulate, and $A = l/t$ is the particulate aspect ratio. In the case of equiaxed particle, the equation is reduced to [63,101,106] :

$$\Delta\sigma_l = \frac{1}{2} V_p \sigma_m \qquad \textbf{(8)}$$

ii. Ductility:

Improvements in the ductility of magnesium have been reported by many researchers when reinforced with nanosized particles. In contrast to the case of other metal matrices that are ductile, addition of hard nanoparticles to magnesium have been found to play a beneficial role in brittle HCP matrix, this have been attributed to the coupled effect of grain refinement, reasonable uniform distribution of reinforcement and slip on extra non basal slip system activated as a result of nano particle addition. Uniformly dispersed nanoparticle in magnesium matrix acts to provide sites where cleavage crack may open in front of advancing crack to dissipate stress concentration at or near crack front; the dissipation also effect a change in stress state from plain strain to plain stress near the crack tip. XRD analysis has also shown that the addition of nanoparticle to magnesium activates non basal slip system and they become more active during tensile loading.

i. Effect of processing method and reinforcement type on Tensile Properties

The degree of improvement in tensile properties has been shown to greatly depend on the type of reinforcement and processing technique employed. The overall effect of processing techniques and type of reinforcement on the tensile properties of developed magnesium based composite is shown in Figure 6 as adapted from reference [47].

SF Hassan and M Gupta[20] studied the effect of type of primary processing on magnesium based composites containing 2.5 wt.% of nano-sized Al_2O_3 (50 nm) particulates. Two different processing techniques of disintegrated melt deposition (DMD) of ingot processing and blend-press-sinter (BPS) of powder metallurgy were used to synthesize the magnesium nanocomposites followed by hot extrusion. Mechanical property characterization revealed an increase in hardness, elastic modulus, 0.2% yield strength, ultimate tensile strength and the fracture strain of magnesium matrix due to the addition of nano-Al_2O_3 particulates. The sample developed with the ingot metallurgy technique exhibits superior ductility and modulus while superior yield strength and ultimate tensile strength was observed in the sample processed by the powder metallurgy technique. Significant increase in yield stress and marginal increase in UTS for powder metallurgy processed composite over the DMD processed composite might be due to the presence of oxide in the initial matrix particulates while the finer grains achieved in the DMD material might be responsible for the additional increase in ductility over the PM processed material.

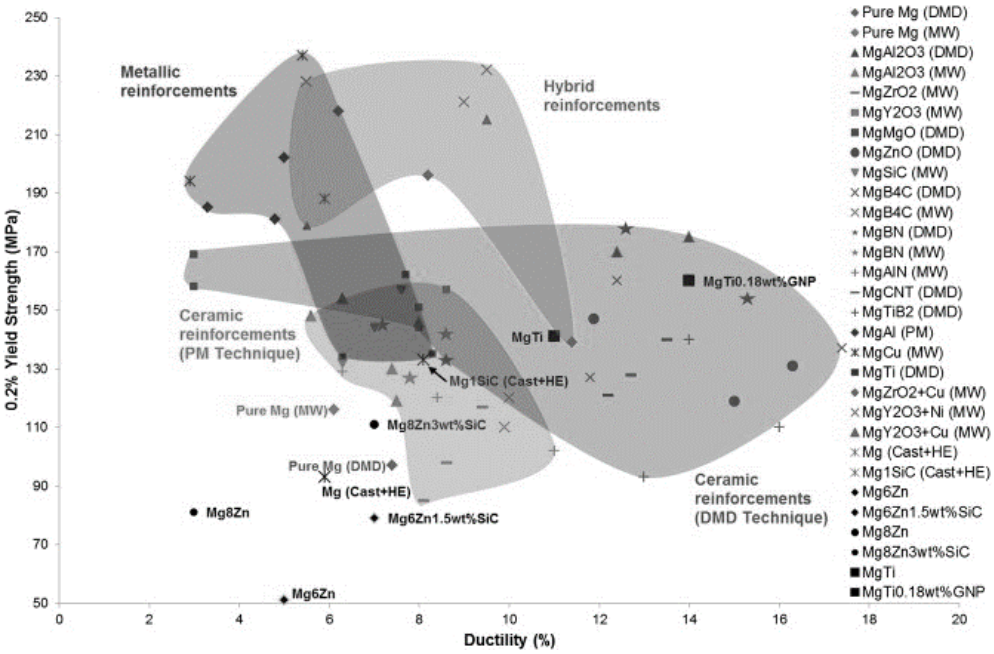

Figure 6: Bubble chart illustrating the improvement in 0.2% yield strength and ductility for magnesium nanocomposites adapted from reference [47]

In another research work by SF Hassan [42]**,** nanocomposite reinforced with nano sized Y_2O_3 was also synthesized by both DMD and BPS technique, the BPS synthesized nanocomposite achieved up to 18% increase in 0.2%YS and 9% increase in UTS while the DMD synthesized nanocomposite improvement was more pronounce, showing up to 222% increase in 0.2%YS and 84% increase in UTS compare to the monolithic magnesium, however the BPS synthesized composite showed a more improvement in ductility up to 276% in 0.2vol% Y2O3 while the improvement was 72% for the DMD produced composite. The disintegrated melt deposition process was more effective in the exploring the strengthening effect of Y_2O_3, hence, the DMD processed composites showed superior 0.2%YS and UTS when compared to the samples processed with the powder metallurgy technique of blend-press-sinter. The DMD technique is found to be relatively more effective in exploring the contribution of nano reinforcement to grain refinement and

the improvement in the mechanical properties of magnesium while the PM processing technique is more effective in exploring the contribution of nano reinforcement in improving the formability and resistance of magnesium to fracture.

A study by K.B Nie t al [89] on the effect of extrusion temperature on 1vol% SiC reinforced magnesium AZ91 alloy, in their study, the nanocomposite was developed by a semisolid method where the stirring was assisted by ultrasonic vibration and then subjected to extrusion at different temperatures of 250, 300 and 350^{o}C, Tensile property characterization reveals and increase in the yield strength, ultimate tensile strength and ductility of the nanocomposites as the extrusion temperature is increased indicating the usefulness of high extrusion temperature in enhancing the mechanical properties of the magnesium.

Hassan and Gupta [87] synthesized magnesium nanocomposite by adding 0.7 vol.% of nano yttria powder by the powder metallurgy technique using hybrid microwave sintering technique to study the effect of extrusion ratio on the mechanical properties of magnesium. The sintered billets were extruded at 350^{o}C using three different extrusion ratios of 12:1, 19:1, and 25:1. Results of tensile test reveals a corresponding increment in the yield stress and ultimate tensile stress with the increase in extrusion ratio while the maximum fracture strain was observed at an extrusion ratio of 19.1 for both pure and reinforced magnesium. The increase in 0.2%YS and UTS is attributed to the reduction in matrix grain size and the decrease in amount of porosity with increasing extrusion ratio.

The effect of sintering technique employed during powder metallurgy was studied by Hassan et al [90] on nano-Y_2O_3 reinforced magnesium, 0.2 and 0.7 vol.% Y_2O_3 reinforced Mg were synthesized by the powder metallurgy technique of blend-press-sinter followed

by hot extrusion, result of tensile test results revealed a marginal increase in the strength values of microwave assisted rapid sintered nanocomposite materials compared to those processed using conventional slow heating sintering, while the ductility of the nanocomposites sintered using conventional slow heating method was significantly superior. The tensile result reveals that the 0.2%YS value increases with increasing Y_2O_3 content in the case of microwave assisted rapid sintering while the value reaches its peak at 0.2vol% Y_2O_3 content for the conventional slow heating sintering method. The results obtained translates that rapid microwave sintering technique is more effective for strength based designs while the conventional sintering technique is more effective for damage tolerant designs. KS Tun and Gupta [83] also studied the effect of heating rate during hybrid microwave sintering of nano Y_2O_3 reinforced magnesium composite, heating rates of 49 and 20^oC were used and tensile tests reveals an increase in strength and reduction in ductility at higher heating rate.

2.5.3. Compressive Properties

Not much work have been done to investigate to compressive properties of magnesium reinforced composites, In all the papers reviewed here [30,38,46,67,107–110], nano reinforced magnesium composites shows an improved mechanical properties compared to the pure magnesium composites. The mechanism for improved compressive properties in reinforced magnesium is the same as the mechanism for improved tensile properties, however, the formation of twins during compressive deformation can also play an important role in the observed property improvement, the formed twins during compressive deformation act similar to grain boundary by impeding the movement of dislocation. Also,

the transformation of the dislocation as they pass across the twining boundary can result in an increased hardening rate within the twin.

Qizhen Li and Bing Tian synthesized carbon nanotube reinforced magnesium with 0.05%, 0.2%, 0.5%, 1.2% and 5% CNT and tested them compressively along the normal and in-plane orientation. Results reveals that the yield strength was higher for the plain normal direction than for the in plain orientation for all composites synthesized, however the maximum yield strength of 125.9MPa corresponding to a 129vol% increment was achieved for 0.5% CNT reinforced composite, the drop in yield strength after 0.5% CNT was attributed to the agglomeration of the CNT reinforcements at higher volume % [110]

Nguyen and Gupta investigated the influence of 50nm sized alumina on the compressive properties of magnesium AZ31B alloy synthesized by the DMD process followed by hot extrusion. Experimental results reveals a 32% increase in compressive yield strength, 10% increase in ultimate strength and 13% increase in failure strain for 1.5 vol% Alumina [108]. Another research work by Meenashisundaram eta al on TiB_2 reinforced magnesium reveals similar trend in improvement in compressive properties, a 47% increment in CYS and 10%increment in UCS was reported while the fracture strain did not significantly [46].

Recently, Meenashisundaram et al developed a TiO_2 reinforced magnesium targeting biomedical applications, the compressive examination reveals a significant increase in the CYS up to 85% with the addition of 2.5vol% TiO_2 and up to 30% increase I the fracture strain, however, the compressive ultimate strength was found to decrease by approximately 7.5% [38]

Effect of hybrid reinforcement of Cu and Y_2O_3 on the compressive strength of magnesium reveals an increase in the 0.2 compressive yield stress and ultimate compressive strength with increase in the volume percent of copper of while the ductility was adversely affected, increase in strength was attributed to the change in crystallographic texture and the ability of the secondary phase to restrict dislocation motion leading to high yield strength and to further resist plastic flow leading to high ultimate strength while the reduction in ductility was attributed to limited slip system in the composite compared to the monolithic material with more twin formation.

2.6 Summary

Based on reports available in open literature, it was observed that magnesium based composites are fabricated from two major techniques of powder metallurgy and melt based technique. The addition of reinforcements had also led to significant improvement in hardness, tensile strength and ductility of magnesium matrix. Micro sized metallic reinforcements generally increase the strength with adverse effect on ductility of the magnesium matrix, this had led to the development of nano sized particle reinforced magnesium composites in order to achieve simultaneous increase in strength and ductility. Addition of nano sized reinforcement had been found to increases the strength without adverse effect on ductility however, the strength improvement still fall short of that due to micron size reinforcement. This led to the development of hybrid composite to take advantage of both type of reinforcements to achieve the desired simultaneous improvement in strength and ductility, a number of researchers [23,30–32,48–50,52,71,104,111] have attempted to combine metallic and ceramic reinforcement to magnesium both at nano scale, however only few [48,50,51,71,111] had attempted to study the combined effect of micro sized metal reinforcement and nanoscale ceramic reinforcement and none have hybridized the effect of micron sized nickel with nano metallic oxide reinforcement despite the great potential shown by elemental micron sized nickel to effectively reduce grain size and significantly increase the strength of magnesium [36,112,113] and only one research work [38] was carried out on the effect of TiO_2 reinforcement on magnesium matrix using a melt based processing technique. Accordingly, in the present study, attempt is made to develop a magnesium based composite by the economical powder metallurgy technique of blend-press-sinter using micron sized elemental nickel as the metallic reinforcement and nano sized TiO_2 as ceramic

reinforcement individually and their combination to create a hybrid reinforcement. The effect of the individual and combined effect of the reinforcements on the microstructure and mechanical properties of the magnesium matrix have been investigated.

CHAPTER 3

MATERIALS AND EXPERIMENTAL PROCEDURE

3.1 Raw Materials

In the present study, commercially pure magnesium powder with <0.1mm average size and 97.5+% purity was used as the base material while elemental nickel particles with average particle size of 10 μm and of 99+% purity and titanium dioxide particles with average particle size of 32nm were used as the reinforcement phases. Both magnesium and nickel metal powder were manufactured by Merck KGaA, Germany while the titanium dioxide powder was manufactured by NanoTek Company, USA.

3.2 Material Processing

Conventional powder metallurgy process route of blend-press-sinter followed by hot extrusion was used for the processing of all the reinforced composites and monolithic magnesium.

3.2.1 Blending

Calculated amount of magnesium particles and the desired amount of reinforcement required to produce a billet of 35mm diameter and 40mm height were blended together at a speed of 200 rpm for 1hr to obtain homogeneity using Fritsch Pulverisette 5 planetary ball milling machine. No balls or process control agent was used during the blending step. Amount of nickel added was equivalent to 1.5 volume percent (Mg-1.50Ni) while amount of TiO_2 equivalent to 0.33, 0.66 and 1.00 volume percentages

was used in this study to produce samples labelled as Mg-0.33TiO_2, Mg-0.66TiO_2 and Mg-1.00TiO_2 respectively. The volume percent with best combination of mechanical properties was used with the nickel reinforcement to produce the hybrid nanocomposite labelled as Mg-1.50Ni-0.33TiO_2.

3.2.2 Powder Compaction/Consolidation

The blended powder mixture was cold compacted using 150Ton uniaxial hydraulic press. The loose powder was poured into the die cavity and pressure equivalent to 570MPa was applied in a single direction and held for 1min to form billets of 35-mm diameter and 40-mm height. The compacted billet is subsequently removed from the die. The schematic process of powder consolidation is shown schematically in Figure 7.

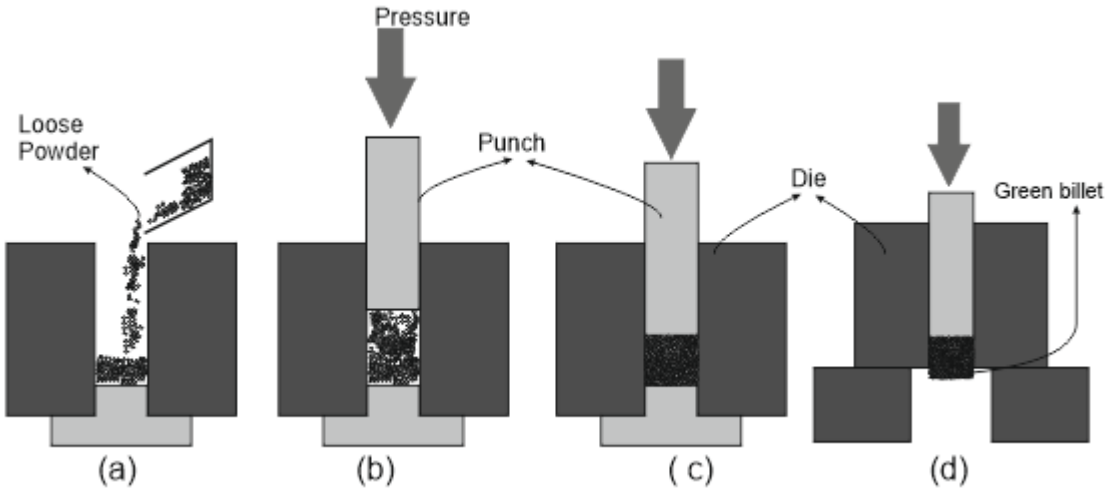

Figure 7: Schematic diagrams showing the powder consolidation steps. a) loose particles are filled into the die cavity b) & c) Pressure is applied uniaxially d) removing the green billet from the die

3.2.3 Sintering

Sintering of the green compacts was carried out in a tube furnace (model: MTI GSL-1700X, MTI corporation, USA) shown in Figure 8. The samples were heated at a heating rate of 10^{o}C/min up to 500°C and held for 2-hours under argon atmosphere. The compacted billets were coated with colloidal graphite and wrapped with aluminum foil to prevent any possible oxidation.

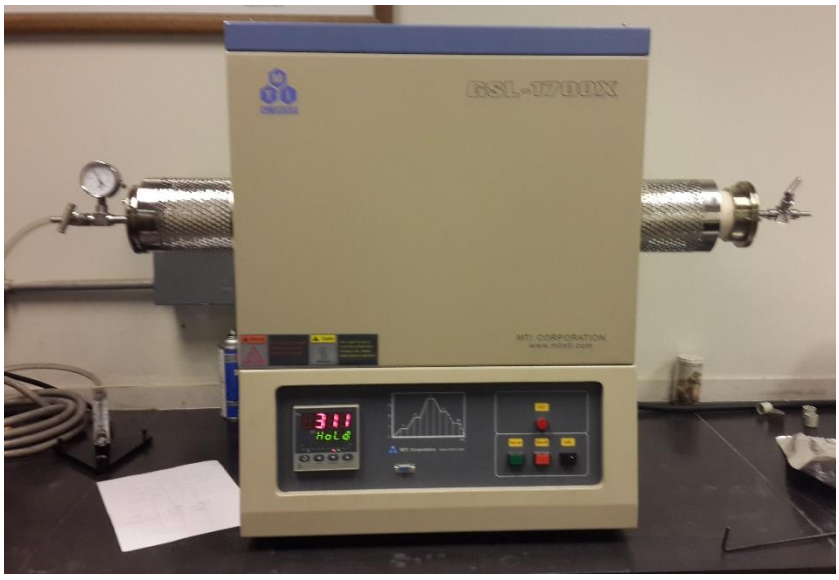

Figure 8: Photograph of tube furnace used for sintering

3.2.4 Extrusion

The sintered reinforced magnesium composites and monolithic magnesium billets were hot extruded using an extrusion ratio of 19.14: 1 to obtain rods of 8 mm diameter using a 150 ton hydraulic press. Extrusion was carried out at 250°C. The billets were held at 300°C for 1hr in a constant temperature furnace before extrusion. Colloidal graphite was used as lubricant.

3.2.5 Density Measurement

Density (ρ) measurements were performed on polished extruded samples of reinforced magnesium composites and monolithic magnesium in accordance with Archimedes' principle[113] using a Mettler Toledo model AG285 Electronic balance, with an accuracy of ±0.0001 g. The process involves carefully weighing the samples in air and in liquid (distilled water was used for this experiment). Equation 9 was then used to calculate the experimental density of the sample.

$$\rho_o = \left(\frac{\mathrm{A}}{\mathrm{A-B}}\right) * (\rho_l - \rho_a) + \rho_a \qquad \textbf{(9)}$$

Where ρ_o = density of composite, ρ_l = Density of Liquid, A = Weight in Air, B = Weight in liquid and ρ_a = Density of Air

The theoretical density of pure Mg, Ni and TiO_2 are 1.738 g/cm3, 8.91 g/cm3 and 4.23 g/cm3 respectively. Hence, the theoretical density of composites was obtained using the rule of mixture equation in equation 10

$$\rho_c = \rho_m V_m + \rho_r V_r \qquad \textbf{(10)}$$

Where ρ_m = Density of Matrix, ρ_r = Density of reinforcement, V_m = Volume fractions of matrix, and V_r = Volume fractions of reinforcement.

The percentage porosity was calculated after obtaining the densities of the samples using equation 11:

$$\%Porosity = \frac{\rho_o}{\rho_c} * 100 \qquad \textbf{(11)}$$

3.2.6 X-ray Diffraction Studies

X-ray diffraction analysis of monolithic and reinforced magnesium composite was conducted using an automated Bruker-AXS D8 Advance -40kv/40Ma diffractometer with Cu *Kα* (λ = 1.5418 Å) radiation. Each specimen was scanned at a step size of 0.02º and for a count time of 1s with diffraction angles varying between 10º and 100º. Scanning was done in both longitudinal and transverse direction to the extrusion direction, the X-ray diffraction data were used for calculating the texture coefficients in both directions to determine the level of crystallographic texture in the sample.

3.2.7 Microstructural Characterization

Microstructural characterization studies were carried out on metalloraphically polished and prepared extruded samples to investigate the distribution of reinforcement, matrix – reinforcement interfacial integrity and the grain morphology. A JEOL SEM (model JSM 6460), Tescan Lyra-3 (Czech Republic) FESEM equipped with energy dispersive spectroscopy (EDS) and a Meji MX7100 optical microscope was utilized for this purpose.

Sample preparation is very important in achieving good results in this process, the samples were prepared by section the extruded rod appropriately and mounting in an epoxy to ease the metallographic preparation of the sample, the surface of the mounted sample was prepared by standard metallographic preparation of magnesium and its alloys as reported by John Vander Voort [114] which involves a stepwise fine grinding process starting from the use of 240, 320, 400, 600 grit grinding papers successively using water as lubricant, followed by a rough polishing with a nylon cloth using 6μm metadi lapping oil as lubricant. The final polishing was done with a mirocloth and use of distilled water as lubricant. Samples for electron microscopy were coated with a thin layer of gold to enhance electron

conduction to avoid electron charging on the samples. X-ray energy dispersive spectrometry (EDS) analysis of the composite was carried out to analyze the elemental composition of the sample. Area mapping, Line Scanning and Spot analysis were all performed on the sample to confirm the presence and level of distribution of the reinforcements in the Mg matrix. Constant number of frames was maintained throughout for ease of comparison. The samples for grain morphology analysis were etched using a solution of acetic picral (containing 10mL acetic acid, 4.2g picric acid, 70mL ethanol and 10mL distilled water) to reveal the grain boundaries, microstructural images of the samples were taken at a different magnification. A MATLAB based image analysis software (LINECUT) was used to determine the grain size and grain distribution.

3.2.8 Mechanical Characterization

Macrohardness and Microhardness measurements were made on the polished monolithic and reinforced extruded magnesium composites. Rockwell 15T (HR15T) superficial scale was used for macrohardness measurement in accordance with ASTM E18-03 standard. Microhardness tests were carried out using a load of 50gf and dwell time of 15secs on a Beuhler MMT-3 automatic digital microhardness tester in accordance to ASTM: E384-08 standard. Ten hardness values were taken from different locations on each sample and the average values were recorded as the hardness value

Extension-to-failure tensile tests on monolithic and reinforced magnesium composites were carried out on an Instron 3367 machine in accordance with ASTM E8M−01 standard. The tensile tests were conducted on smooth round tension test specimens machined from the extruded rod to a diameter 5 mm and gauge length 25 mm as shown in Figure 9. The crosshead speed of the machine was set at 0.254 mm/min and kept constant for all the

samples for easy comparison. Three set of samples was tested for each composition and the average values of the extension and force was recorded.

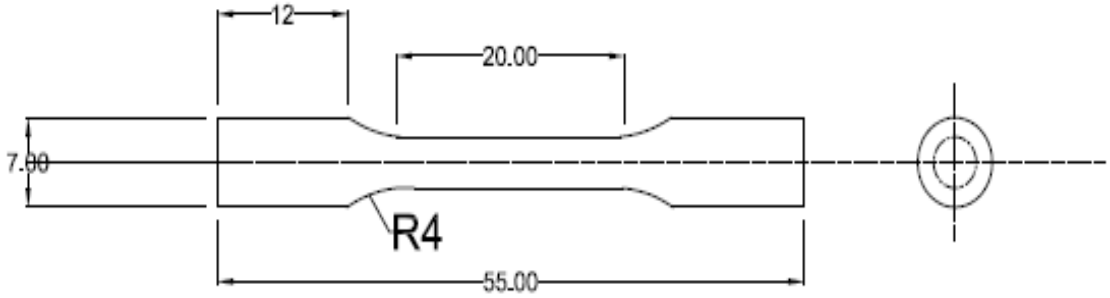

Figure 9: Schematic of tensile specimen

Compressive test on monolithic and reinforced composites were carried out using an Instron 3367 machine in accordance with ASTM: E9-89a standard, the smooth bar compressive test was carried out on specimen of 8mm diameter and length ~ 8 to achieve an l/d ratio of ~ 1, the specimen was sectioned from the extruded rod. The compressive properties were determined at ambient temperature with a strain rate of $8.334 \times 10^{-5}\ s^{-1}$. 4samples were tested for each composition to ensure repeatable values.

For both tensile and compressive tests, stress and strain values were determined for each values of force and extension respectively using equation 3.1 and 3.2 with the aid of excel sheet program and the values of stress were plotted against the strain values to generate the stress-strain curve for each sample tested.

$$Stress\ (\sigma) = \frac{Force\ (F)}{Original\ Area\ (A_o)} \quad \textbf{(12)}$$

$$Strain\ (\varepsilon) = \frac{Extension\ (e)}{Original\ Length\ (l_o)} \quad \textbf{(13)}$$

From the stress-strain curve of both tensile and compressive tests, a line was constructed parallel to the initial portion of the plot but offset by 0.002 mm/mm (0.2%) from the origin. The 0.2% offset yield strength is the stress at which the constructed line intersects the stress-strain curve, the ultimate strength (UTS for tensile and UCS for compressive) was taken as the maximum stress value. The fracture strain is the maximum strain value at which fracture occur and the work of fracture (WoF) was also calculated from the stress-strain curve as the area under the curve.

$$WoF = \sum_{i=2}^{N}\{\frac{1}{2}(\varepsilon_i - \varepsilon_{i-1})(\sigma_i + \sigma_{i-1})\} \quad \textbf{(14)}$$

3.2.9 Fracture characterization

Fracture surface characterization studies were carried out on the tensile and compressive fractured surfaces of the samples to provide insight into the fracture mechanisms operative during tensile and compressive loading. The fractography samples were kept in a desiccator to avoid oxidation and contamination of the fractured surface. Fractography was accomplished using a JEOL JSM-6460 LV SEM equipped with EDS.

CHAPTER 4

EXPERIMENTAL RESULTS

4.1 Magnesium-Nickel Composite

4.1.1 Macrostructural Characteristics

Macrostructural characterization of the compacted and sintered monolithic and elemental nickel reinforced magnesium composite samples did not show the presence of any macrodefects. The outer surfaces were found to be smooth and no longitudinal or circumferential cracks were observed before and after extrusion as shown in Figure 10

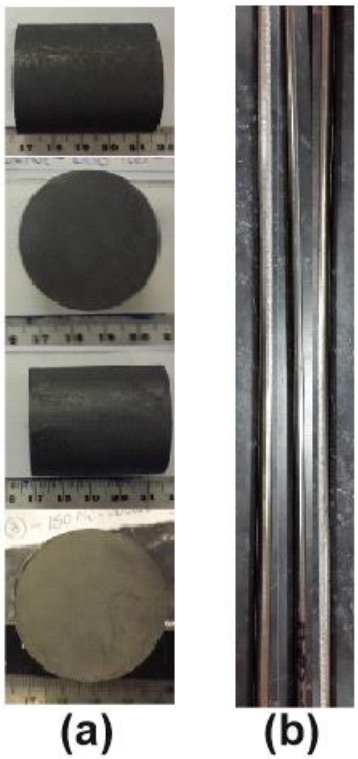

Figure 10: Photograph of some a) sintered billets and b) extruded rods showing no visible macrostructural defect

4.1.2 Density Measurement

The density and porosity measurements conducted on the extruded reinforced and monolithic magnesium samples are listed in Table 1. The porosity level in all the samples remained below 1% indicating the near net shape forming capability of the blend-press-sinter followed by extrusion process adopted in this study

Table 1: Results of Density, porosity and grain size

Materials	**Reinforcement (wt %)**	**Density (g/cm^3)**		**% Porosity**	**Grain Size (µm)**
		Theoretical	Experimental		
Mg-Pure	-	1.738	1.734 ± 0.0099	0.2193	10.1 ± 5.7
Mg-1.50Ni	7.3	1.8456	1.8309 ± 0.0162	0.7965	2.12 ±0.77

4.1.3 X-RAY Diffraction Studies

The X-ray diffraction results corresponding to the extruded reinforced and monolithic magnesium samples were analyzed, Scanning was done in both longitudinal (parallel) and transverse direction to the extrusion direction as shown in Figure 11 and Figure 12 respectively. The obtained lattice spacing (d-spacing) and diffraction angle (2Φ) values compared with the standard values for Mg, Ni, Mg_2Ni and various phases of the Mg–O and Ni–O systems, however, only magnesium and elemental nickel and magnesium were identified, no peaks corresponding to Mg_2Ni were present, The peaks corresponding to the prismatic plane $(10\bar{1}0)$, basal plane (0002) and pyramidal plane $(10\bar{1}1)$ of magnesium are labelled.

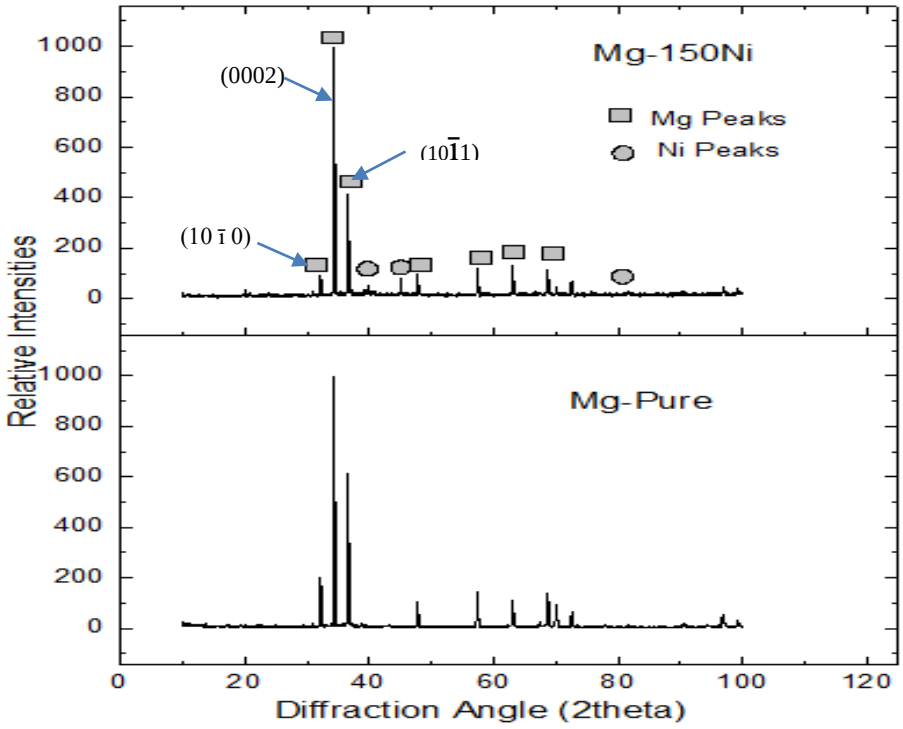

Figure 11: X-ray diffraction spectrum of samples in direction parallel to extrusion direction

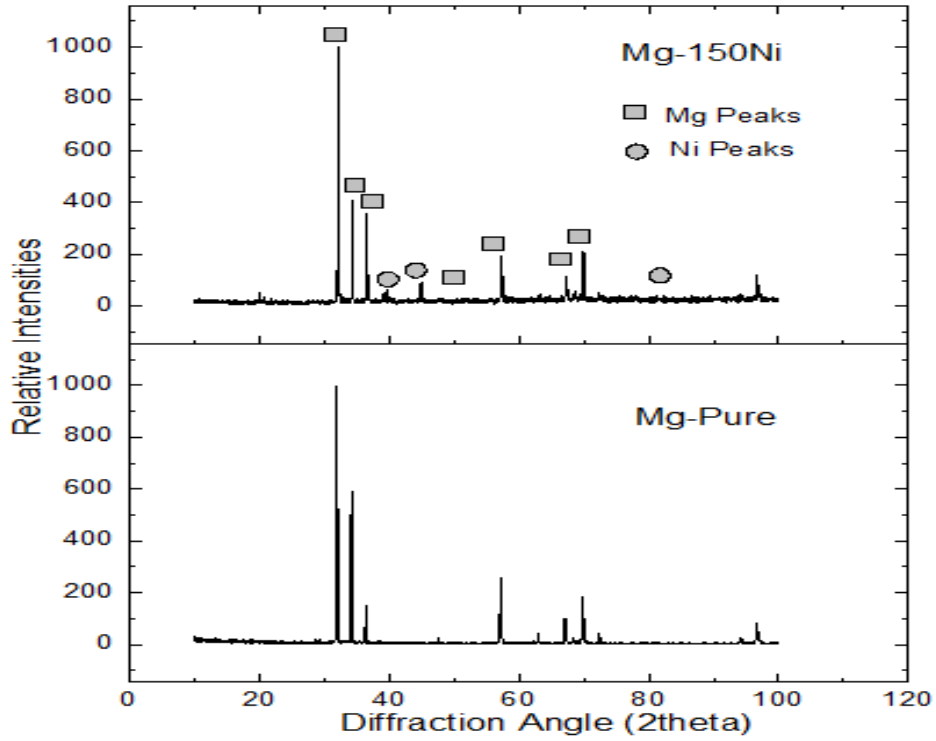

Figure 12: X-ray diffraction spectrum of samples in direction perpendicular to extrusion direction

4.1.4 Microstructural Characteristics

The microstructural characterization of the reinforced composite revealed fairly uniform distribution of nickel reinforcement in the magnesium matrix as shown in the SEM image at lower magnification in Figure 13a, while, at higher magnification, the interface between the magnesium matrix and nickel particle reveals good interfacial integrity between the matrix and reinforcement without any noticeable presence of nickel–magnesium reaction product, debonded areas or voids as also evident from the EDX linescan analysis in Figure 13c. There were some sporadic presence of high-concentration nickel particle zone without cluster. Optical micrographs of the etched samples revealed significant refinement in the grains of magnesium matrix due to the presence of fine elemental nickel particles as evident from the micrographs in Figure 14 and grain size measurement in Table 1

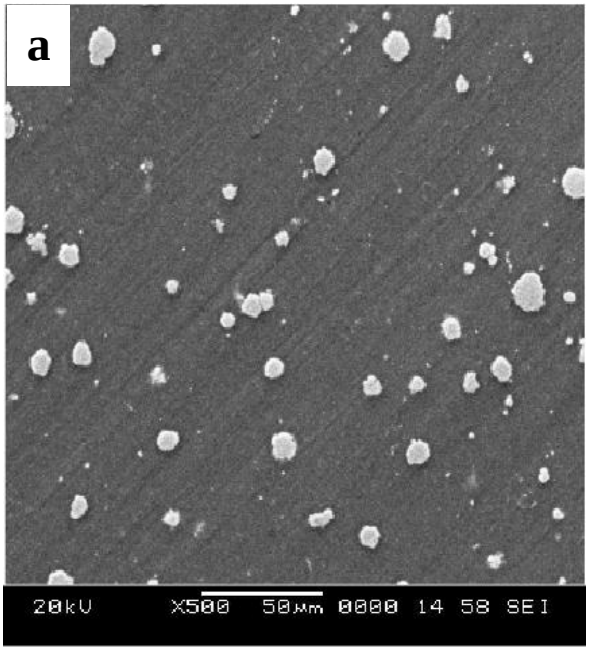

Continued . . . .

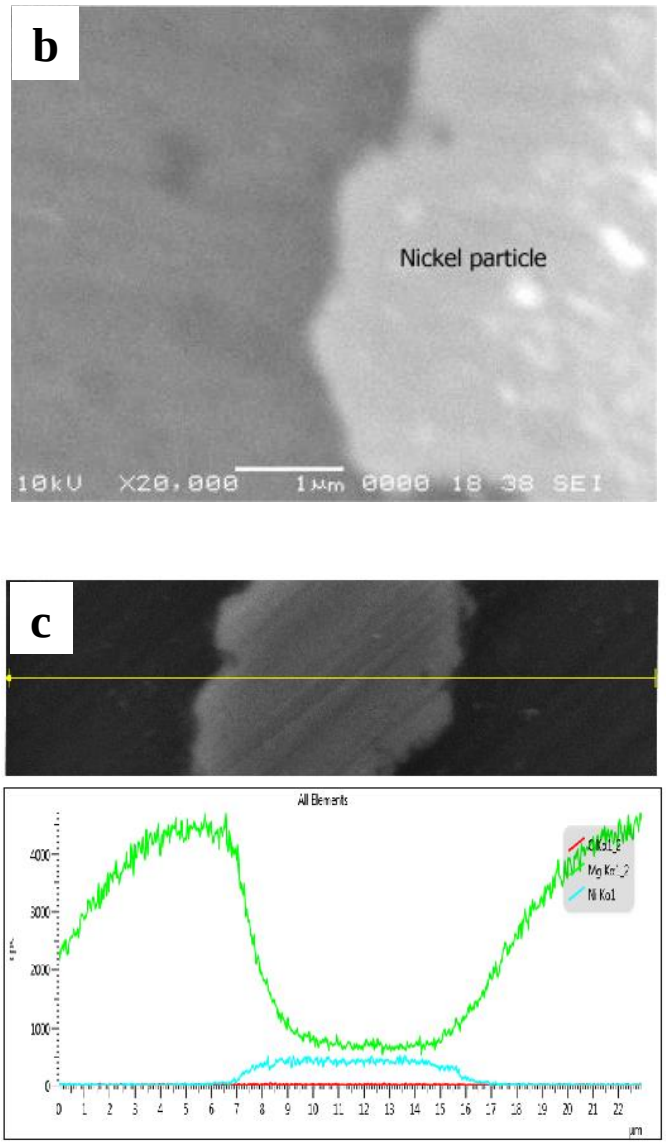

Figure 13: Scanning electron micrographs showing elemental nickel particle: (a) distribution pattern and (b) interfacial characteristics in Mg-1.50Ni composite and c) EDX linescan analysis showing elements across the line indicating good interfacial integrity

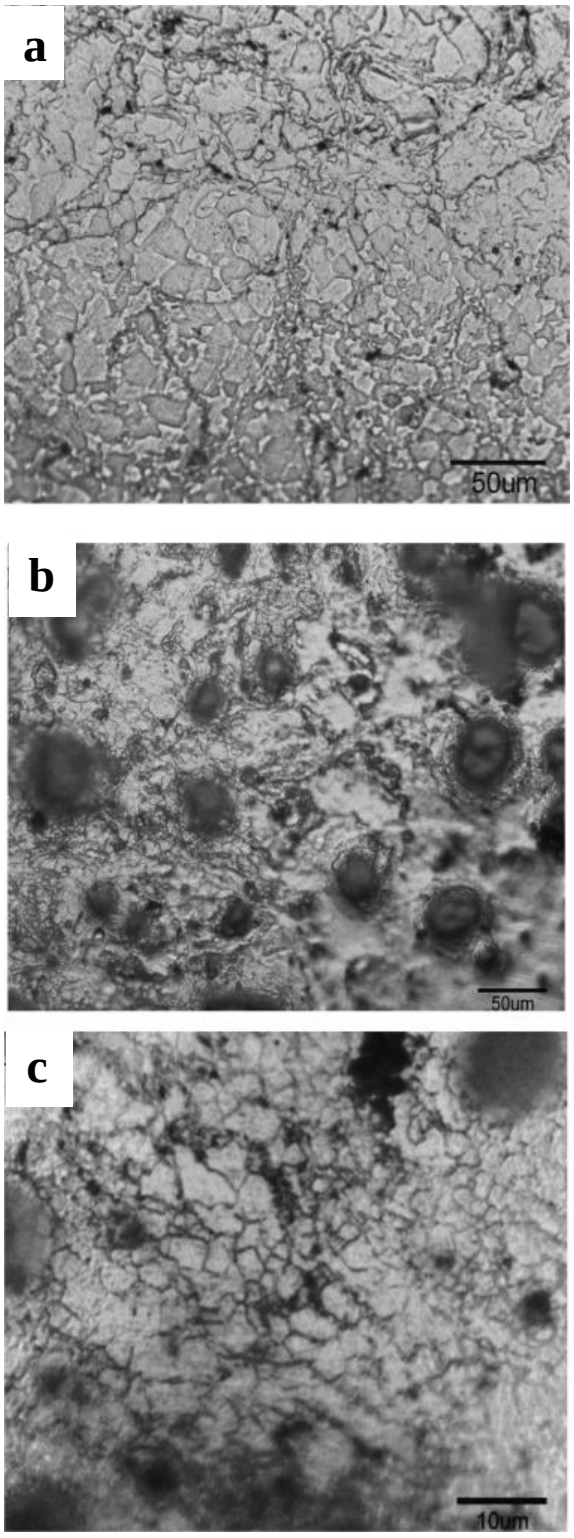

Figure 14: Optical micrographs showing grain morphology in: (a) monolithic magnesium, and (b) and (c) elemental nickel reinforced magnesium, respectively.

4.1.5 MECHANICAL PROPERTIES

i. Micro and Macro Hardness Values

The result of macrohardness and microhardness measurement on the extruded monolithic and reinforced magnesium composite samples are shown in Table 2.

Significant improvement in magnesium hardness due to the presence of nickel particle reinforcement was observed.

Table 2: Results of Microhardness and Macrohardness for Mg-Pure and Mg-1.50Ni

Materials	Micro Hardness (HV)	Macro Hardness (HR15T)
Mg-Pure	39.96 ± 0.32	49.09 ± 1.42
Mg-1.50Ni	54.22 ± 0.79	63.82 ± 1.35

ii. Tensile Test Results

The results of room temperature elongation-to-failure tensile test for monolithic and nickel particle reinforced composites are shown in Table 3 and Figure 15. Results of Mg-150Ni composites revealed that tensile strength of the magnesium was significant improvement due to the incorporation of elemental nickel particle, while its yield strength remained unaffected and ductility affected adversely, the results also revealed relative less energy absorption of magnesium while reinforced with elemental nickel particle.

Table 3: Result of room temperature tensile testing for Mg-Pure and Mg-1.50Ni

Materials	0.2% YS (MPa)	UTS (MPa)	% Elongation	WoF (MJ/m^3)
Mg-Pure	125.5 ± 3.12	199.56 ± 9.37	10.29 ± 2.85	17.12 ± 5.69
Mg-1.50Ni	127 ± 2.29	242 ± 10.32	7.64 ± 0.78	13.35 ± 1.97

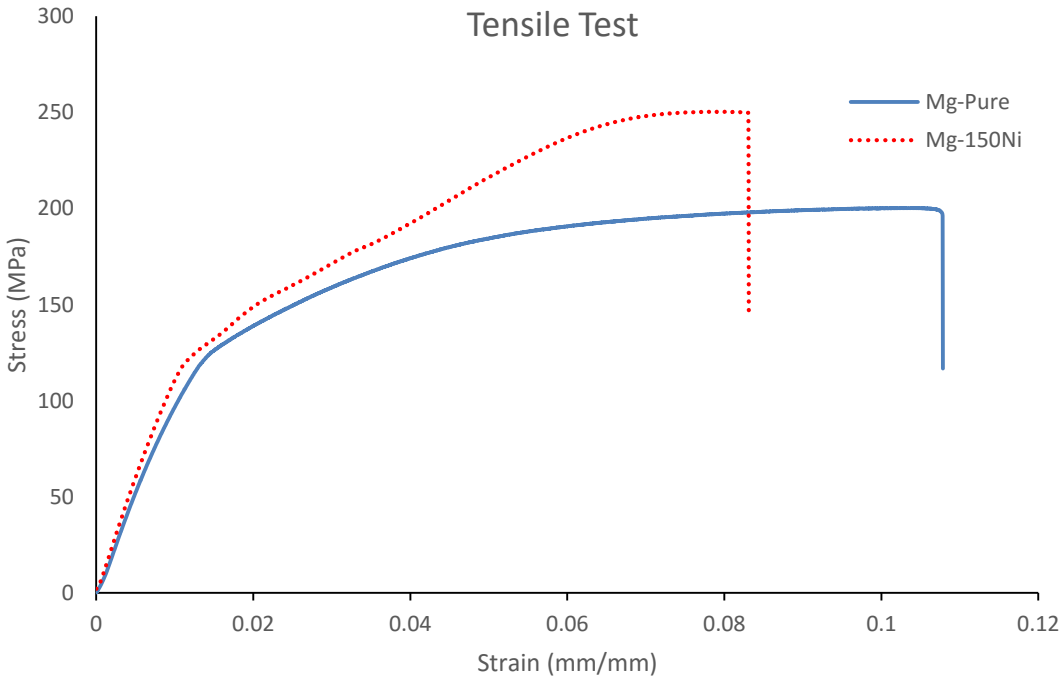

Figure 15: Tensile Stress-Strain curves of Mg-Pure and Mg-150Ni composites

iii. Compressive Test Result

The results of room temperature compressive test for monolithic and nickel particle reinforced composites are shown in Table 4 and Figure 16. Results of Mg-150Ni composites revealed a significant improvement in the compressive yield strength (~80% increase) and compressive strength (~23% increase) of the magnesium due to the

incorporation of elemental nickel particles, while its compressive ductility reduced (~16% reduction).

Table 4: Result of room temperature compressive testing for Mg-Pure and Mg-1.50Ni composite

Materials	0.2% YS (MPa)	UCS (MPa)	% Elongation	WoF (MJ/m^3)
Mg-Pure	66 ± 4.00	185.66 ± 1.72	22.01 ± 0.99	27.99 ± 1.89
Mg-1.50Ni	120 ± 12.5	228 ± 11.57	18.34 ± 3.13	31.07 ± 9.8

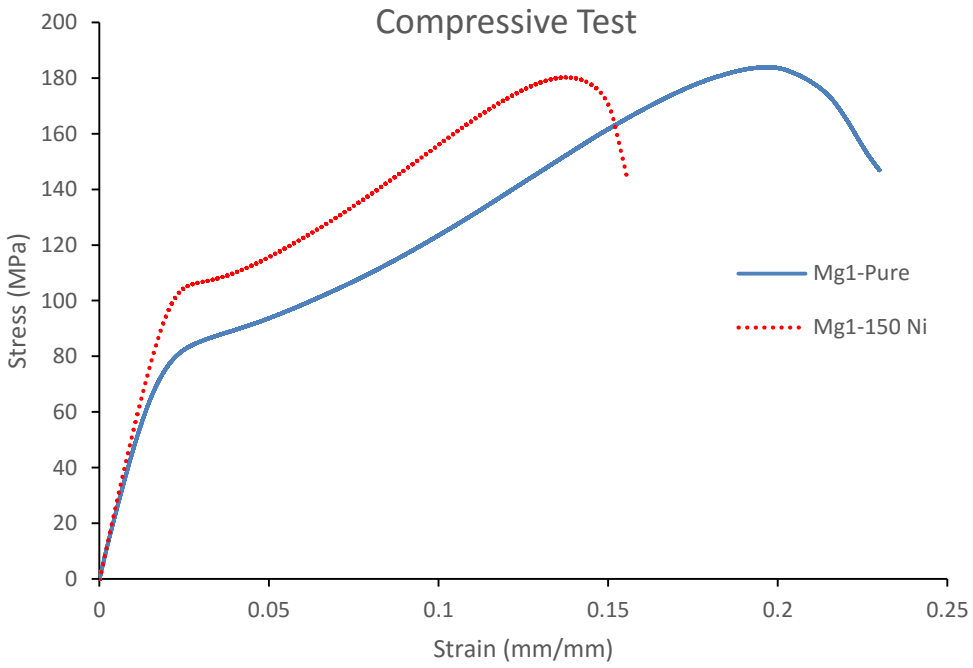

Figure 16: Compressive Stress-Strain curves of Mg-Pure and Mg-1.50Ni composites

4.1.6 Fractography

i. Tensile Fractography

Tensile fracture surfaces of extruded monolithic and nickel particle reinforced magnesium are shown in Figure 17. Fracture surface of monolithic magnesium samples indicates the presence pseudo-dimple (Figure 17a-b) and intergranular crack propagation (Figure 17c) while the reinforced Mg-150Ni sample showed brittle features with reinforcement particle cracking (Figure 17d-e).

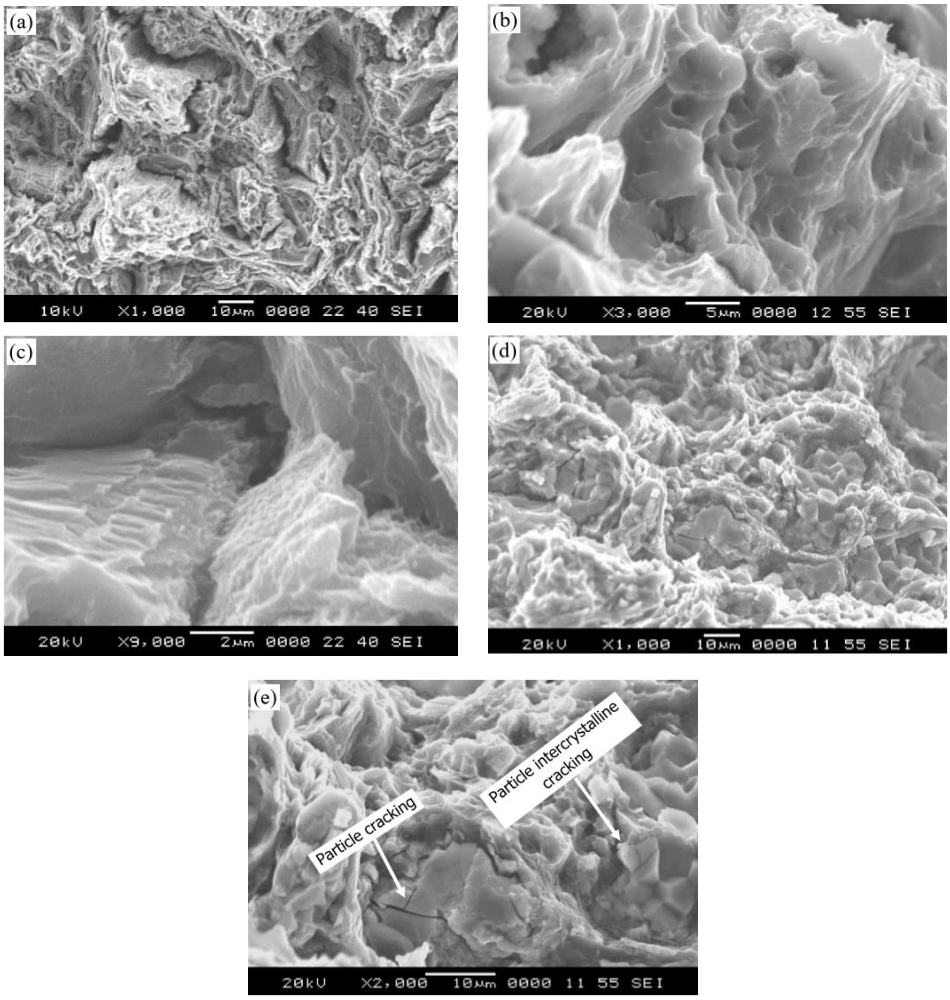

Figure 17: Scanning electron fractographs showing: ductile pseudo-dimple in (a) and (b), and inter-crystalline feature in (c) for monolithic magnesium, and brittle-ductile matrix in (d) with particle cracking in (e) for elemental nickel particle reinforced magnesium respectively

ii. Compressive Fractography

Compressive fracture surfaces of extruded monolithic and nickel particle reinforced magnesium are shown in Figure 18. The fracture surface showed the presence of shear band on the fracture surface of both the monolithic and reinforced composite.

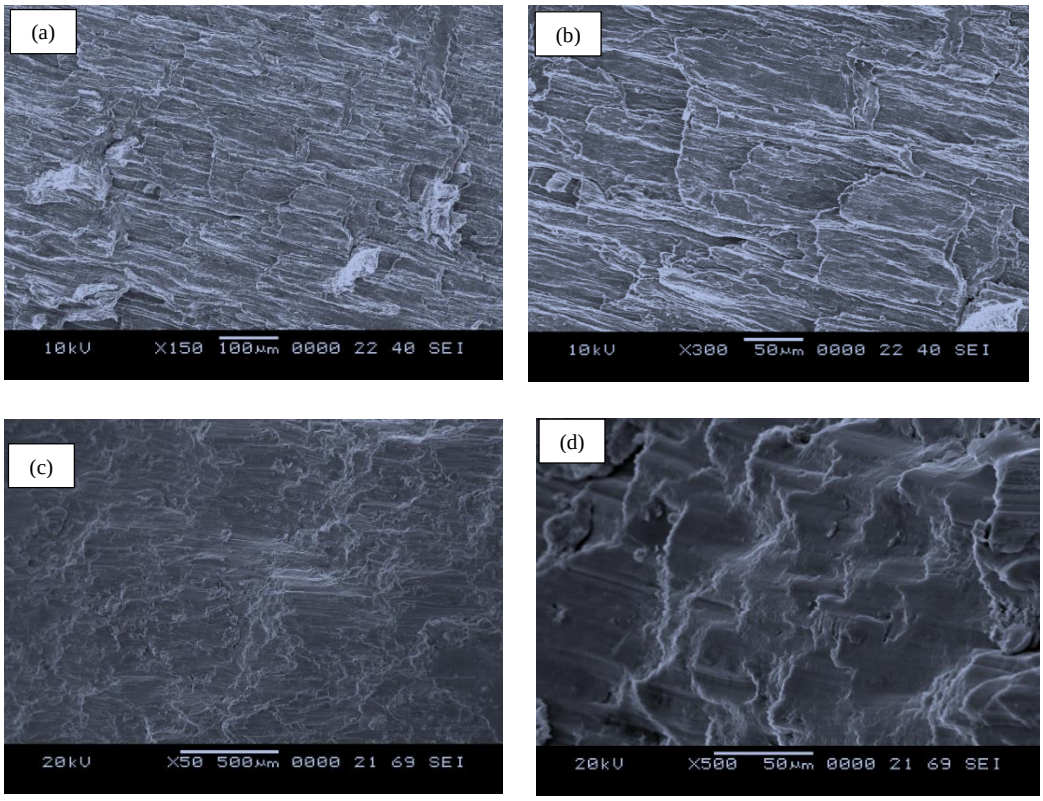

Figure 18: Compressive fracture surface image of a & b) pure magnesium and (c &d) Ni reinforced magnesium composite

4.2 Magnesium-TiO_2 Nanocomposite

4.2.1 Macrostructural Characteristics

Macrostructural characterization of the compacted and sintered monolithic and TiO_2 reinforced magnesium nanocomposite samples did not reveal presence of any macrodefects. The outer surfaces of the samples were free from any form of circumferential or longitudinal cracks before and after the extrusion process as shown in Figure 19.

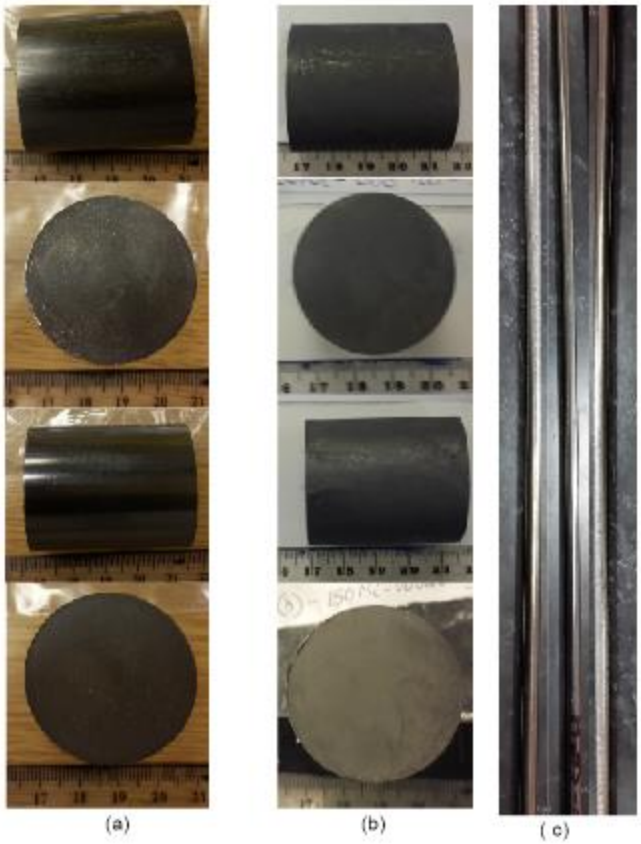

Figure 19: Photograph of some a) compacted billets b) sintered billets and c) extruded rods of TiO_2 reinforced samples

4.2.2 Density Measurement

The result of density and porosity measurements conducted on the extruded monolithic magnesium and reinforced nanocomposite samples are listed in Table 5. The porosity level in all the samples remained below 1% indicating the near net shape forming capability of the blend-press-sinter followed by extrusion process adopted in this study

Table 5: Results of Density, Porosity and Grain size measurement for Mg-TiO_2 nanocomposites

Materials	Reinforcement (wt %)	Density (g/cm^3)		% Porosity	Grain Size (μm)
		Theoretical	Experimental		
Mg-Pure	-	1.738	1.734 ± 0.0099	0.2193	10.1 ± 5.7
Mg-0.33TiO_2	0.80	1.7462	1.7392 ± 0.0024	0.4033	5.605 ±3.4
Mg-0.66TiO_2	1.60	1.7544	1.7479 ± 0.0001	0.3716	4.62 ±2.02
Mg-1.00TiO_2	2.40	1.7629	1.7572 ± 0.0153	0.3258	4.04 ±1.04

4.2.3 X-RAY Diffraction Studies

The X-ray diffraction results corresponding to the extruded reinforced and monolithic magnesium samples were analyzed, Scanning was done in both longitudinal (parallel) and transverse direction to the extrusion direction as shown in Figure 20 and Figure 21 respectively. The obtained lattice spacing (d-spacing) and diffraction angle (2Φ) values compared with the standard values for Mg, MgO and TiO_2, systems, however, only magnesium peaks was identified, no peaks corresponding to nano sized titania were present, this can be attributed to the limitation of the filtered X-ray to detect phases with amount less than 2 vol. % [115,116]. The peaks labelled x, y and z corresponds to the $(10\bar{1}0)$, (0002) and $(10\bar{1}1)$ planes of magnesium respectively.

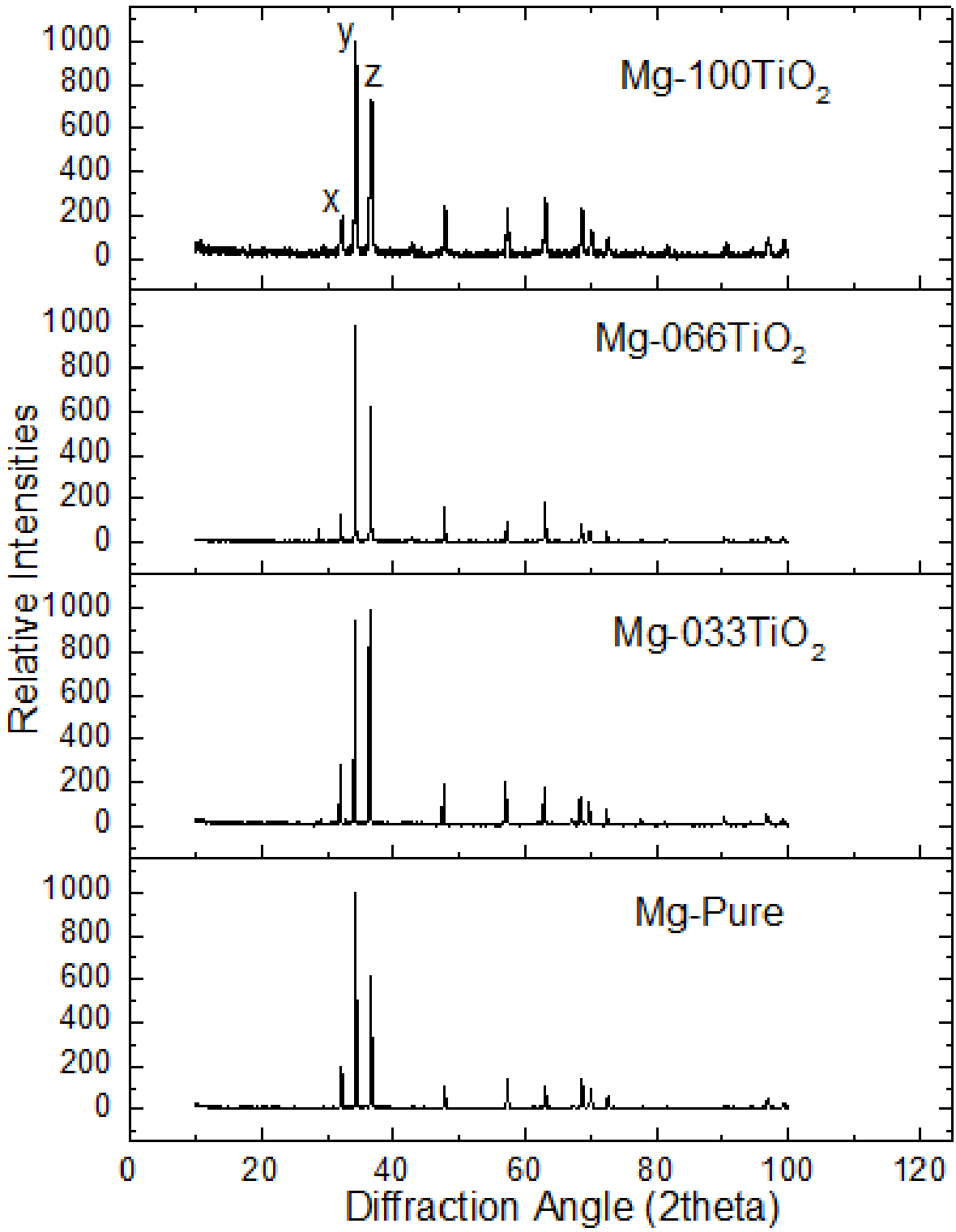

Figure 20: X-ray diffraction spectrum of Mg-TiO2 samples in direction parallel to extrusion direction

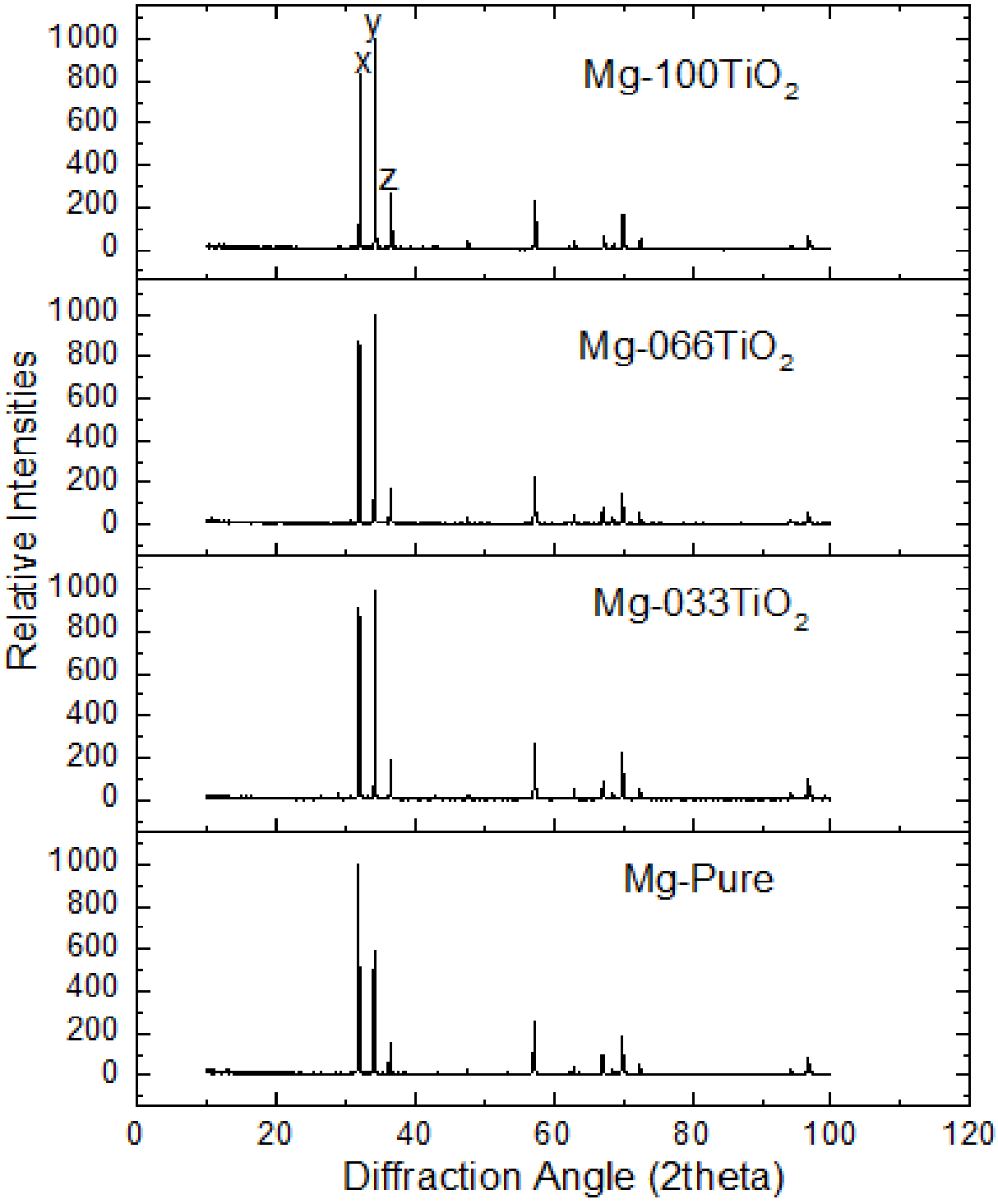

Figure 21: X-ray diffraction spectrum of Mg-TiO2 samples in direction perpendicular to extrusion direction

4.2.4 Microstructural Characteristics

The microstructural characterization of all the nano TiO_2 reinforced Magnesium nanocomposite samples revealed uniform distribution of nano TiO_2 particles (indicated with arrows) in the magnesium matrix, no significant cluster of nano powder was observed as shown in Figure 23. The EDX mapping of the sample confirms the presence of Mg, Ti and O_2 in the samples as seen in Figure 22, no evidence of void was found in the sample. Optical micrographs of the etched samples revealed significant refinement in the grains of magnesium matrix due to the presence of nano sized TiO_2 particles as evident from the micrographs in Figure 24 and grain size measurement in Table 5.

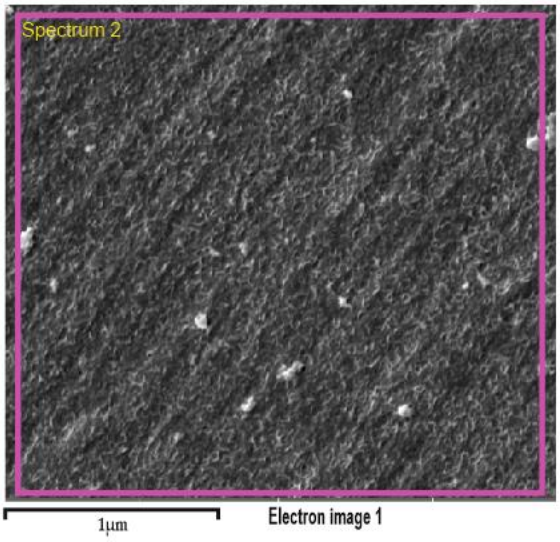

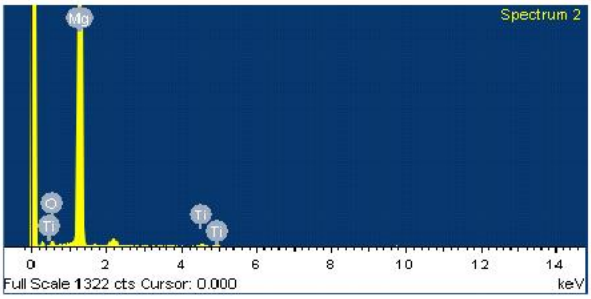

Element	Weight%	Atomic%
O K	5.96	8.85
Mg K	92.62	90.45
Ti K	1.42	0.70
Totals	100.00	

Figure 22: EDX analysis of Mg-TiO2 nanocomposite sample

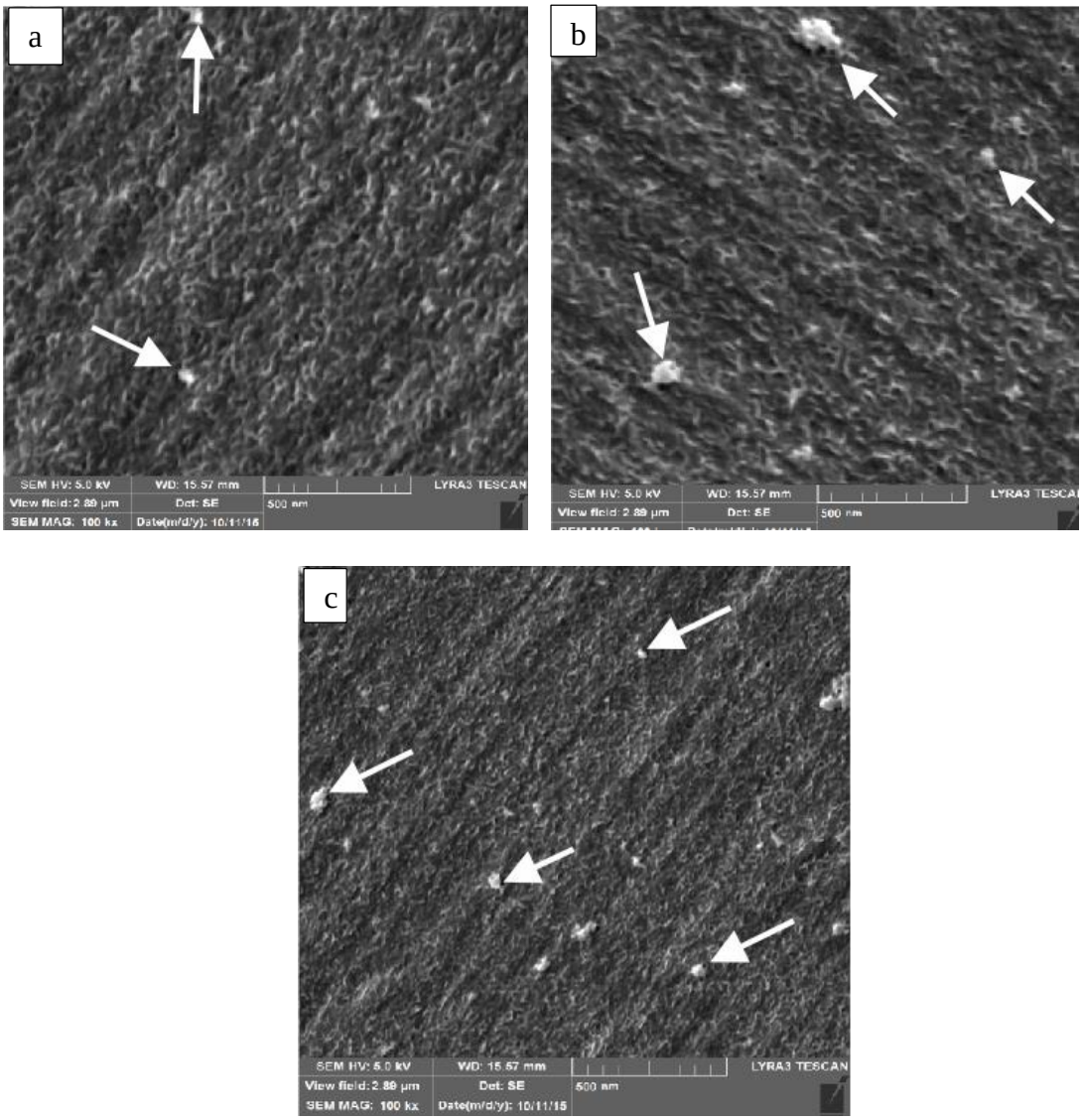

Figure 23: Representative FESEM images reinforcement distribution in (a) Mg-033TiO2 b) Mg-066TiO2 c) Mg-100TiO2 samples (few pointed arrows indicate TiO2 nanoparticles)

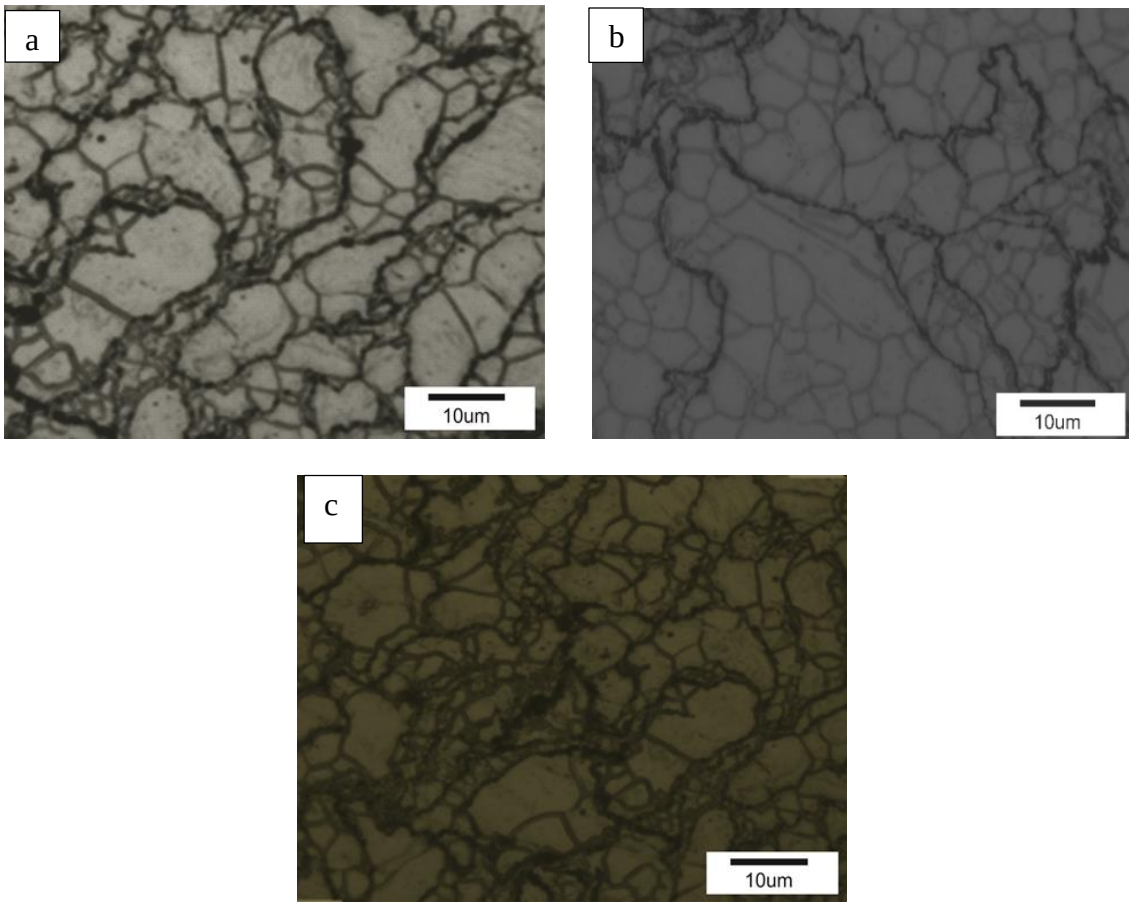

Figure 24: Representative optical micrograph of (a) Mg-033TiO2, (b) Mg-066TiO2 and (c) Mg-100TiO2

4.2.5 Mechanical Properties

i. Micro and Macro Hardness Values

The result of macrohardness and microhardness measurement on the extruded monolithic and TiO_2 reinforced magnesium nanocomposite samples are shown in Table 6. The addition of TiO_2 nanoparticles show was no significant influence on the hardness values of magnesium.

Table 6: Results of Microhardness and Macrohardness for Mg-TiO2 nanocomposites

Materials	**Micro Hardness (HV)**	**Macro Hardness (HR15T)**
Mg-Pure	39.96 ± 0.32	49.09 ± 1.42
Mg-0.33TiO_2	37.35 ± 0.25	46.30 ± 0.99
Mg-0.66TiO_2	39.2 ± 0.47	48.41 ± 0.92
Mg-1.00TiO_2	39.95 ± 1.44	52.42 ± 0.67

ii. Tensile Test Results

The results of room temperature elongation-to-failure tensile test for monolithic and all the nano TiO_2 reinforced nano composites are shown in Table 7 and Figure 25. Results of Mg/TiO_2 nanocomposites reveals no significant improvement in the yield strength and tensile strength due to the addition of TiO_2 nanoparticles, while its ductility was significantly improved, however, the increase in ductility was not significantly affected by the increase in volume percent of TiO_2. The ability of a material to absorb energy up to fracture under tensile loading corresponds to the area under the stress-strain curve indicated by the work of fracture was higher for 0.33 volume% reinforced nanocomposite indicating the material capability to tolerate damage.

Table 7: Result of room temperature tensile testing for Mg-Pure and Mg-TiO2 nanocomposites

Materials	0.2% YS (MPa)	UTS (MPa)	% Elongation	WoF (MJ/m^3)
Mg-Pure	125.5 ± 3.12	199.56 ± 9.37	10.29 ± 2.85	17.12 ± 5.69
Mg-0.33TiO_2	115.63 ± 13.63	201.97 ± 6.40	12.12 ± 1.21	17.07 ± 2.63
Mg-0.66TiO_2	112.96 ± 12.80	197.36 ± 5.76	11.46 ± 3.17	16.68 ± 6.35
Mg-1.00TiO_2	112.61 ± 5.45	190.12 ± 9.40	11.76 ± 1.62	13.37 ± 6.70

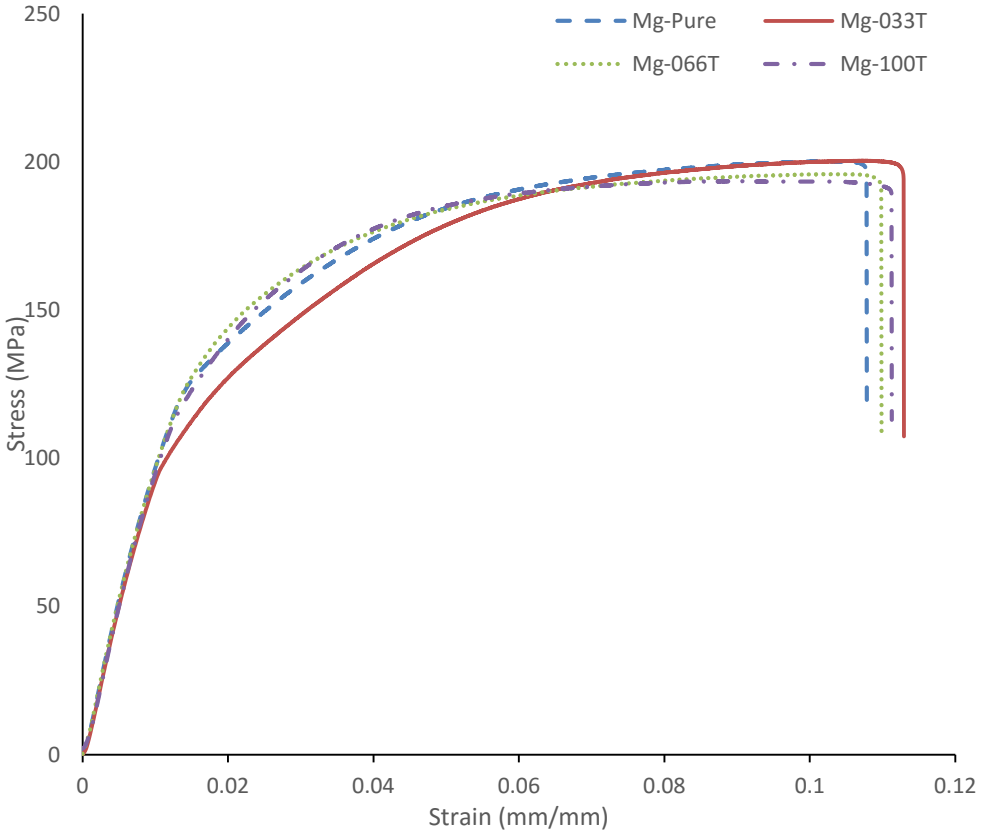

Figure 25: Tensile Stress-Strain curves of for Mg-Pure and Mg-TiO2 nanocomposites

iii. Compressive Test Result

The results of room temperature compressive test for monolithic and all the nano TiO_2 reinforced nano composites are shown in Table 8 and Figure 26. The results of Mg-TiO_2 nanocomposites reveals simultaneous increase in the compressive yield strength, ultimate compressive strength and compressive ductility of magnesium with increasing volume % of TiO_2. The highest combination of mechanical properties was obtained with 1.00 volume % of Titania where a maximum of ~ 65% increase in compressive yield strength and ~39% increase in UCS with ~6% increase in fracture strain of pure magnesium was observed.

Table 8: Result of room temperature compressive testing for Mg-Pure and Mg-TiO2 nanocomposites

Materials	**0.2% YS (MPa)**	**UCS (MPa)**	**% Elongation**	**WoF (MJ/m^3)**
Mg-Pure	66 ± 4.00	185.66 ± 1.72	22.01 ± 0.99	27.99 ± 1.89
Mg-0.33TiO_2	75.00 ± 3.54	201.20 ± 4.42	23.15 ± 4.23	33.60 ± 6.5
Mg-0.66TiO_2	91.83 ± 4.94	249.11 ± 6.10	20.22 ± 2.44	31.03 ± 3.66
Mg-1.00TiO_2	109.00 ± 4.00	255.78 ± 4.0	23.32 ± 1.22	35.18 ± 10.88

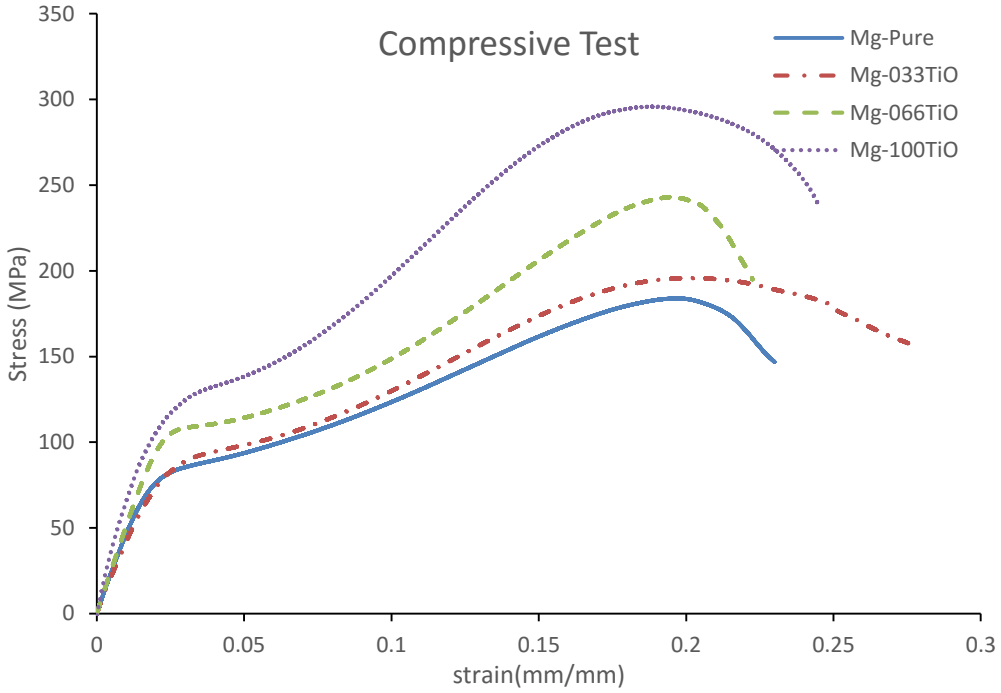

Figure 26: Compressive Stress-Strain curves of developed composites for Mg-Pure and Mg-TiO2 nanocomposites

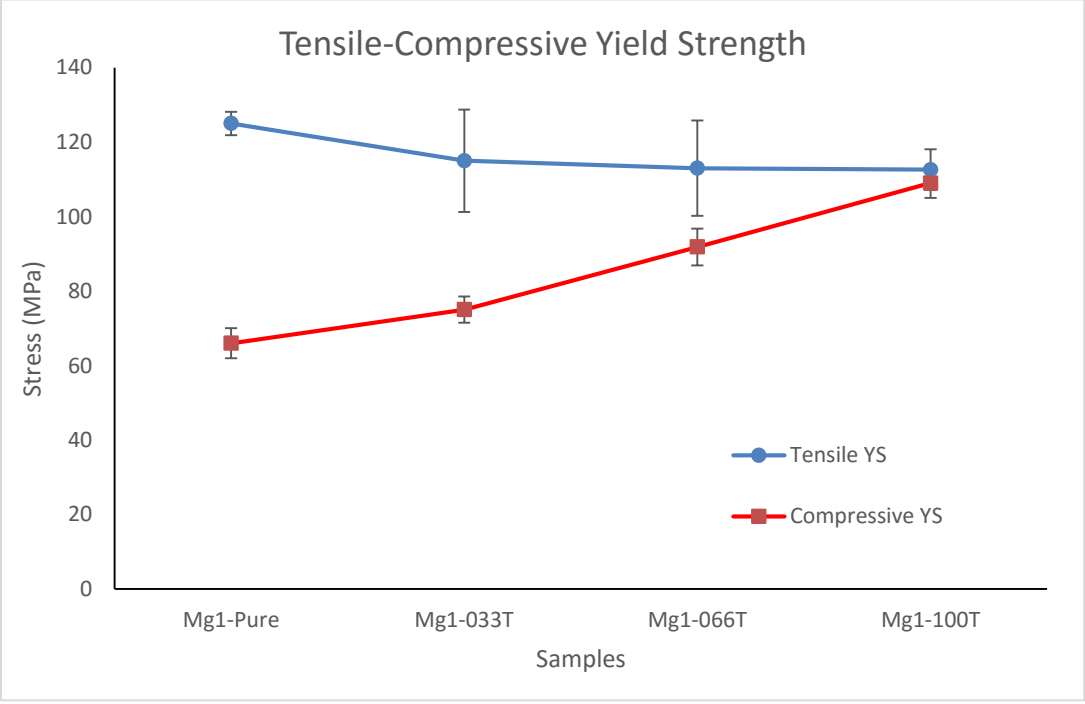

Figure 27: Tensile compressive yield stress of Pure Mg and Mg/TiO2 composites indicating the Tensile Compression Asymmetry

4.2.6 Fractography

i. Tensile Fractography

Tensile fracture surfaces of extruded monolithic and nano TiO_2 reinforced magnesium nanocomposite are shown in Figure 28. Fracture surface of monolithic magnesium samples indicates the presence pseudo-dimple and intergranular crack propagation.

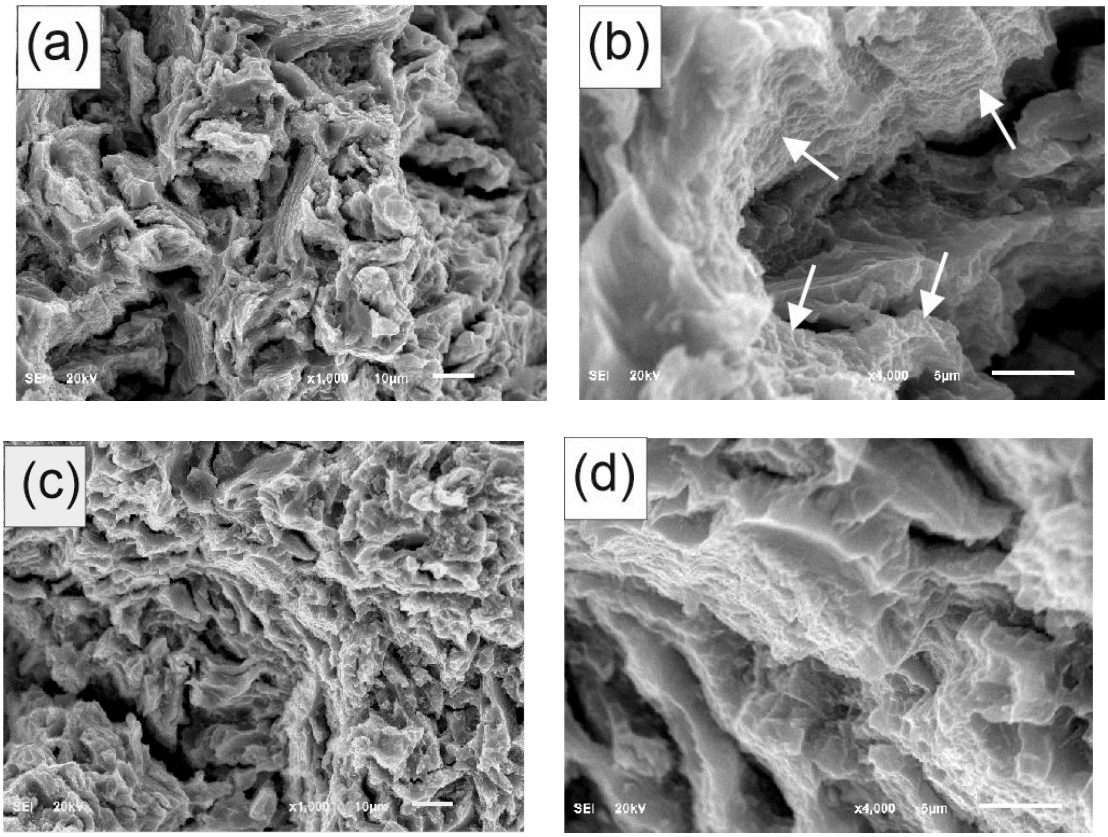

Continued. .

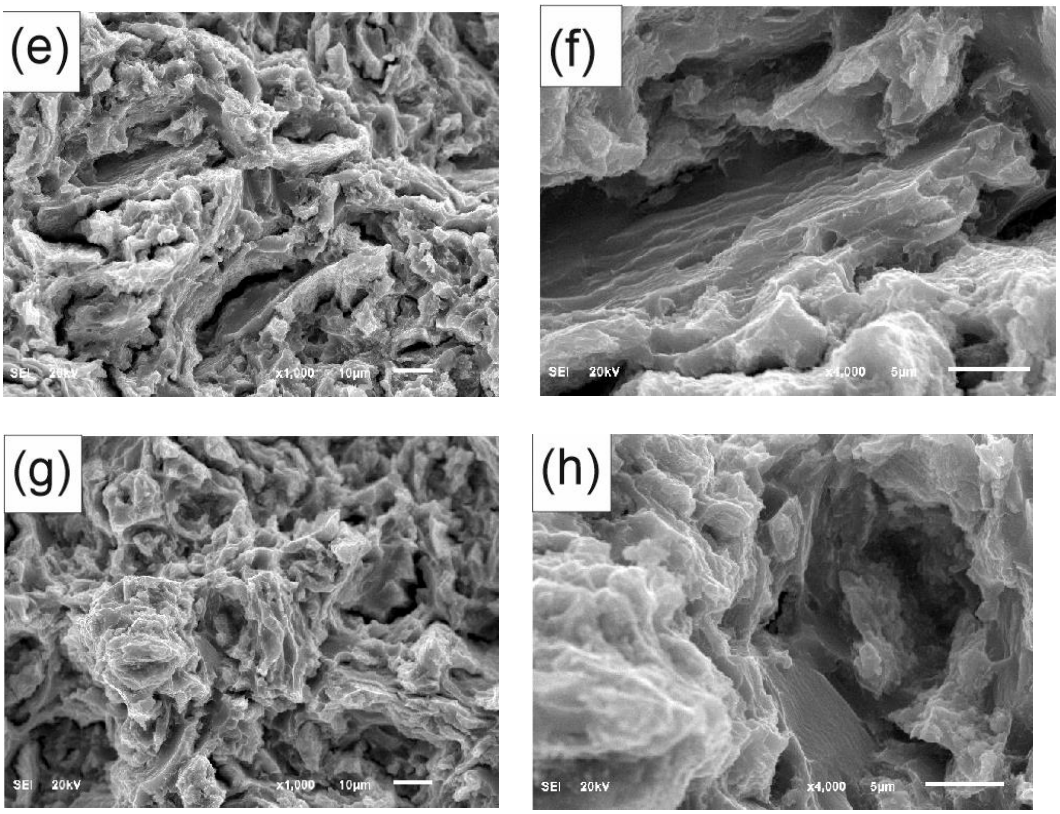

Figure 28: Scanning electron fractographs showing the tensile fracture surface of a) & b) monolithic Mg, c) & d) Mg-033TiO_2 e) & f) Mg-066TiO_2 g) & h) Mg-100TiO_2

ii. Compressive Fractography

The fracture surface of the pure Mg and nano TiO_2 reinforced nanocomposite samples under compressive loading are shown in Figure 29.

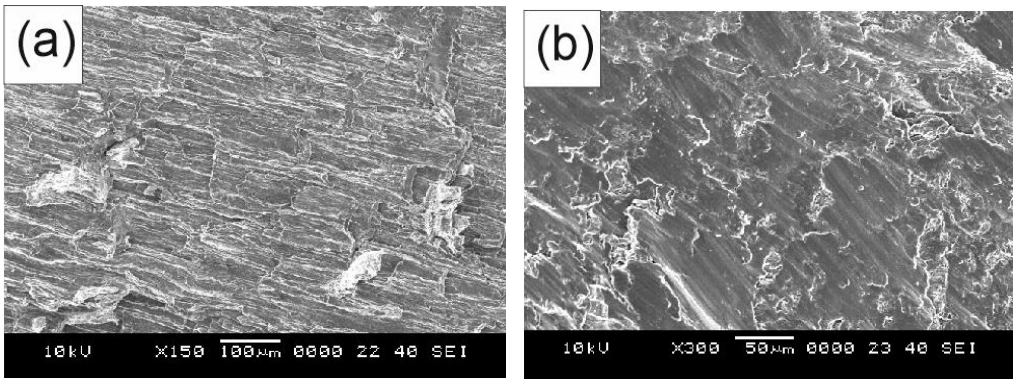

Continued . . . .

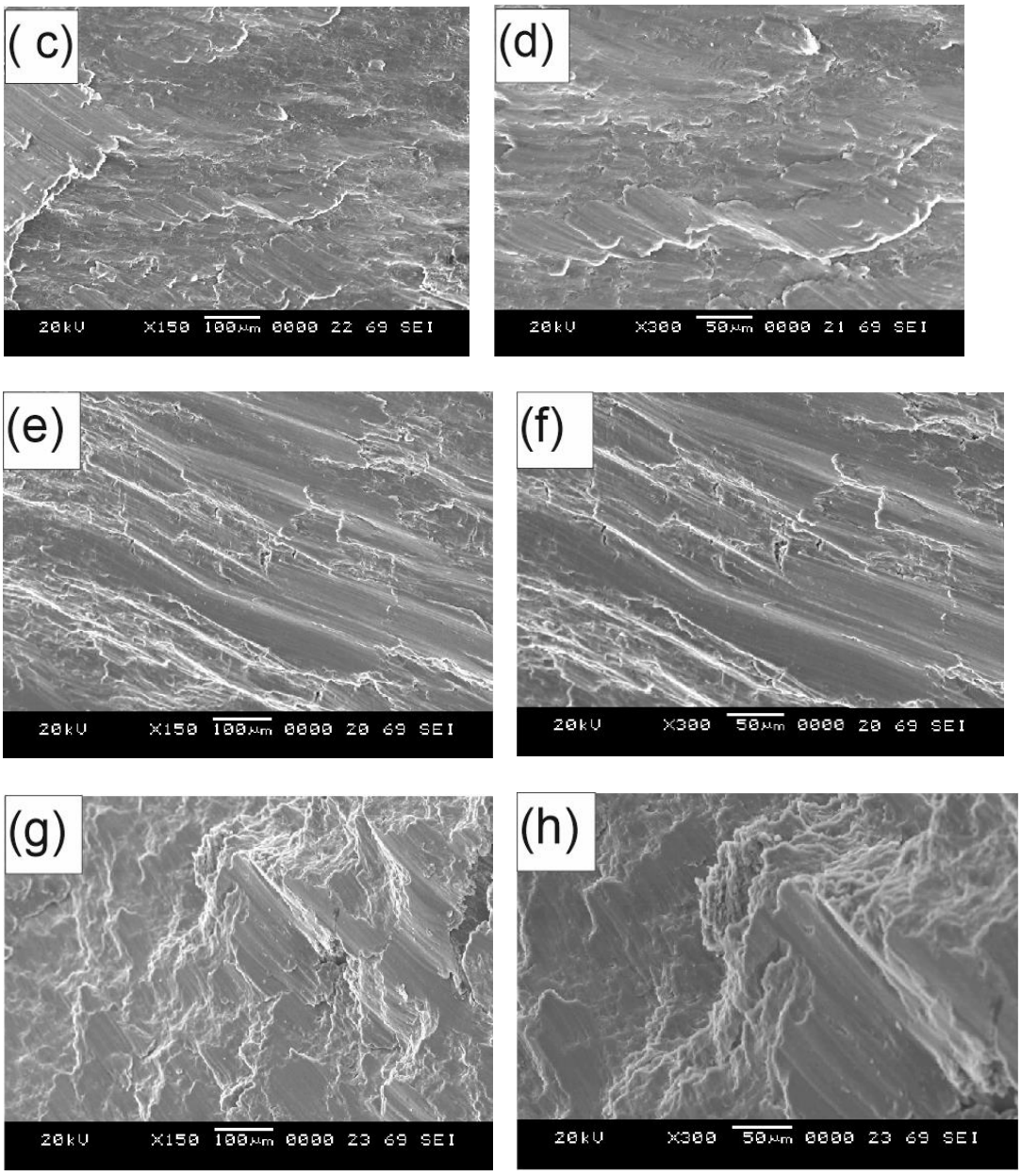

Figure 29: Scanning electron fractographs showing the compressive fracture surface of a) & b) monolithic Mg, c) & d) Mg-033TiO2 e) & f) Mg-066TiO2 g) & h) Mg-100TiO2

4.3 Magnesium-Hybrid Nanocomposite

4.3.1 Macrostructural Characteristics

Macrostructural characterization of the compacted and sintered hybrid magnesium nanocomposite containing 0.33vol% TiO_2 and 1.50vol% Ni reinforcements did not reveal presence of any macro-defects. The outer surfaces were found to be smooth and free from all forms of longitudinal and circumferential cracks both on the sintered sample and extruded sample.

Figure 30: Photograph of some hybrid (Mg-1.50Ni-0.33TiO_2) samples

4.3.2 Density Measurement

The results of density and porosity measurements conducted on the extruded monolithic magnesium and hybrid nanocomposite samples are listed in Table 9. The porosity level in all the samples remained below 1% indicating the near net shape forming capability of the blend-press-sinter followed by extrusion process adopted in this study

Table 9: Results of Density. Porosity and Grain size Measurement for hybrid sample

Materials	Reinforcement (wt %)	Density (g/cm^3)		% Porosity	Grain Size (µm)
		Theoretical	Experimental		
Mg-Pure	-	1.738	1.734 ± 0.0099	0.2193	10.1 ± 5.7
Mg-1.50Ni-0.33TiO_2	7.2Ni and 0.75 TiO_2	1.8538	1.8431 ± 0.0044	0.5714	2.1 ± 0.8

4.3.3 X-Ray Diffraction Studies

The X-ray diffraction results corresponding to the extruded reinforced and monolithic magnesium samples were analyzed, Scanning was done in both longitudinal (parallel) and transverse direction to the extrusion direction as shown in Figure 31 and Figure 32 respectively. The obtained lattice spacing (d-spacing) and diffraction angle (2Φ) values compared with the standard values for Mg, TiO_2, Ni, Mg_2Ni and various phases of the Mg–O and Ni–O systems, however, only magnesium and elemental nickel and magnesium was identified, no peaks corresponding to TiO_2 and Mg_2Ni was present, The peaks corresponding to the prismatic plane $(10\bar{1}0)$, basal plane (0002) and pyramidal plane $(10\bar{1}1)$ of magnesium are labeled.

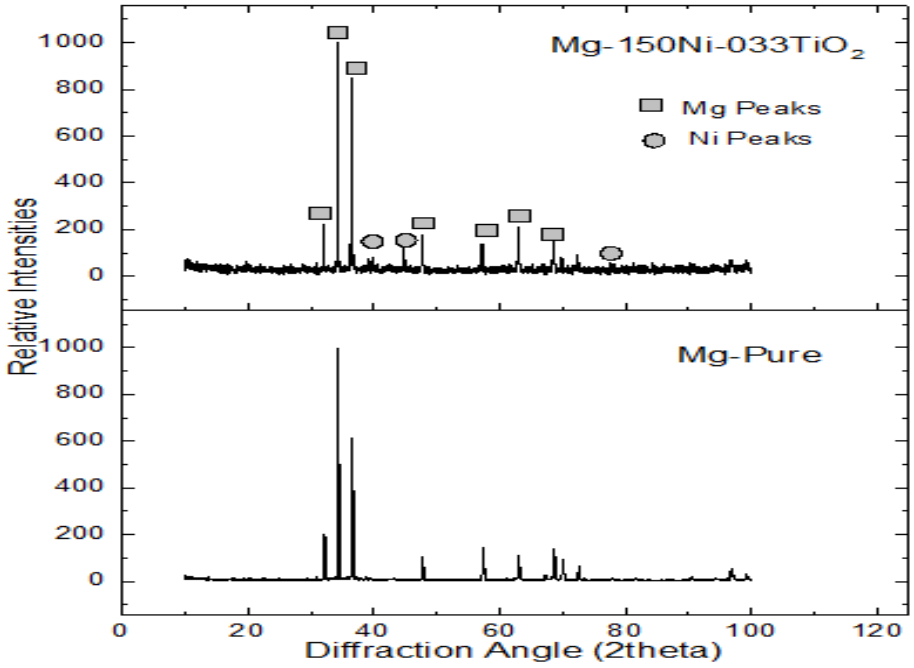

Figure 31: X-ray diffraction spectrum of pure Mg and Mg-1.50Ni-0.33TiO_2 samples in direction parallel to extrusion direction

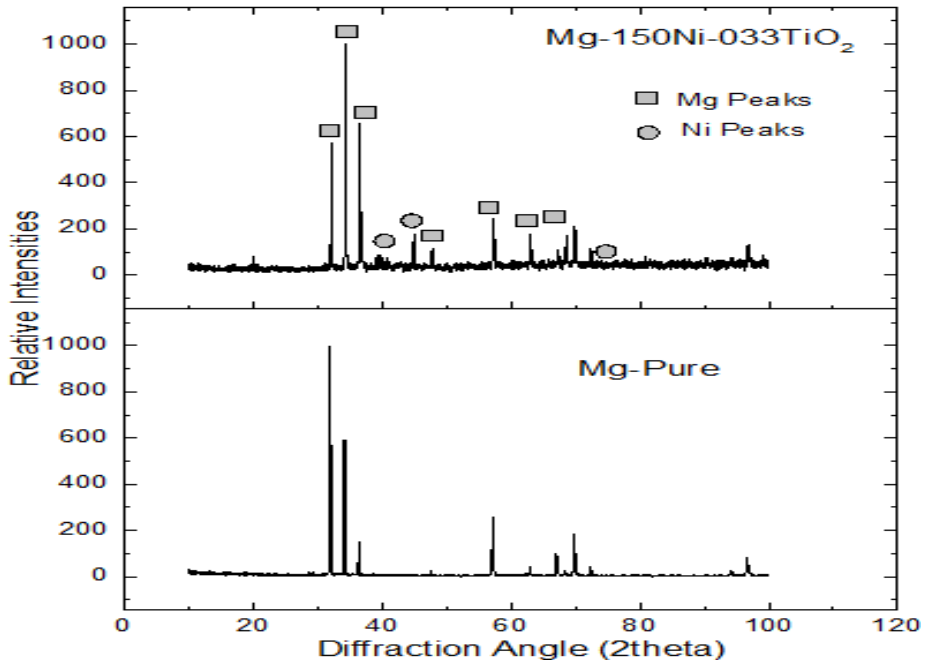

Figure 32: X-ray diffraction spectrum of pure Mg and Mg-1.50Ni-0.33TiO_2 samples in direction perpendicular to extrusion direction

4.3.4 Microstructural Characteristics

The microstructural characterization of the hybrid reinforced Magnesium nanocomposite revealed fairly uniform distribution of the reinforcement in the magnesium matrix as shown in Figure 34. There was no noticeable presence of nickel-magnesium reaction products at the boundary between Mg and Ni, the interface reveals good interfacial integrity between the matrix and reinforcement, there was also no presence of debonded areas or voids. EDX map and EDX elemental scan analysis (Figure 33) of the hybrid nanocomposite confirm the presence of Nickel, Titanium and oxygen in the magnesium matrix, the XRAY map shows that the TiO_2 nanoparticles are more concentrated at the interface between the larger nickel particle and the magnesium matrix (Figure 35). Optical micrographs of the etched hybrid reinforced sample revealed significant refinement in the grains of magnesium matrix due to the presence of fine elemental Ni and TiO_2 particles as evident from the micrographs in Figure 36 and grain size measurement in Table 9.

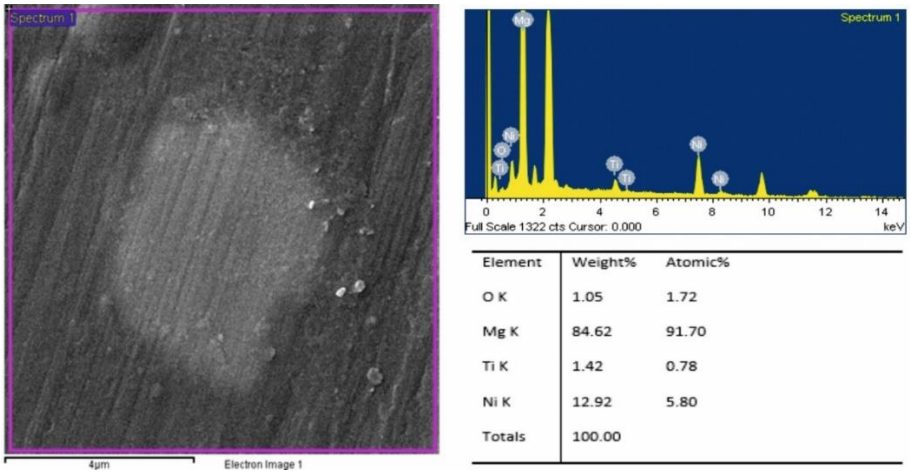

Element	Weight%	Atomic%
O K	1.05	1.72
Mg K	84.62	91.70
Ti K	1.42	0.78
Ni K	12.92	5.80
Totals	100.00	

Figure 33: EDX analysis of Mg-150-0.33TiO2 nanocomposite sample

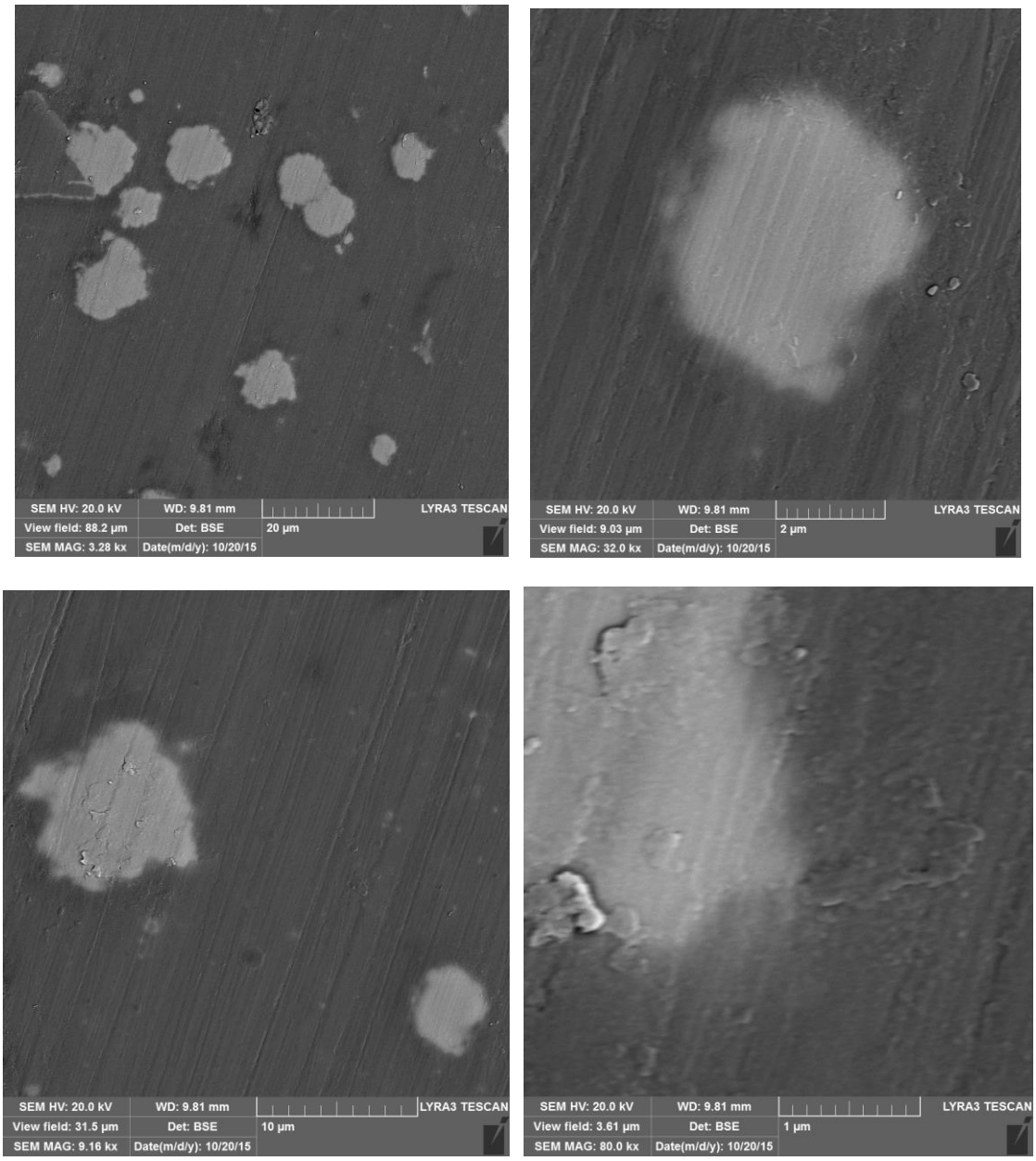

Figure 34: SEM image of hybrid sample showing distribution of reinforcement

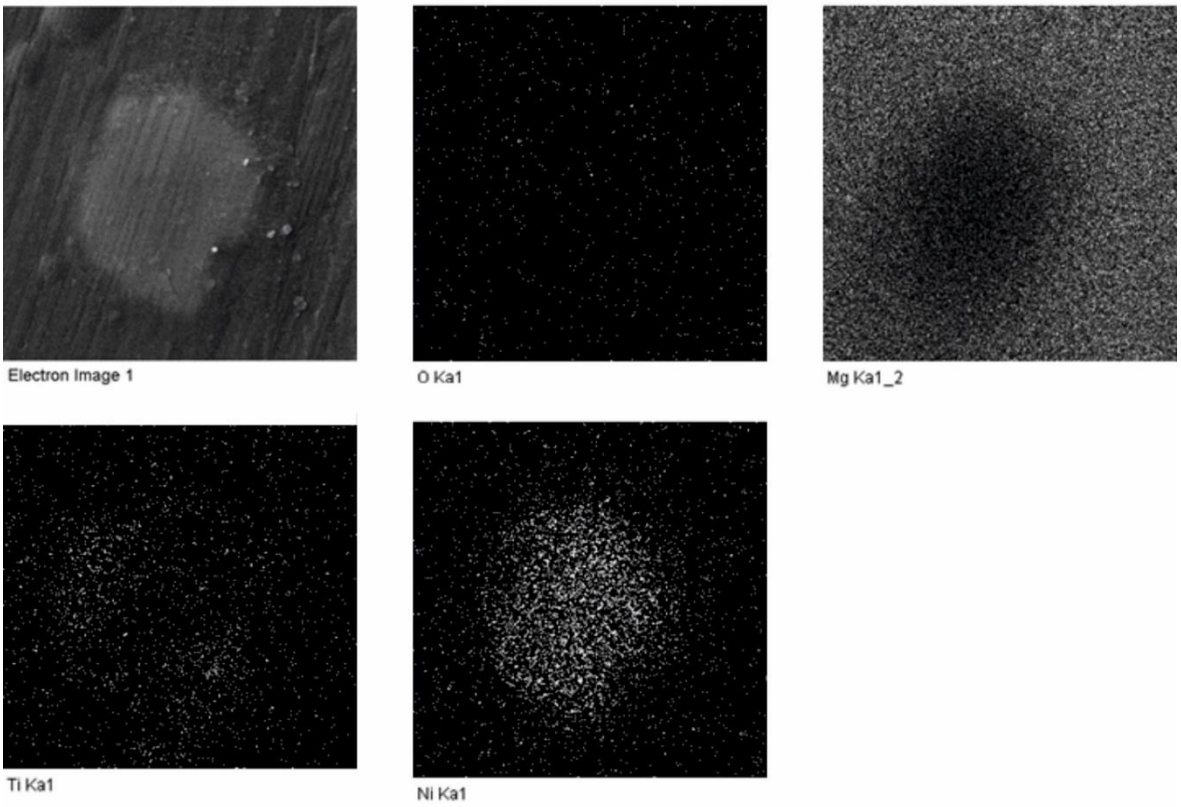

Figure 35: EDX mapping of Mg-150Ni-033TiO2 sample

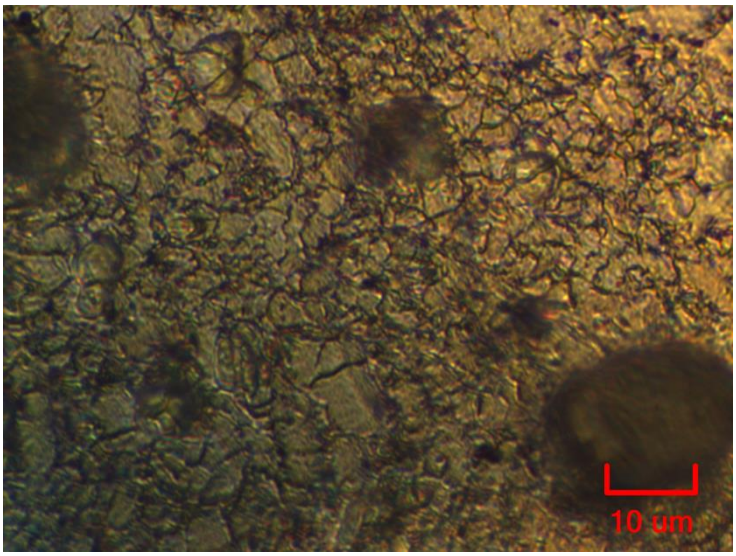

Figure 36: Micrograph of etched hybrid nanocomposite

4.3.5 Mechanical Properties

i. Micro and Macro Hardness Values

The result of macrohardness and microhardness measurement on the extruded monolithic and reinforced magnesium composite samples are shown in

Table 10. Significant improvement in magnesium hardness due to the presence of Nickel and TiO_2 particle reinforcement was observed, the microhardness of the Mg-Ni interfacial region in the hybrid composite was found to be higher when compared to that of the matrix region. The hardness value of the hybrid nanocomposite (Mg-1.50Ni-0.33TiO_2) was found to be higher than that of the nickel reinforced and TiO_2 reinforced composite.

Table 10: Results of Microhardness and Macrohardness of Mg-Pure and Mg-1.50Ni-0.33TiO_2 sample

Materials	**Micro Hardness (HV)**	**Macro Hardness (HR15T)**
Mg-Pure	39.96 ± 0.32	49.09 ± 1.42
Mg-1.50Ni-0.33TiO_2	60.52 ± 0.99	64.16 ± 0.57

ii. Tensile Test Results

The results of room temperature elongation-to-failure tensile test for monolithic and all the reinforced composites are shown in Table 11 and Figure 37.

The results of hybrid nanocomposite (Mg-150Ni-033TiO_2) reveal a significant simultaneous improvement in the tensile strength and the ductility of magnesium matrix due to the addition of nickel particle and TiO_2 nanoparticle while its yield strength was adversely affected.

Table 11: Result of room temperature tensile testing for Mg—Pure and Mg-1.50Ni-0.33TiO_2 sample

Materials	0.2% YS (MPa)	UTS (MPa)	% Elongation	WoF (MJ/m^3)
Mg-Pure	125.5 ± 3.12	199.56 ± 9.37	10.29 ± 2.85	17.12 ± 5.69
Mg-1.50Ni-0.33TiO_2	43.68 ± 7.85	248.43 ± 11.32	11.93 ± 1.04	17.64 ± 1.86

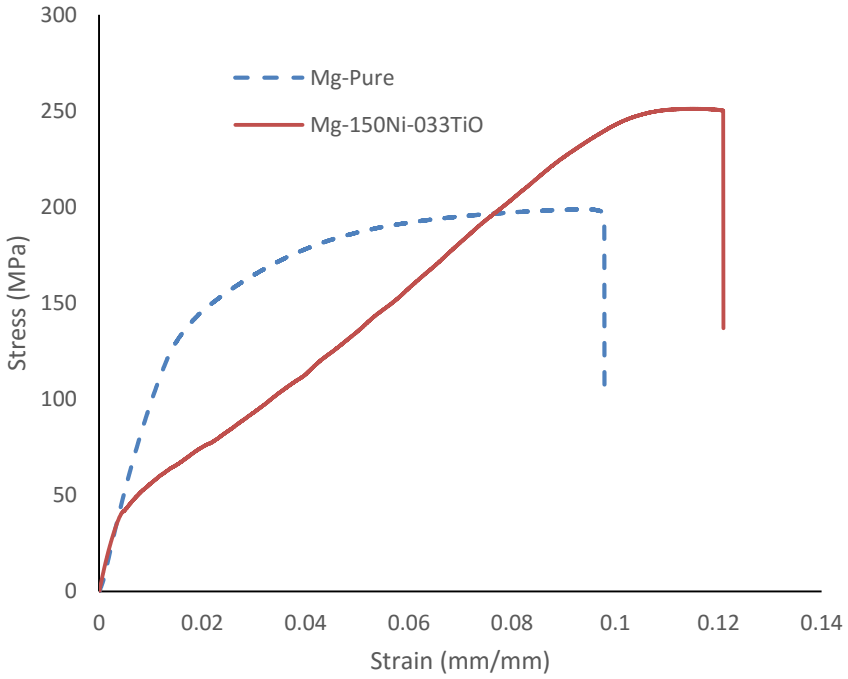

Figure 37: Tensile Stress-Strain curves of developed Mg-Pure and Mg-1.50Ni-0.33TiO2 sample

iii. Compressive Test Result

The results of room temperature compressive test for monolithic and all the reinforced composites are shown in

Table 12 and Figure 38.

Compressive test results of the developed hybrid nanocomposites (Mg-150Ni-033TiO2) reveals a significant increase in the compressive yield and ultimate compressive strength

of magnesium when compared with the monolithic and Ni particle reinforced composite, however a decrease in ductility was observed when compared with the monolithic magnesium composite.

Table 12: Result of room temperature compressive testing for Mg-Pure and Mg-1.50Ni-0.33TiO2 sample

Materials	**0.2% YS (MPa)**	**UCS (MPa)**	**% Elongation**	**WoF (MJ/m^3)**
Mg-Pure	66 ± 4.00	185.66 ± 1.72	22.01 ± 0.99	27.99 ± 1.89
Mg-1.50Ni-0.33TiO_2	140.33 ± 10.66	239.68 ± 9.54	19.40 ± 1.45	29.85 ± 6.35

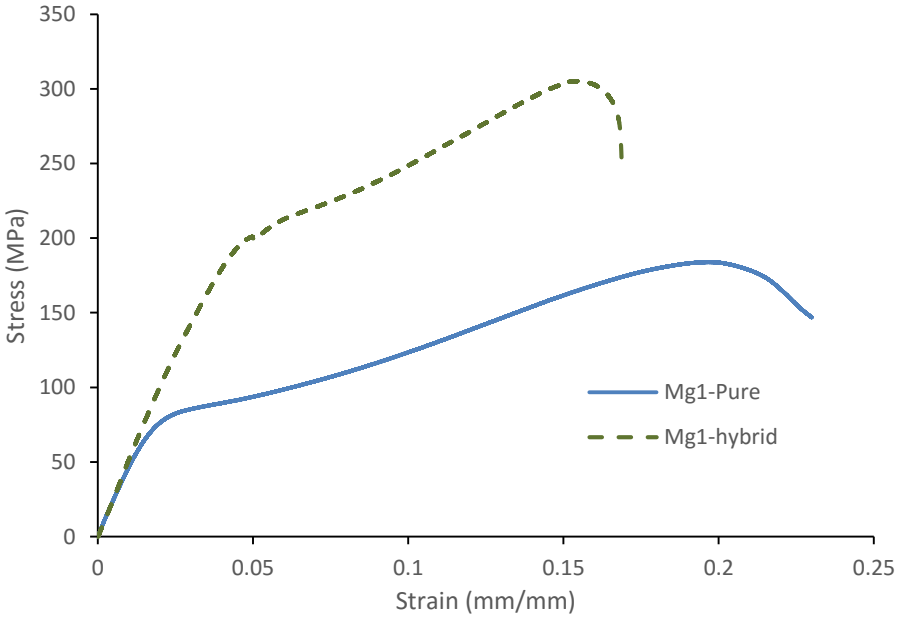

Figure 38: Compressive Stress-Strain curves of developed composites for Mg-Pure and Mg-1.50Ni-0.33TiO2 sample

4.3.6 Fractography

i. Tensile Fractography

Tensile fracture surfaces of extruded hybrid reinforced magnesium composite are shown in Figure 39. The fracture surface of the developed hybrid nanocomposite showed mixed mode of facture with uniform fracture surface at microscopic level.

Hybrid reinforced nanocomposite sample showed brittle features with reinforce particle cracking was observed in the elemental nickel reinforced magnesium sample fracture surface.

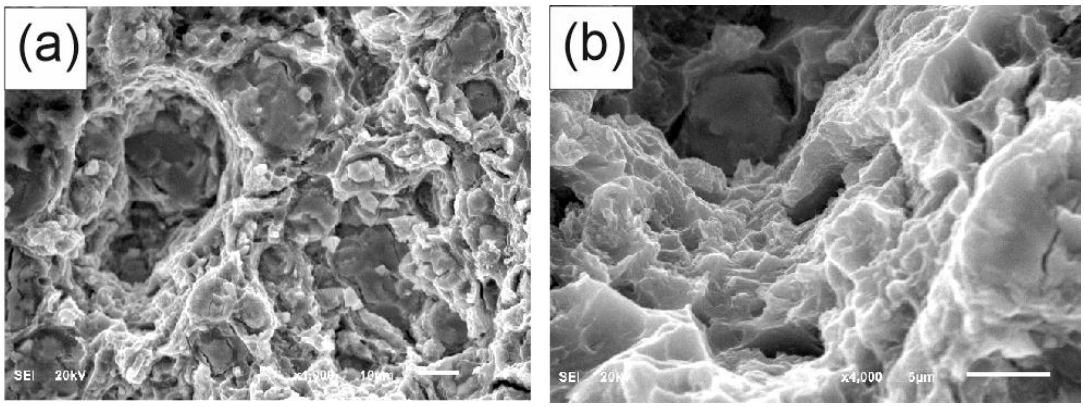

Figure 39: Scanning electron fractographs showing the tensile fracture surface of Mg-150Ni-033TiO2 samples at different magnification.

ii. Compressive Fractography

Compressive fracture surfaces of extruded monolithic and nickel particle reinforced magnesium are shown in Figure 40. The fracture surface showed the presence of shear band on the fracture surface of the reinforced composite.

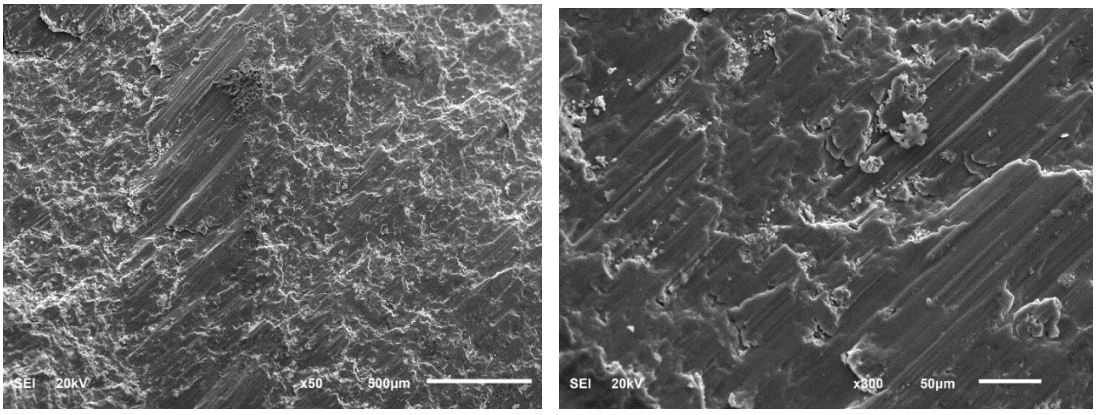

Figure 40: Scanning electron fractographs showing the compressive fracture surface of Mg-150Ni-033TiO_2 samples at different magnification.

CHAPTER 5

DISCUSSIONS

5.1. Mg-Ni Composite

5.1.1. Synthesis of reinforced and monolithic magnesium

The synthesis of monolithic and nickel particle reinforced magnesium composite was successfully accomplished by the blend-press-sinter powder metallurgy technique followed by hot extrusion. No macroscopic defects like oxidation, deformation or surface cracks were observed in compact and sintered billets and as well on the extruded rods. The density of the samples were greater than 99% of the theoretical density (Table 1) for both the monolithic and reinforced samples which indicates the appropriateness of the processing parameters used in this study. Large compaction pressure of 570 MPa and high extrusion ratio of 19.41:1 could be attributed as main reason in achieving the high density for the processed materials.

5.1.2. Microstructural characteristics

The microstructural characterization process of the elemental nickel reinforced magnesium is discussed in terms of the distribution pattern of nickel particle, nickel particle-magnesium matrix interfacial characteristics, the grain size of the samples and porosity. The distribution of nickel particles in the magnesium matrix were found to be reasonable uniformly (see Figure 13a) while some sporadic high-particle concentration area was noticed. The relative uniform distribution pattern of nickel particle in extruded reinforced magnesium is also supported by the almost zero standard deviation in the measured density

values (see Table 1) can be attributed to the use of: (i) suitable blending parameters, and (ii) high extrusion ratio. Secondary processing with a large enough deformation can homogeneously distribute reinforcements regardless of the size difference between matrix powder and reinforcement particulates [23]. The presence of the noticeable sporadic high particle concentration of nickel in the extruded reinforced magnesium composite can be attributed to the large difference in density between nickel (8.90 g/cm^3) and magnesium (1.74 g/cm^3) particles [36]. The Scanning electron microscopy image, EDX analysis and XRD results established the presence of elemental nickel particle as reinforcement without any identifiable nickel–magnesium reaction product and could be attributed to the relatively low sintering temperature of 500^{o}C used in this study [117]. Microstructural characterization also revealed defect-free interface formed between elemental nickel reinforcement-magnesium matrix, which was assessed in terms of presence of debonding and/or microvoid at interface.

The grains size analysis of the extruded samples revealed significant grain refinement due to the presence of elemental nickel particle in the magnesium matrix (see Table 1 and Figure 14). The nearly equal size and shaped fine grain in the nickel reinforced magnesium matrix can be attributed to the cumulative effect of dynamic recrystallization of the matrix with restricted grain growth specifically around the nickel reinforcement particle.

Microstructural characterization also shows negligible presence of minimal porosity in the elemental nickel reinforced magnesium matrix (see Table 1), which can be attributed to the cumulative effect of: (i) appropriate primary processing parameters, (ii) large extrusion ratio, and (iii) good compatibility between magnesium matrix and elemental nickel particles [117]. Earlier studies has established convincingly that an extrusion ratio of as

low as 12:1 is capable to nearly close micrometer-size porosity associated to metal-based reinforced materials [21,58,113,118].

5.1.3. Mechanical characteristics

The result of micro and macro hardness revealed significant increase due to the incorporation of nickel particle into magnesium matrix up to 30% and 36% in macro and micro hardness respectively, the improvement can attributed primarily to the presence of relatively harder reinforcement phase [36,113] and reduction in grain size which cumulatively increased the constrain to the localized matrix deformation during the indentation process. It may be noted that hardness results obtained for reinforced magnesium in the present study are similar to the findings reported for metallic and ceramic reinforced magnesium matrices [37].

The result of uniaxial tensile test revealed that the strength characteristics of the developed pure magnesium in this study was similar to the values reported by other's [34]. However, the yield strength of magnesium remained unchanged despite the inclusion of reasonable dispersed and well bonded particles of a much stiffer elemental nickel which induced significant grain refinement. The yield stress of a material is defined as the minimum stress required to mobilize dislocation and is governed by the dislocation density and magnitude of all the obstacles that restricts the motion of dislocation in the matrix. Increase in yield strength of reinforced metal matrix arises due to the presence of: (i) large dislocation density as a result of mismatch between coefficient of thermal expansion and elastic modulus of matrix and reinforcement, and (ii) increasing number of obstacle, stiffer reinforcement particle and grain boundaries in the case of grain refinement, to the dislocation motion [119–121]. Presence of low volume percentage of elemental nickel

particle (1.5vol%) as reinforcement in this study was apparently unable to increase dislocation density significantly during hot extrusion process and also unable to act well as effective barrier to the initiation of dislocation motion which led to the unchanged yield strength in this study. However, the onset of plastic deformation led to active dislocation-nickel particle interaction which induced effective strain hardening (see Figure 15) in the magnesium matrix and significantly increased (21%) the tensile strength.

The failure strain of the monolithic magnesium was found to be good (see Table 3) and reasonable higher that those reported in the literature for pure magnesium, the increment can be attributed to the fine grain of the hexagonal close packed structure matrix with grain boundary dislocation pile-up leading to intergranular crack propagation (see Figure 17b), the improvement in ductility was also justified by the fractography of the fractured tensile samples which reveals revealed pseudo-dimples (see Figure 17a and b) and intergranular crack propagation (see Figure 17c) for the monolithic magnesium sample. On the other hand, the presence of nickel led to a cumulative effect of brittle fracture of strain hardened nickel particles and presence of relatively higher level of porosity which outweigh the further refinement of the grains in the reinforced magnesium matrix leading to the relatively poor failure strain achieved, the fractographs of the fractures surface of the nickel reinforced magnesium composite also reveals brittle fracture features (see Figure 17d) with the presence of reinforcement particle cracking (see Figure 17e). The work of fracture expresses the ability of magnesium matrix to absorb energy up to fracture under tensile load, computed using stress-strain diagram, reduced when incorporated with elemental nickel due to the reduction in failure strain value.

The result of room temperature compressive test of the monolithic and nickel particle reinforced composite shows an increase in the 0.2% YS and UCS of magnesium due to the addition of nickel reinforcement, while the compressive fracture strain was reduced. It is well established that yielding in magnesium materials is due mainly to twinning effects. The increase in 0.2% Compressive yield strength and ultimate compressive strengths of magnesium can be attributed to the reduction in the twinning activity through grain refinement[47], the reduction in the twinning activities could also be responsible for the reduction in fracture strain [30]. The fractographs of the compressive fracture surface reveals the presence of shear bands which represents intense localized plastic deformation [30].

5.2. Mg-TiO_2 nanocomposite

5.2.1. Synthesis of reinforced and monolithic magnesium

The synthesis of monolithic and TiO_2 nanoparticle reinforced magnesium nanocomposite was successfully accomplished by the blend-press-sinter powder metallurgy technique followed by hot extrusion. No visible defects like oxidation, deformation or surface cracks were observed in compact and sintered billets and as well on the extruded rods.

5.2.2. Density Measurements

The results of density measurement on monolithic magnesium and Mg-TiO_2 nanocomposites indicate that the density of the samples was greater than 99% of the theoretical density (see Table 5). An increase in the experimental density was observed with the incorporation of TiO_2 nanoparticles, this is due to the higher density of Titania ($4.23 g/cm^3$) compared to Magnesium. The density result indicates the appropriateness of the processing parameters used in this study and that by using these process and parameters, near dense material can be obtained. Large compaction pressure of 570MPa and high extrusion ratio of 19.41:1 could be attributed as main reason in achieving the high density for the processed materials.

5.2.3. Microstructural characteristics

The FESEM image and EDX analysis established the presence of TiO_2 nanoparticle as reinforcement (see Figure 23) distribution of TiO_2 nanoparticles in the magnesium matrix were found to be reasonable uniformly as observed in the FESEM images (see Figure 4.14) indicating minimal agglomeration of the reinforcement in the composites. The relative uniform distribution pattern of nano-TiO_2 nanoparticle in extruded reinforced magnesium is also supported by the almost zero standard deviation in the measured experimental

density values (see Table 5) can be attributed to the use of suitable blending parameters, and high extrusion ratio of 22.5:1 capable of breaking down any agglomerates that might be present.

The grain size measurements using optical micrographs of etched monolithic Mg and reinforced Mg–TiO_2 nanocomposites indicate relatively finer grains for the reinforced Mg–TiO_2 nanocomposites when compared to that of monolithic pure Mg. The decrease in grain size with the addition of TiO_2 reinforcements can be attributed to a) recrystallization during hot extrusion b) recrystallization of Mg matrix through particle simulated nucleation (PSN) at the Mg-TiO_2 interface c) pinning effect due to uniformly distributed titania particles presented in the mg matrix and d) restriction of the grain growth of newly recrystallized grains by the TiO_2 nanoparticle [19].

5.2.4. Mechanical characteristics

The result of micro and macro hardness revealed no significant increase due to the incorporation of TiO_2 nanoparticle into magnesium matrix, increase in micro and micro hardness as a result of addition of nanoparticles into magnesium matrix usually arise dues to the constrain to localized matrix deformation during indentation process, it is obvious in this study that the volume percent of the TiO_2 nanoparticles used is small and could not effective increase the constrain to localized deformation of the magnesium matrix, hence the non-significant increase in the hardness values observed.

The result of uniaxial tensile test revealed that the strength characteristics of the reinforced composite were similar to that of the unreinforced sample. Considering the standard deviation, the 0.2% YS and the UTS was similar between the monolithic and the reinforced magnesium composites. In similar studies where addition of nanoscale reinforcement led

to superior strength, the improvement is attributed to Hall-Petch effect, in this study however, the addition of nano sized TiO_2 in this study is expected to improve the strength, however due to the observed change in Mg-crystal orientation (Figure 20 and Figure 21), the increase in strength is not significant, this is because the texture weakening would result in the activation of basal slip at relatively lower stress levels[118]. The ductility of the reinforced nanocomposite indicated by the fracture strain was increased due to the incorporation of TiO_2 nanoparticles. The increase in fracture strain was more noticeable for composite containing 0.33vol % and can be attributed to the combined effect of grain refinement, possible activation of non-basal slip systems as evident from the increase in the peak of the pyramidal plane in Figure 20. Similar observation have been previously reported for magnesium containing ultrafine nano particle reinforcement [38,46,67]. The fractography image for all the developed Mg materials under tensile loading revealed similar fracture features of a cleavage fracture mode which indicates that the fracture behavior was largely controlled by the Mg matrix deformation mechanism.

The room temperature compressive test results reveals an increase in the 0.2% CYS, UCS and fracture strain of magnesium due to the incorporation of TiO_2 nanoparticles, the improvement in compressive properties can be attributed to the effective transfer of load from the magnesium matrix to the TiO_2 nanoparticles and a number of other important mechanism which includes i) Orowan strengthening due to the presence of uniformly distributed nano TiO_2 particles [42,46], ii) Mismatch in the thermal expansion coefficient values of Mg and TiO_2 that could lead to the increased generation of dislocations [23,108], iii) Hall-Petch strengthening mechanism due to grain size reduction [42,45,122] and iv)

Taylor strengthening arising from the mismatch in the modulus values between the Mg matrix and TiO_2 reinforcements [38,67]

The ability of magnesium to absorb energy before fracture under compressive loading which corresponds to the area under the stress-strain curve was found to increase with the addition of TiO_2 nano particles as reflected in the Work of Fracture values, a maximum increase of ~44% was observed with 1.00 volume % of TiO_2

Fracture in pure Mg and Mg–TiO_2 nanocomposite was found to occur at approximately 45° with respect to the compression loading axis and the fractography images shows the presence of shear bands in all the developed Mg materials, the presence of shear bands indicates the twinning mode of plastic deformation which is common in Mg materials, no change in the fracture mode under compressive loading was observed.

5.2.5. Tension-Compression Asymmetry (TCA) of Mg-TiO_2 nanocomposite.

From the tensile and compressive test results (Table 7 and Table 8), it can be noted that the developed Mg materials display different yield strengths under tension and compression loading. The inclusion of nano-TiO_2 particles to monolithic Mg is observed to reduce the tension/compression yield asymmetry significantly. The ratio of tension–compression yield asymmetry (TCA) of Mg-1.00TiO_2 being ~1. The TCA of the monolithic composite was approximately 2 as common with magnesium and Mg alloys, the significant reduction in tension-compression asymmetry can be attributed to the strong influence of TiO_2 on the crystallographic orientation of magnesium. The high basal plane intensity along longitudinal and low intensity along transverse section of monolithic Mg as seen in the XRD spectrums (Figure 20 and Figure 21) are indicative of a typical basal texture of pure Mg with basal planes aligned parallel to the extrusion direction. However, the addition of

nanoscale TiO_2 particles has resulted in a reduction in the intensity of the basal planes along longitudinal section and its corresponding increase along the transverse-section, this is an indication of weakening of basal texture in Mg/TiO_2 nanocomposites relative to monolithic Mg, this will make basal slip more admissible in tension because they are no more parallel to the stress direction (extrusion direction). The presence of second phases is also expected to restrict the twining process under compression and reduce compressive ductility, however, no significant changes in compressive ductility was observed with the addition of TiO_2 and this could be from the effect of texture changes due to addition of TiO_2.

5.3. Magnesium hybrid nanocomposite

5.3.1. Synthesis of hybrid nanocomposite

The synthesis of the hybrid nanocomposite was successfully accomplished by the blend-press-sinter powder metallurgy technique followed by hot extrusion just as the Ni-particle reinforced and TiO_2 reinforced composites. Absence of visible defects such as macropores and blowhole on the samples after the process of compaction, sintering and extrusion indicates the appropriateness of the processing parameters used in each of the process. The result of density and porosity measurement indicates that near dense material can be obtained with the powder metallurgy process route using the processing parameters adopted in this study, increase in experimental density is obviously as a result of the relatively higher density of Ni and TiO_2 particles.

5.3.2. Microstructural characteristics

The microstructural characterization process of the hybrid magnesium composite is discussed in terms of the distribution of reinforcements, reinforcement-matrix interfacial characteristics and the grain size of the matrix. The distribution of reinforcements in the magnesium matrix was found to be reasonable uniformly while some few negligible pores were noticed. The relatively uniform distribution pattern of reinforcements in the magnesium matrix can be can be attributed to the use of suitable blending parameters and high extrusion ratio. The Scanning electron microscopy image, EDX analysis and XRD results established the presence of elemental nickel particle and TiO_2 as reinforcements without any identifiable reinforcement–matrix reaction product and could be attributed to the relatively low sintering temperature of 500^{o}C [117] used in this study. EDX mapping analysis reveals that the nano sized TiO_2 particles are more concentrated at the interface

between the micron sized nickel particle and the magnesium matrix (see Figure 35), this can be attributed to the difference in density of TiO_2 (4.23g/cm^3) compared to that of Ni (8.908g/cm^3) and Mg (1.74g/cm^3) and the smaller size of the TiO_2 particles making them to adhere more to the boundary between the matrix and the micron sized Ni reinforcement.

Significant grain refinement was achieved due to the presence of the hybrid reinforcement compare to the addition of individual reinforcement of Nickel and TiO_2, this can be attributed to the combined effect of the reinforcements to act effectively as nucleation site for the recrystallization of new nuclei and also to effectively restrict the growth of recrystallized grains specifically around the reinforcement particles.

5.3.3. Mechanical characteristics

Hardness measurement revealed significant increase in the hardness of the matrix due to the presence of hybrid reinforcement, the hardness values were greater than that of the individual reinforcement reinforced composites, the increase in hardness can be attributed to the more significant grain refinement resulting from the presence of relatively harder reinforcement phase [36,113] which will cumulatively increase the constrain to the localized matrix deformation during the hardness indentation process.

The result of room temperature uniaxial tensile test revealed that the tensile strength and fracture strain of the hybrid composite was significantly improved while the yield stress was adversely affected. The decrease in 0.2%YS can be attributed to the interaction between the micron sized Ni particulates and TiO_2 nano particles, due to the smaller size of the TiO_2 particles, they tend to agglomerates and adhere to the sharp corners or edges of Ni particles forming clusters at the Mg-Ni boundary, thus preventing direct load transfer from the magnesium matrix to the nickel particles. The TiO_2 nano particle can also cause

a relief of interfacial stress at the Mg-Ni interface during hot extrusion which will eventually lead to a decrease in the initial stress required to mobilize dislocation in that particular region and lead to a softening effect on the matrix, the presence of TiO_2 nano particle can also delay the nucleation and growth of cavities in advances of the crack tip under tensile loading. The decrease in stress required to move dislocation in the boundary of the matrix-reinforcement led to softening of the matrix and hence, the observed reduced yield stress while the delay of the growth of cavities in advance of the crack tip led to the observed elongated strain hardening in the stress-strain curve after yielding which resulted in the improved tensile strength, ductility and work of fracture [52,119,123]. The increase in tensile strength can also be attributed to the difference in the coefficient of thermal expansion of the reinforcements and Mg matrix. The presence of nano TiO_2 particles in the Mg matrix can also simultaneously activate non basal slip system which will delay the fracture process and result in the increased ductility observed [38].

The fractographs of the tensile facture surface reveals a mix mode of fracture, some micro voids are noticed around some of the nickel-matrix interface while it is absent in some interfaces. The micovoid noticed could have been generated by interfacial stress even in the absence of load as earlier established by Sankaranarayanan et al [52], while the absence of micro-voids around some of the Mg-Ni particles boundary confirms the relief of stress due to the presence of TiO_2 nano particles.

The result of room temperature compressive test of the hybrid reinforced composite revealed an increase in the 0.2% YS and UCS of magnesium due to the addition of nickel reinforcement, while the compressive fracture strain was reduced. It is established that in pure magnesium, twin formation and its propagation have been reported to be at favored

at relatively lower strength levels which results in high ductility during compression[47], while the addition of reinforcement obstructs the nucleation and propagation of twin which results in delayed yielding process leading to the higher strength properties and the poor ductility as a result of the restricted twinning process [30]. The significant improvement in tensile strength of the hybrid composite compared to the individual reinforcement can be attributed to the finer grain size.

The fractographs of the compressive fracture surface reveals the presence of shear bands, the developed hybrid composites also showed rough fracture surfaces with mixed mode of shear and brittle features. The presence of shear bands generally attributes to the twinning mode of plastic deformation as common with Mg materials.

CHAPTER 6

CONCLUSIONS

Mg composites reinforced with micron size nickel, nano sized titania and an hybrid of nickel and TiO_2 reinforcements were successfully developed using the conventional cost effective powder metallurgy route of blend-press-sinter followed by hot extrusion, the effect of the reinforcements on the microstructure and mechanical properties of magnesium were studied and base on the structure-property correlation, the following conclusions are drawn.

1. The addition of nickel particle reinforcement significantly reduced the average grain size and increased the hardness when compared to monolithic magnesium.
2. Elemental nickel particle is capable of improving the hardness and ultimate tensile strength of commercially pure magnesium matrix without affecting the yield strength. However, ductility of magnesium matrix was adversely affected by nickel particles.
3. Under compressive loading, the addition of nickel particle to magnesium significantly improves the compressive yield strength and ultimate compressive strength while the ductility was reduced owing to difficulty in twinning.
4. The addition of nano-sized TiO_2 reinforcement led to significant grain refinement compared to the monolithic Mg sample.
5. XRD studies conducted on the nano-TiO_2 reinforced composite revealed the weakening of the basal texture of magnesium matrix.

6. Under tensile loading, the developed Mg-TiO_2 nanocomposite exhibits similar strength characteristics as the monolithic Mg and enhanced ductility attributed to the activation of non-basal slip system.
7. Under compressive loading, addition of nano TiO_2 led to significant improvement in the 0.2% yield stress and UTS, while no significant change was observed in the compressive ductility.
8. The addition of nano TiO_2 to magnesium matrix led to a reduction in the tension-compression asymmetry ratio which was attributed to the weakening of the strong basal texture in pure Mg.
9. The composite sample containing 0.33vol % of TiO_2 had the best combination of mechanical properties and was chosen for the hybrid composite.
10. Addition of hybrid reinforcement (1.5Vol% Ni and 0.33vol%TiO_2) led to significant grain refinement of the magnesium matrix and improvement in its hardness.
11. Under tensile loading, the hybrid reinforcement led to significant improvement in the ultimate tensile strength and ductility of magnesium but with a deteriorating effect on the ductility.
12. Significant improvement in the compressive yield strength, ultimate compressive strength of the hybrid reinforced Mg composite was achieved without adverse effect on its ductility.

CHAPTER 7

RECCOMENDATIONS

The present work led to the development of near dense monolithic and reinforced magnesium composites through powder metallurgy process route of blend-press-sinter and their microstructural characterization of their microstructure and mechanical properties were examined. Further microstructural analysis of the developed reinforced materials is recommended. This may include:

- TEM characterization of the microstructure to further investigate the formation of secondary phases, interface between matrix and reinforcements.
- Pole figure analysis of the Mg-TiO_2 and hybrid nanocomposites to investigate the effect of the nanoparticle on the crystallographic texture of magnesium.
- Investigation of the coefficient of thermal expansion of the developed composites to determine its thermal stability.
- Investigation of the corrosion behavior of the Mg-TiO_2 nanocomposites in body simulated fluid to establish its biocompatibility.
- Evaluation of mechanical properties of magnesium as function of very small difference in volume fraction of nano size reinforcement.

References

[1] M. Gupta, N.M.L. Sharon, Magnesium, Magnesium Alloys, and Magnesium Composites, John Wiley & Sons, 2011.

[2] G. Neite, K. Kubota, K. Higashi, F. Hehmann, Magnesium-Based Alloys, Wiley-VCH Verlag GmbH & Co. KGaA, Weinheim, Germany, 2006. doi:10.1002/9783527603978.

[3] H.Z. Ye, X.Y. Liu, Review of recent studies in magnesium matrix composites, J. Mater. Sci. 9 (2004) 6153–6171. doi:10.1023/B:JMSC.0000043583.47148.31.

[4] E.L. Bray, 2013 Minerals Yearbook (Magnesium), U.S. Geol. Surv. (2015).

[5] J.J. Kim, D.S. Han, Recent Development and Applications of Magnesium Alloys in the Hyundai and Kia Motors Corporation, Mater. Trans. 49 (2008) 894–897. doi:10.2320/matertrans.MC200731.

[6] K.U. Kainer, Magnesium Alloys and Technology, John Wiley & Sons, 2003.

[7] G.D. COLE, MAGNESIUM, Chem. Eng. News. 81 (2003) 52. doi:10.1021/cen-v081n036.p052.

[8] H.E. Friedrich, B.L. Mordike, Magnesium Technology: Metallurgy, Design Data, Applications, (2006) 677.

[9] M.P. Staiger, A.M. Pietak, J. Huadmai, G. Dias, Magnesium and its alloys as orthopedic biomaterials: A review, Biomaterials. 27 (2006) 1728–1734. doi:10.1016/j.biomaterials.2005.10.003.

[10] K.F. Farraro, K.E. Kim, S.L.Y. Woo, J.R. Flowers, M.B. McCullough, Revolutionizing orthopaedic biomaterials: The potential of biodegradable and bioresorbable magnesium-based materials for functional tissue engineering, J. Biomech. 47 (2014) 1979–1986. doi:10.1016/j.jbiomech.2013.12.003.

[11] F. Witte, F. Feyerabend, P. Maier, J. Fischer, M. Störmer, C. Blawert, et al., Biodegradable magnesium-hydroxyapatite metal matrix composites, Biomaterials. 28 (2007) 2163–2174. doi:10.1016/j.biomaterials.2006.12.027.

[12] S. Zhang, X. Zhang, C. Zhao, J. Li, Y. Song, C. Xie, et al., Research on an Mg-Zn alloy as a degradable biomaterial, Acta Biomater. 6 (2010) 626–640. doi:10.1016/j.actbio.2009.06.028.

[13] T. Liu, C. Wang, Y. Wu, Mg-based nanocomposites with improved hydrogen storage performances, Int. J. Hydrogen Energy. 39 (2014) 14262–14274. doi:10.1016/j.ijhydene.2014.03.125.

[14] T. Liu, C. Chen, C. Qin, X. Li, Improved hydrogen storage properties of Mg-based nanocomposite by addition of LaNi5 nanoparticles, Int. J. Hydrogen Energy. 39 (2014) 18273–18279. doi:10.1016/j.ijhydene.2014.03.041.

[15] T. Liu, C. Chen, F. Wang, X. Li, Enhanced hydrogen storage properties of magnesium by the synergic catalytic effect of TiH1.971 and TiH1.5 nanoparticles at room temperature, J. Power Sources. 267 (2014) 69–77. doi:10.1016/j.jpowsour.2014.05.066.

[16] I.P. Jain, C. Lal, A. Jain, Hydrogen storage in Mg: A most promising material, Int. J. Hydrogen Energy. 35 (2010) 5133–5144. doi:10.1016/j.ijhydene.2009.08.088.

[17] S. Sankaranarayanan, R.K.K. Sabat, S. Jayalakshmi, S. Suwas, M. Gupta, Effect of nanoscale boron carbide particle addition on the microstructural evolution and mechanical response of pure magnesium, Mater. Des. 56 (2014) 428–436. doi:10.1016/j.matdes.2013.11.031.

[18] H. Ferkel, B.L.L. Mordike, Magnesium strengthened by SiC nanoparticles, Mater. Sci. Eng. A. 298 (2001) 193–199. doi:10.1016/S0921-5093(00)01283-1.

[19] S.F. Hassan, M. Gupta, Effect of different types of nano-size oxide particulates on microstructural and mechanical properties of elemental Mg, J. Mater. Sci. 41 (2006) 2229–2236. doi:10.1007/s10853-006-7178-3.

[20] S.F. Hassan, M. Gupta, Effect of type of primary processing on the microstructure, CTE and mechanical properties of magnesium/alumina nanocomposites, Compos. Struct. 72 (2006) 19–26. doi:10.1016/j.compstruct.2004.10.008.

[21] C.S. Goh, J. Wei, L.C. Lee, M. Gupta, Development of novel carbon nanotube reinforced magnesium nanocomposites using the powder metallurgy technique, Nanotechnology. 17 (2005) 7–12. doi:10.1088/0957-4484/17/1/002.

[22] H. Yu, H.S. Yu, Z.Y. Zhang, G.H. Min, C. Chen, Microstructural Evolution and Mechanical Properties of AZ91 and SiCp/AZ91 Magnesium Alloys upon Rapid Solidification/Powder Metallurgy Followed by Hot Extrusion, in: Adv. Mater. Res., 2011: pp. 734–737. http://www.scientific.net/AMR.146-147.734 (accessed May 5, 2015).

[23] S.F. Hassan, M. Gupta, Development of high strength magnesium copper based hybrid composites with enhanced tensile properties, Mater. Sci. Technol. 19

(2003) 253–259. doi:10.1179/026708303225009346.

[24] M. Paramsothy, S.F. Hassan, N. Srikanth, M. Gupta, Toughening mechanisms in Mg/Al macrocomposites: texture and interfacial mechanical interlocking, J. Phys. D. Appl. Phys. 41 (2008) 175402. doi:10.1088/0022-3727/41/17/175402.

[25] R. Casati, M. Vedani, Metal Matrix Composites Reinforced by Nano-Particles—A Review, Metals (Basel). 4 (2014) 65–83. doi:10.3390/met4010065.

[26] S.C. Tjong, Novel Nanoparticle-Reinforced Metal Matrix Composites with Enhanced Mechanical Properties, Adv. Eng. Mater. 9 (2007) 639–652. doi:10.1002/adem.200700106.

[27] V.K. Lindroos, M.J. Talvitie, Recent advances in metal matrix composites, J. Mater. Process. Technol. 53 (1995) 273–284. doi:10.1016/0924-0136(95)01985-N.

[28] D.J. Lloyd, Particle reinforced aluminium and magnesium matrix composites, Int. Mater. Rev. 39 (1994) 1–23. doi:10.1179/095066094790150982.

[29] C. Suryanarayana, Synthesis of nanocomposites by mechanical alloying, J. Alloys Compd. 509 (2011) S229–S234. doi:10.1016/j.jallcom.2010.09.063.

[30] K.S. Tun, M. Gupta, Role of Microstructure and Texture on Compressive Strength Improvement of Mg/(Y2O 3 + Cu) Hybrid Nanocomposites, J. Compos. Mater. 44 (2010) 3033–3050. doi:10.1177/0021998310369591.

[31] K.S. Tun, M. Gupta, Development of magnesium/(yttria+nickel) hybrid nanocomposites using hybrid microwave sintering: Microstructure and tensile properties, J. Alloys Compd. 487 (2009) 76–82.

doi:10.1016/j.jallcom.2009.07.117.

[32] K.S. Tun, M. Gupta, T.S. Srivatsan, Investigating influence of hybrid (yttria + copper) nanoparticulate reinforcements on microstructural development and tensile response of magnesium, Mater. Sci. Technol. 26 (2010) 87–94. doi:10.1179/174328408X388095.

[33] F. Moll, K.U. Kainer, Particle-Reinforced Magnesium Alloys, Magnes. Alloy. Technol. (2003). doi:10.1002/3527602046.ch12.

[34] W.L.E. Wong, M. Gupta, Enhancing Thermal Stability, Modulus and Ductility of Magnesium using Molybdenum as Reinforcement, Adv. Eng. Mater. 7 (2005) 250–256. doi:10.1002/adem.200400137.

[35] S.F. Hassan, M. Gupta, Development of ductile magnesium composite materials using titanium as reinforcement, J. Alloys Compd. 345 (2002) 246–251. doi:10.1016/S0925-8388(02)00413-9.

[36] S.F. Hassan, O.O. Nasirudeen, N. Al-Aqeeli, N. Saheb, F. Patel, M.M.A. Baig, Magnesium–nickel composite: Preparation, microstructure and mechanical properties, J. Alloys Compd. 646 (2015) 333–338. doi:10.1016/j.jallcom.2015.06.099.

[37] S.. Hassan, K.. Ho, M. Gupta, Increasing elastic modulus, strength and CTE of AZ91 by reinforcing pure magnesium with elemental copper, Mater. Lett. 58 (2004) 2143–2146. doi:10.1016/j.matlet.2004.01.011.

[38] G.K. Meenashisundaram, M.H. Nai, A. Almajid, M. Gupta, Development of high

performance Mg–TiO2 nanocomposites targeting for biomedical/structural applications, Mater. Des. 65 (2015) 104–114. doi:10.1016/j.matdes.2014.08.041.

[39] K.B. Nie, X.J. Wang, X.S. Hu, L. Xu, K. Wu, M.Y. Zheng, Microstructure and mechanical properties of SiC nanoparticles reinforced magnesium matrix composites fabricated by ultrasonic vibration, Mater. Sci. Eng. A. 528 (2011) 5278–5282. doi:10.1016/j.msea.2011.03.061.

[40] C.S. Goh, J. Wei, L.C. Lee, M. Gupta, Simultaneous enhancement in strength and ductility by reinforcing magnesium with carbon nanotubes, Mater. Sci. Eng. A. 423 (2006) 153–156. doi:10.1016/j.msea.2005.10.071.

[41] K.B. Nie, X.J. Wang, K. Wu, L. Xu, M.Y. Zheng, X.S. Hu, Processing, microstructure and mechanical properties of magnesium matrix nanocomposites fabricated by semisolid stirring assisted ultrasonic vibration, J. Alloys Compd. 509 (2011) 8664–8669. doi:10.1016/j.jallcom.2011.06.091.

[42] S.F. Hassan, Effect of primary processing techniques on the microstructure and mechanical properties of nano-Y2O3 reinforced magnesium nanocomposites, Mater. Sci. Eng. A. 528 (2011) 5484–5490. doi:10.1016/j.msea.2011.03.063.

[43] V.H. Hammond, Magnesium Nanocomposites : Current Status and Prospects for Army Applications, (2011) ARL–TR–5728.

[44] W. WONG, M. GUPTA, Development of Mg/Cu nanocomposites using microwave assisted rapid sintering, Compos. Sci. Technol. 67 (2007) 1541–1552. doi:10.1016/j.compscitech.2006.07.015.

[45] S. Fida Hassan, K.S. Tun, F. Patel, M. Gupta, Effect of copper nano particles on high temperature tensile behavior of Mg-Y2O3 nanocomposite, Met. Mater. Int. 21 (2015) 588–592. doi:10.1007/s12540-015-4188-1.

[46] G.K. Meenashisundaram, S. Seetharaman, M. Gupta, Enhancing overall tensile and compressive response of pure Mg using nano-TiB2 particulates, Mater. Charact. 94 (2014) 178–188. doi:10.1016/j.matchar.2014.05.021.

[47] M. Gupta, W.L.E. Wong, Magnesium-based nanocomposites: Lightweight materials of the future, Mater. Charact. 105 (2015) 30–46. doi:10.1016/j.matchar.2015.04.015.

[48] K. Tun, V. Tungala, Q. Nguyen, J. Chan, R. Kwok, J. Kuma, et al., Enhancing tensile and compressive strengths of magnesium using nanosize (Al2O3 + Cu) hybrid reinforcements, J. Compos. Mater. 46 (2011) 1879–1887. doi:10.1177/0021998311427767.

[49] S. Sankaranarayanan, S. Jayalakshmi, M. Gupta, Effect of ball milling the hybrid reinforcements on the microstructure and mechanical properties of Mg–(Ti+n-Al2O3) composites, J. Alloys Compd. 509 (2011) 7229–7237. doi:10.1016/j.jallcom.2011.04.083.

[50] Q.B. Nguyen, K.S. Tun, J. Chan, R. Kwok, J.V.M. Kuma, T.H. Phung, et al., Simultaneous effect of nano-Al 2 O 3 and micrometre Cu particulates on microstructure and mechanical properties of magnesium alloy AZ31, Mater. Sci. Technol. 28 (2012) 227–233. doi:10.1179/1743284711Y.0000000023.

[51] S. Sankaranarayanan, S. Jayalakshmi, M. Gupta, Effect of individual and

combined addition of micro/nano-sized metallic elements on the microstructure and mechanical properties of pure Mg, Mater. Des. 37 (2012) 274–284. doi:10.1016/j.matdes.2012.01.009.

[52] S. Sankaranarayanan, S. Jayalakshmi, M. Gupta, Effect of nano-Al2O3 addition and heat treatment on the microstructure and mechanical properties of Mg-(5.6Ti+3Al) composite, Mater. Charact. 75 (2012) 150–164. doi:10.1016/j.matchar.2012.10.005.

[53] J. Jayakumar, Recent Development and Challenges in Synthesis of Magnesium Matrix Nano Composites- A Review, 1 (2012).

[54] M.M. Avedesian, H. Baker, ASM Specialty Handbook: Magnesium and Magnesium Alloys, ASM International, 1999. https://books.google.com/books?id=0wFMfJg57YMC&pgis=1 (accessed December 9, 2015).

[55] N. Chawla, K.K. Chawla, Metal Matrix Composites, Springer, 2006. https://books.google.com/books?id=gU1tagimjIcC&pgis=1 (accessed December 9, 2015).

[56] J. Lan, Y. Yang, X. Li, Microstructure and microhardness of SiC nanoparticles reinforced magnesium composites fabricated by ultrasonic method, Mater. Sci. Eng. A. 386 (2004) 284–290. doi:10.1016/j.msea.2004.07.024.

[57] G. Cao, H. Konishi, X. Li, Mechanical properties and microstructure of SiC-reinforced Mg-(2,4)Al-1Si nanocomposites fabricated by ultrasonic cavitation based solidification processing, Mater. Sci. Eng. A. 486 (2008) 357–362.

doi:10.1016/j.msea.2007.09.054.

[58] K.B.B. Nie, X.J.J. Wang, K. Wu, L. Xu, M.Y.Y. Zheng, X.S.S. Hu, Processing, microstructure and mechanical properties of magnesium matrix nanocomposites fabricated by semisolid stirring assisted ultrasonic vibration, J. Alloys Compd. 509 (2011) 8664–8669. doi:10.1016/j.jallcom.2011.06.091.

[59] S.Y. Liu, F.P. Gao, Q.Y. Zhang, X. Zhu, W.Z. Li, Fabrication of carbon nanotubes reinforced AZ91D composites by ultrasonic processing, Trans. Nonferrous Met. Soc. China (English Ed. 20 (2010) 1222–1227. doi:10.1016/S1003-6326(09)60282-X.

[60] X.Y. Jia, S.Y. Liu, F.P. Gao, Q.Y. Zhang, W.Z. Li, Magnesium matrix nanocomposites fabricated by ultrasonic assisted casting, Int. J. Cast Met. Res. 22 (2009) 196–199. doi:10.1179/136404609X367704.

[61] L.-Y. Chen, J.-Y. Peng, J.-Q. Xu, H. Choi, X.-C. Li, Achieving uniform distribution and dispersion of a high percentage of nanoparticles in metal matrix nanocomposites by solidification processing, Scr. Mater. 69 (2013) 634–637. doi:10.1016/j.scriptamat.2013.07.016.

[62] J.C. Wong, M. Paramsothy, M. Gupta, Using Mg and Mg-nanoAl2O3 concentric alternating macro-ring material design to enhance the properties of magnesium, Compos. Sci. Technol. 69 (2009) 438–444. doi:10.1016/j.compscitech.2008.11.009.

[63] M. Habibnejad-Korayem, R. Mahmudi, W.J. Poole, Enhanced properties of Mg-based nano-composites reinforced with Al2O3 nano-particles, Mater. Sci. Eng. A.

519 (2009) 198–203. doi:10.1016/j.msea.2009.05.001.

[64] S.F. Hassan, M. Gupta, Effect of submicron size Al2O3 particulates on microstructural and tensile properties of elemental Mg, J. Alloys Compd. 457 (2008) 244–250. doi:10.1016/j.jallcom.2007.03.058.

[65] M.E. Alam, A.M.S. Hamouda, Q.B. Nguyen, M. Gupta, Improving microstructural and mechanical response of new AZ41 and AZ51 magnesium alloys through simultaneous addition of nano-sized Al 2O3 particulates and Ca, J. Alloys Compd. 574 (2013) 565–572. doi:10.1016/j.jallcom.2013.04.207.

[66] C. GOH, J. WEI, L. LEE, M. GUPTA, Properties and deformation behaviour of Mg–Y2O3 nanocomposites, Acta Mater. 55 (2007) 5115–5121. doi:10.1016/j.actamat.2007.05.032.

[67] G.K. Meenashisundaram, M. Gupta, Synthesis and characterization of high performance low volume fraction TiC reinforced Mg nanocomposites targeting biocompatible/structural applications, Mater. Sci. Eng. A. 627 (2015) 306–315. doi:10.1016/j.msea.2015.01.007.

[68] Q.B. Nguyen, Y.H.M. Sim, M. Gupta, C.Y.H. Lim, Tribology characteristics of magnesium alloy AZ31B and its composites, Tribol. Int. (2014). doi:10.1016/j.triboint.2014.02.024.

[69] J. Jayakumar, B.K. Raghunath, T.H. Rao, Enhancing microstructure and mechanical properties of AZ31-MWCNT nanocomposites through mechanical alloying, Adv. Mater. Sci. Eng. 2013 (2013) 1–6. doi:10.1155/2013/539027.

[70] S.F. Hassan, M. Gupta, Effect of Nano-ZrO2 Particulates Reinforcement on Microstructure and Mechanical Behavior of Solidification Processed Elemental Mg, J. Compos. Mater. 41 (2007) 2533–2543. doi:10.1177/0021998307074187.

[71] S. Sankaranarayanan, R.K. Sabat, S. Jayalakshmi, S. Suwas, M. Gupta, Microstructural evolution and mechanical properties of Mg composites containing nano-B4C hybridized micro-Ti particulates, Mater. Chem. Phys. 143 (2014) 1178–1190. doi:10.1016/j.matchemphys.2013.11.019.

[72] C.D. Li, X.J. Wang, K. Wu, W.Q. Liu, S.L. Xiang, C. Ding, et al., Distribution and integrity of carbon nanotubes in carbon nanotube/magnesium composites, J. Alloys Compd. 612 (2014) 330–336. doi:10.1016/j.jallcom.2014.05.153.

[73] M.K.K. Oo, P.S. Ling, M. Gupta, Characteristics of Mg-based composites synthesized using a novel mechanical disintegration and deposition technique, Metall. Mater. Trans. A. 31 (2000) 1873–1881. doi:10.1007/s11661-006-0241-5.

[74] M. Güvendiren, E. Baybörü, T. Öztürk, Effects of additives on mechanical milling and hydrogenation of magnesium powders, Int. J. Hydrogen Energy. 29 (2004) 491–496. doi:10.1016/S0360-3199(03)00091-0.

[75] L. Lü, M.O. Lai, W. Liang, Magnesium nanocomposite via mechanochemical milling, Compos. Sci. Technol. 64 (2004) 2009–2014. doi:10.1016/j.compscitech.2004.02.018.

[76] X.L. Zhong, W.L.E. Wong, M. Gupta, Enhancing strength and ductility of magnesium by integrating it with aluminum nanoparticles, Acta Mater. 55 (2007) 6338–6344. doi:10.1016/j.actamat.2007.07.039.

[77] S. Hwang, C. Nishimura, P.G. McCormick, Mechanical milling of magnesium powder, Mater. Sci. Eng. A. 318 (2001) 22–33. doi:10.1016/S0921-5093(01)01767-1.

[78] J. Liu, C. Suryanarayana, D. Ghosh, G. Subhash, L. An, Synthesis of Mg-Al2O3 nanocomposites by mechanical alloying, J. Alloys Compd. 563 (2013) 165–170. doi:10.1016/j.jallcom.2013.01.113.

[79] J. Bridgwater, Fundamental powder mixing mechanisms, Powder Technol. 15 (1976) 215–236. doi:10.1016/0032-5910(76)80051-4.

[80] M.O. Lai, L. Lu, W. Laing, Formation of magnesium nanocomposite via mechanical milling, Compos. Struct. 66 (2004) 301–304. doi:10.1016/j.compstruct.2004.04.052.

[81] Powder Metallurgy, (n.d.). http://thelibraryofmanufacturing.com/powder_processes.html (accessed November 15, 2015).

[82] W.W.L. Eugene, M. Gupta, Characteristics of aluminum and magnesium based nanocomposites processed using hybrid microwave sintering., J. Microw. Power Electromagn. Energy. 44 (2010) 14–27.

[83] K.S. Tun, M. Gupta, Effect of heating rate during hybrid microwave sintering on the tensile properties of magnesium and Mg/Y2O3 nanocomposite, J. Alloys Compd. 466 (2008) 140–145. doi:10.1016/j.jallcom.2007.11.047.

[84] W.L.E. Wong, M. Gupta, Improving Overall Mechanical Performance of

Magnesium Using Nano-Alumina Reinforcement and Energy Efficient Microwave Assisted Processing Route, Adv. Eng. Mater. 9 (2007) 902–909. doi:10.1002/adem.200700169.

[85] M. Gupta, W.L.E. Wong, Enhancing overall mechanical performance of metallic materials using two-directional microwave assisted rapid sintering, Scr. Mater. 52 (2005) 479–483. doi:10.1016/j.scriptamat.2004.11.006.

[86] M.K. Habibi, M. Qian, A.S. Hamouda, M. Gupta, Differentiating the mechanical response of hierarchical magnesium nano-composites as a function of temperature, Mater. Des. 42 (2012) 102–110. doi:10.1016/j.matdes.2012.05.037.

[87] K.S. Tun, M. Gupta, Effect of extrusion ratio on microstructure and mechanical properties of microwave-sintered magnesium and Mg/Y2O3 nanocomposite, J. Mater. Sci. 43 (2008) 4503–4511. doi:10.1007/s10853-008-2649-3.

[88] J. Liu, K. Zhao, M. Zhang, Y. Wang, L. An, High performance heterogeneous magnesium-based nanocomposite, Mater. Lett. 143 (2015) 287–289. doi:10.1016/j.matlet.2014.12.099.

[89] K.B. Nie, X.J. Wang, L. Xu, K. Wu, X.S. Hu, M.Y. Zheng, Influence of extrusion temperature and process parameter on microstructures and tensile properties of a particulate reinforced magnesium matrix nanocomposite, Mater. Des. 36 (2012) 199–205. doi:10.1016/j.matdes.2011.11.020.

[90] S.F. Hassan, K.S. Tun, M. Gupta, Effect of sintering techniques on the microstructure and tensile properties of nano-yttria particulates reinforced magnesium nanocomposites, J. Alloys Compd. 509 (2011) 4341–4347.

doi:10.1016/j.jallcom.2011.01.064.

[91] K.B. Nie, K.K. Deng, X.J. Wang, W.M. Gan, F.J. Xu, K. Wu, et al., Microstructures and mechanical properties of SiCp/AZ91 magnesium matrix nanocomposites processed by multidirectional forging, J. Alloys Compd. 622 (2015) 1018–1026. doi:10.1016/j.jallcom.2014.11.045.

[92] X. Xia, Q. Chen, Z. Zhao, M. Ma, X. Li, K. Zhang, Microstructure, texture and mechanical properties of coarse-grained Mg–Gd–Y–Nd–Zr alloy processed by multidirectional forging, J. Alloys Compd. 623 (2015) 62–68. doi:10.1016/j.jallcom.2014.10.084.

[93] S.F. Hassan, M. Gupta, Development of high performance magnesium nano-composites using nano-Al2O3 as reinforcement, Mater. Sci. Eng. A. 392 (2005) 163–168. doi:10.1016/j.msea.2004.09.047.

[94] S.F. Hassan, M. Gupta, Development of nano-Y2O3 containing magnesium nanocomposites using solidification processing, J. Alloys Compd. 429 (2007) 176–183. doi:10.1016/j.jallcom.2006.04.033.

[95] D. Zhang, P. Shen, L. Shi, Q. Jiang, Wetting of B4C, TiC and graphite substrates by molten Mg, Mater. Chem. Phys. 130 (2011) 665–671. doi:10.1016/j.matchemphys.2011.07.040.

[96] K.K. Chawla, Mechanical Behavior of Materials, 1999. https://books.google.com.sa/books/about/Mechanical_Behavior_of_Materials.html?id=caJRAAAAMAAJ&pgis=1 (accessed December 23, 2015).

[97] D. Witkin, Z. Lee, R. Rodriguez, S. Nutt, E. Lavernia, Al–Mg alloy engineered with bimodal grain size for high strength and increased ductility, Scr. Mater. 49 (2003) 297–302. doi:10.1016/S1359-6462(03)00283-5.

[98] Y. Li, Y.H. Zhao, V. Ortalan, W. Liu, Z.H. Zhang, R.G. Vogt, et al., Investigation of aluminum-based nanocomposites with ultra-high strength, Mater. Sci. Eng. A. 527 (2009) 305–316. doi:10.1016/j.msea.2009.07.067.

[99] Z. Zhang, D. Chen, Consideration of Orowan strengthening effect in particulate-reinforced metal matrix nanocomposites: A model for predicting their yield strength, Scr. Mater. 54 (2006) 1321–1326. doi:10.1016/j.scriptamat.2005.12.017.

[100] S.F. Hassan, M.J. Tan, M. Gupta, High-temperature tensile properties of Mg/Al2O3 nanocomposite, Mater. Sci. Eng. A. 486 (2008) 56–62. doi:10.1016/j.msea.2007.08.045.

[101] Z. Zhang, D.L. Chen, Contribution of Orowan strengthening effect in particulate-reinforced metal matrix nanocomposites, Mater. Sci. Eng. A. 483-484 (2008) 148–152. doi:10.1016/j.msea.2006.10.184.

[102] R.E. Smallman, A.H.W. Ngan, Physical Metallurgy and Advanced Materials Engineering, Elsevier, 2007. doi:10.1016/B978-075066906-1/50015-9.

[103] A. Sanaty-Zadeh, Comparison between current models for the strength of particulate-reinforced metal matrix nanocomposites with emphasis on consideration of Hall–Petch effect, Mater. Sci. Eng. A. 531 (2012) 112–118. doi:10.1016/j.msea.2011.10.043.

[104] Q.B. Nguyen, M. Gupta, Enhancing compressive response of AZ31B using nano-Al2O3 and copper additions, J. Alloys Compd. 490 (2010) 382–387. doi:10.1016/j.jallcom.2009.09.188.

[105] a. Sanaty-Zadeh, Comparison between current models for the strength of particulate-reinforced metal matrix nanocomposites with emphasis on consideration of Hall–Petch effect, Mater. Sci. Eng. A. 531 (2012) 112–118. doi:10.1016/j.msea.2011.10.043.

[106] R. Kapoor, N. Kumar, R.S. Mishra, C.S. Huskamp, K.K. Sankaran, Influence of fraction of high angle boundaries on the mechanical behavior of an ultrafine grained Al–Mg alloy, Mater. Sci. Eng. A. 527 (2010) 5246–5254. doi:10.1016/j.msea.2010.04.086.

[107] S. Hwang, C. Nishimura, P.G. McCormick, Compressive mechanical properties of Mg-Ti-C nanocomposite synthesised by mechanical milling, Scr. Mater. 44 (2001) 2457–2462. doi:10.1016/S1359-6462(01)00925-3.

[108] Q. NGUYEN, M. GUPTA, Enhancing compressive response of AZ31B magnesium alloy using alumina nanoparticulates, Compos. Sci. Technol. 68 (2008) 2185–2192. doi:10.1016/j.compscitech.2008.04.020.

[109] Q. Li, A. Viereckl, C. a. Rottmair, R.F. Singer, Improved processing of carbon nanotube/magnesium alloy composites, Compos. Sci. Technol. 69 (2009) 1193–1199. doi:10.1016/j.compscitech.2009.02.020.

[110] Q. Li, B. Tian, Compression behavior of magnesium/carbon nanotube composites, J. Mater. Res. 28 (2013) 1877–1884. doi:10.1557/jmr.2013.167.

[111] M. Wong, W.L.E., Gupta, Effect of hybrid length scales (micro + nano) of SiC reinforcement on the properties of magnesium, Solid State Phenom. 111 (2006) 91–94. doi:10.4028/www.scientific.net/SSP.111.91.

[112] S.F. Hassan, M. Gupta, Development of a novel magnesium/nickel composite with improved mechanical properties, J. Alloys Compd. 335 (2002) L10–L15. doi:10.1016/S0925-8388(01)01841-2.

[113] S.F. Hassan, M. Gupta, Development of high strength magnesium based composites using elemental nickel particulates as reinforcement, J. Mater. Sci. 37 (2002) 2467–2474. doi:10.1023/A:1015475103720.

[114] G. Vander Voort, Metallography of Magnesium and its Alloys, Beuler Publ. 4 (n.d.). doi:10.1038/156614b0.

[115] B.D. Cullity, S.R. Stock, Elements of X-ray diffraction, 3rd edition, Prentice Hall. (2001) Chapter 1.

[116] M.E. Alam, S. Han, Q.B. Nguyen, A.M. Salem Hamouda, M. Gupta, Development of new magnesium based alloys and their nanocomposites, J. Alloys Compd. 509 (2011) 8522–8529. doi:10.1016/j.jallcom.2011.06.020.

[117] A.A. Nayeb-Hashemi, J.B. Clark, The Mg−Ni (Magnesium-Nickel) system, Bull. Alloy Phase Diagrams. 6 (1985) 238–244. doi:10.1007/BF02880406.

[118] S. Seetharaman, J. Subramanian, K. Tun, A. Hamouda, M. Gupta, Synthesis and Characterization of Nano Boron Nitride Reinforced Magnesium Composites Produced by the Microwave Sintering Method, Materials (Basel). 6 (2013) 1940–

1955. doi:10.3390/ma6051940.

[119] R. Abbaschian, R.E. Reed-Hill, Physical Metallurgy Principles, n.d. https://books.google.com.sa/books/about/Physical_Metallurgy_Principles.html?id=wh4v6UWjYdIC&pgis=1 (accessed January 31, 2016).

[120] V.L.E.M. Addison-, Interfacial Phenomena in Metal and Alloys. Wesley Publishing Company, Reading/Mass. 1975, 376 S., 14,50 $, Phys. Unserer Zeit. 8 (1977) 30–30. doi:10.1002/piuz.19770080108.

[121] M.. J. Tan, X. Zhang, Powder metal matrix composites: selection and processing, Mater. Sci. Eng. A. 244 (1998) 80–85. doi:10.1016/S0921-5093(97)00829-0.

[122] K.S. Tun, P. Jayaramanavar, Q.B. Nguyen, J. Chan, R. Kwok, M. Gupta, Investigation into tensile and compressive responses of Mg–ZnO composites, Mater. Sci. Technol. 28 (2012) 582–588. doi:10.1179/1743284711Y.0000000108.

[123] H.E. Friedrich, B.L. Mordike, Magnesium Technology, Springer-Verlag, Berlin/Heidelberg, 2006. doi:10.1007/3-540-30812-1.

Vitae

Name: OGUNLAKIN NASIRUDEEN OLALEKAN

Nationality: NIGERIAN

Date of Birth: 12/17/1985

Email: naslek85@gmail.com

Address 10, Emmanuel Ojeabu Street, Ijeododo Ijegun Ikotun, Lagos state Nigeria

Academic Background:

2016: **Master of Science (Material Science and Engineering),**
King Fahd University of Petroleum and Minerals, Saudi Arabia
CGPA: 4.00/4.00

2010: **Bachelor of Science (Metallurgical and Materials Engineering),**
University of Lagos, Akoka Nigeria
CGPA: 4.68/5.00

2004: **Senior Secondary School Certificate**
Baptist Model High School, Ijegun, Lagos Nigeria

PUBLICATIONS

S. Fida Hassan, **O.O. Nasirudeen**, N. Al-Aqeeli, N. Saheb, F. Patel, and M.M.A. Baig, Magnesium-Nickel Composite: Preparation, Microstructure and Mechanical Properties, Journal of Alloys and Compounds 646 (2015) 333-338

MEMBERSHIPS

American Welding Society (AWS)
The Minerals, Metals and Materials Society (TMS)
The America Ceramic Society (ACerS)
Association of Iron and Steel Technology (AIST)

PROFFESIONAL EXPERIENCE

02/2013 – 01/2014 **Graduate Trainee,** Dangote Industry Ltd.

- Hands-on training on maintenance of mechanical equipment.
- Hands-on training on condition monitoring of mechanical equipment
- Training on operational principles of mechanical components.

06/2011 - 08/2012 **Graduate Research Assistant,** LAUTECH, Ogbomoso

- Reporting directly to Professor performing research and analysis for various projects; data extrapolation and Model designing.
- Tutor students in microsoft office packages, graphical softwares and basics of computer engineering.
- Tutor students in mathematics and science subjects in preparation for their examinations.

02-09/2009 **Intern,** Iron Products Industries, Ikotun**.**

- Supporting the draft men to perfom basic calculatins on work diagrams and dimensions before final approval.
- Visual inspection of welds prior to painting.
- Recording, Updating and reviewing the reports of various test, daily weld reports and coating protection reports.